ABSTRACT

Reprogramming the Immune Environment in Breast Cancer via Dendritic Cells

Te-Chia Wu, Ph.D.

Mentor: Karolina Palucka, M.D., Ph.D.

Breast cancer is the most common cancer among American women. The current therapies are not curative for some forms of braest cancer, especially breast cancers that do not express the growth factor and hormone receptors and metastatic cancers. Recently, immunotherapy become an anticipated option for breast cancer. Before approaching immunotherapy, it is important to firstly understand how is the immune microenvironment regulated in breast cancer to determine how it could be modulated for therapy.

The human breast cancer microenvironment displays features of T helper 2 (Th2) immunity which promotes tumor development. Here we show that human breast cancer cells produce thymic stromal lymphopoietin (TSLP). Breast tumor supernatants, in a manner dependent on TSLP, induce expression of OX40L on dendritic cells (DCs). $OX40L^+$ DCs are found in primary breast tumor infiltrates. $OX40L^+$ DCs drive development of inflammatory Th2 cells producing interleukin 13 and tumor necrosis factor in vitro. Antibodies neutralizing TSLP or OX40L inhibit breast tumor growth and interleukin 13 production in a humanized mouse model of breast cancer. Thus, breast

cancer cell-derived TSLP, by inducing OX40L expression on DCs, contributes to the Th2 immunity conducive to breast tumor development.

In order to reprogram the inflammatory pro-tumor Th2 (iTh2) into anti-tumor Th1 microenvironment, we tested the impact of targeting the innate receptors on DCs to render the resistant to tumor environment. We show that intratumoral delivery of β-glucan, a natural ligand for dectin-1 expressed on DCs, blocks the generation of iTh2 cells leading to decreased IL-13 in the tumor microenvironment and prevents breast cancer development in vivo. β-glucan inhibits OX40L expression on tumor-associated DCs which is due to a block in STAT6 phosphorylation. β-glucan-treated DCs, when exposed to breast cancer supernatant, secrete higher levels of IL-12p70 and do not expand iTh2 cells thereby enabling the T helper 1 cells secreting IFN-γ. β-glucan exposed DCs expand $CD8^+$ T cells that express CD103, a ligand for E-cadherin. These $CD8^+$ T cells, which produce higher IFN-γ, Granzyme A and Granzyme B, accumulate in the tumors leading to enhanced tumor necrosis in vivo. DC reprogramming by β-glucan is dependent upon dectin-1 engagement. The ligand of TLR7/8 (CL075) and TLR3 (polyI:C) show the same effect in Th2 response inhibition but no effect on the functions of CD8 T cells. Taken together, our data demonstrate that exploiting pattern recognition receptors on tumor-infiltrating DCs enables cancer rejection.

Reprogramming the Immune Environment in Breast Cancer via Dendritic Cells

by

Te-Chia Wu, B.S., M.S.

A Dissertation

Approved by the Institute of Biomedical Studies

_____
Robert R. Kane, Ph.D., Director

Submitted to the Graduate Faculty of
Baylor University in Partial Fulfillment of the
Requirements for the Degree
of
Doctor of Philosophy

Approved by the Dissertation Committee

_____
A. Karolina Palucka, M.D., Ph.D., Chairperson

_____
Yong-Jun Liu, M.D., Ph.D.

_____
Sangkon Oh, Ph.D.

_____
Virginia Pascual, M.D.

_____
Robert R. Kane, Ph.D.

_____
Christopher M. Kearney, Ph.D.

Accepted by the Graduate School
August 2013

_____
J. Larry Lyon, Ph.D., Dean

Page bearing signatures is kept on file in the Graduate School.

TABLE OF CONTENTS

LIST OF FIGURES

LIST OF TABLES

LIST OF ABBREVIATIONS

APC ..... Allophycocyanin
APCs ..... Antigen presenting cell
BC or BRCA ..... Breast cancer
BME 2-Beta-mercaptoethanol
CAF ..... Cancer -associated fibroblast
CCL ..... Chemokine (C-C motif) ligand
CCR ..... C-C chemokine receptor
CD ..... Cell differentiation
CFSE ..... Carboxyfluorescein diacetate succinimidyl ester
CLR ..... C-type lectin receptor
CR ..... Complement receptor
CRD ..... Carbohydrate-recognition domain
cRPMI ..... Complete Roswell Park Memorial Institute medium
CSF ..... Colony stimulating factor
CTL ..... Cytotoxic T lymphocyte
DC ..... Dendritic cell
DCIR ..... Dendritic cell immunoreceptor
DC-SIGN ..... Dendritic-cell specific ICAM-3 grabbing non-integrin
DLEC ..... Dendritic cell lectin
DMSO ..... Dimethyl sulfoxide
DNA ..... Deoxyribonucleic acid
ERα ..... Estrogen receptor alpha
FACS ..... Fluorescence-activated cell sorting
FCS ..... Fetal calf serum
FITC ..... Fluorescein
FSC ..... Forward scatter

GM-CSF ..... Granulocyte macrophage colony stimulating factor

HCC ..... hepatocellular carcinoma

HD ..... Healthy donor

HEPES ..... 4-(2-hydroxyethyl)-1-piperazineethanesulfonic acid

HER2 ..... Human epidermal growth factor receptor

HIF-1α ..... Hypoxia-inducible factor-1α

HLA ..... Human leukocyte antigen

iC3b ..... inactivated complement 3b

ICS ..... Intracellular staining

IFN ..... Interferon

IL ..... Interleukin

ITAM ..... immunoreceptor tyrosine-based activation motif

LPS ..... Lipopolysaccharide

M1 ..... Type-1-polarized macrophages

M2 ..... Type-2-polarized macrophages

mAb ..... Monoclonal antibody

M-CSF ..... Macrophage colony stimulating factor

mDC ..... Myeloid DC

MHC ..... Major histocompatibility complex

MMP ..... Matrix metalloproteinases

MRI ..... Magnetic resonance imaging

MUC-1 ..... Mucin-1

NF-κB ..... Nuclear factor kappa B

NK ..... Natural killer cell

NKT ..... Natural killer T cell

NLR ..... Nucleotide oligomerization domain receptor

PAMP ..... Pathogen associated molecular pattern

PBS ..... Phosphate buffered saline

pDC ..... Plasmacytoid DC

PD-1 ..... Programmed death 1

PE ..... Phycoerythrin

PerCP ..... Peridinin chlorophyll

PMA ..... Phorbol 12-myristate 13-acetate

PolyI:C ..... Polyinosinic:polycytidylic acid

PRR ..... Pattern recognition receptors

PR ..... Progesterone receptor

RLR ..... Retinoic-acid inducible gene (RIG)-like receptors

ROS ..... Reactive oxygen species

RNA ..... Ribonucleic acid

SD ..... Standard deviation

SSC ..... Side scatter

STAT ..... Signal transducer and activator of transcription protein

TAM ..... Tumor associated macrophage

TCR ..... T cell receptor

TGF-β ..... Transforming growth factor beta

TIL ..... Tumor infiltratin lymphocyte

Th ..... T helper cell

TLR ..... Toll-like receptor

TNFα ..... Tumor necrosis factor alpha

Treg ..... Regulatory T cell

TSLP ..... Thymic stromal lymphopoietin

VEGF ..... Vascular endothelial growth factor

CHAPTER ONE

Introduction

Breast Cancer

Background

Breast cancer refers to the tumors that form in the breast tissue such as milk ducts and the lobules, which are the glands that produce milk. According to the information from the National Cancer Institute, there were more than 23,000 new cases in 2012 and around 40,000 deaths. Breast cancer is the most common of all cancer incidences among women in the US. Although breast cancer is rare in males, some do get breast cancer and can die from it. Invasive breast cancer cells may break away from the primary tumors, enter the lymphatic system or blood vessels, and spread to other tissues and organs to establish tumor metastasis. The risks factors for breast cancer include age, personal health history, family health history, genome changes, and race. Advanced techniques, mammograms and breast x-rays, allow us to have earlier diagnosis. The further imaging methods such as ultrasound and MRI will be performed if some abnormal regions are found from mammogram examination.

Breast carcinoma in situ is the term used for describing early stage of cancers. It refers to the cancer which remains in the place where it origins as non-invasive breast cancer. When breast cancer becomes invasive, it will spread outside the membrane that lines a duct or lobule, invading the surrounding tissues. Ductal carcinoma which forms in the lining of a milk duct within breast is the most common type of breast cancer. Lobular

carcinoma starts in the lobules of the breast, where breast milk is produced. Sarcoma refers to the cancers that start in connective tissue which are the rare cases.

Different stages describe the severity of breast cancer. Stage 0 refers to the abnormal cells found in situ and not invading other tissues. In stage 1, the abnormal cells form more than 1 tumor inside of the breast. When tumors spread into nearby lymph nodes, this is classified as stage 2. Further spreading to the breastbone and the formation of tumors larger than 5 centimeters across constitute stage 3. When the breast tumor cells spread into other parts of the body and establish metastasis, it is called stage 4.

Histology tumor grade is based on the arrangement of the cells whether they form tubules and how many cancer cells are in the process of dividing. Tumor grading system is only used in invasive breast cancers not in *in situ* carcinomas. The grade can be a predictor for patients' prognosis while a higher number indicates a faster-growing cancer that is most likely to spread. Grade 1 cancers have relatively more normal-like cells and small tubules. The moderately differentiated cancers are grade 2. And the highest grade is grade 3 which lack normal features and tend to grow and spread more aggressively.

It is known that breast cancer cells may highly express hormone receptors (estrogen receptor (ER) and progesterone receptor (PR)) and/or human epidermal growth factor (HER2) protein (except in the case of triple-negative breast cancer, which doesn't express ER and PR and normal level of HER2). Therefore, hormone receptors and HER2 can serve as indicators for early diagnosis of breast cancer. Hormones (estrogen and progesteron) can fuel the growth of breast cancer cells through these receptors.

Breast cancers can be classified based on the expression of receptors. The ER positive cancers are defined as luminal types. Luminal A cancers are low grade, grow

slowly and have best prognosis, whereas luminal B cancers grow faster than luminal A and the outcome is not good as luminal A cancers. Her2 type cancers are those with extra copies of *HER2* gene and show worse prognosis. And the basal type cancers are mostly of the triple-negative types which are the cancers growing fast and high grade.

Current Therapy

Surgery. Lumpectomy is the common method in treating early stages of breast cancer. The regions with abnormal cells are removed and also the lymph nodes under arms are taken for cancer cell examination. If cancer cells are present in the lymph nodes, other treatments may need to be applied.

Radiation therapy. Radiation therapy may be combined with surgery. The high-energy rays are applied on the breast to eliminate the possible remaining cancer cells after surgery. The killing effect is regional, thus affecting only the regions that are treated.

Chemotherapy. Chemotherapy kills rapidly dividing cells. The administration route may be though intravenous injection or oral administration. Usually, multiple drugs are used in combination. However, there are side effects from chemotherapy. The drugs may also kill the normal cells that are regularly dividing such as blood cells, cells in hair roots and cells that line the digestive tract. Loss of hair, increased likelihood of infection and vomiting are the common side effects of chemotherapy drugs.

Hormone therapy. The hormones produced by ovaries (such as estrogen and progesterone) are thought to act on breast cancer cells, promoting cell proliferation and breast tumor formation in some cases. The goals of hormone therapy are to prevent

hormones from acting on cancer cells or to terminate hormone production. Certain hormone therapy drugs block the estrogen and progesterone receptors and are good at attenuating certain types of breast cancer cell growth.

Targeted therapy. In addition, some breast cancers exhibit abnormal expression of human epidermal growth factor receptor 2 (HER2). HER2 is involved in signal transduction pathways, leading to cell growth and differentiation. Targeted therapy introduces anti-HER2 antibodies, which block HER2 protein function and inhibit the growth of cancer cells.

Unfortunately, the current therapies are not curative for some forms of braest cancer, especially breast cancers that do not express the growth factor and hormone receptors and metastatic cancers. Therefore, a deeper knowledge of the mechanisms of breast cancer and how these mechanisms are regulated will enable us to develop effective therapeutic approaches.

Cancer Immunology

Cancer Microenvironment

Tumor development is a complicated process that involves the cross-talk between three components: 1) cancer cells; 2) stroma (including fibroblasts and endothelial cells); 3) cells of the immune system including bone-marrow-derived cells such as dendritic cells (DCs) and macrophages, lymphocytes (T cells, B cells, NK cells and NKT cells) and neutrophils. The tumor microenvironemnt comprises different stromal cells in addition to tumor cells. These include vascular or lymphatic endothelial cells, supporting pericytes,

fibroblasts, and both innate and adaptive infiltrating immune cells. Moreover, the tumor microenvironment contains non-cellular components, including extracellular matrices, growth factors, proteases, protease inhibitors and other signaling molecules that play important roles in stromal reactions (Koontongkaew, 2013).

Immune System in Cancer

The immune system can efficiently sense the molecules produced by infectious agents and elicit specific immune responses to defend against these agents. When encountering pathogens, damaged cells or some irritants, inflammation will be induced to protect host from the injurious stimuli. The inflammation can be classified as acute or chronic. Acute inflammation is the initial response to the harmful stimuli by the increased movement of plasma and leukocytes from the blood into the injured tissue. The chronic inflammation occurred in the site of inflammation with a progressive shift in the present cell types.

However, tumor cells, which exhibit low-immunogenicity and are treated as self-antigens, usually do not give sufficient signals to induce immune responses. Some tumors even actively modulate the surrounding environment to suppress immune responses or secrete factors that form physical barriers, thus creating immune-privileged sites around tumors. Tumors can inhibit DC function by several mechanisms. For example, cancer cells may promote the production of vascular endothelial growth factor (VEGF), which is thought to interrupt DC infiltration (Naoko Inoshima, Takahiro Minami, Koichi Takayama, & Hara, 2002). Tumor-derived cytokines such as IL-6 and IL-10 induce tolerogenic DCs and tumor-associated macrophages, which favor

immunosuppression and Th2 immunity (Solinas, Germano, Mantovani, & Allavena, 2009).

Upon encountering foreign antigens presented by antigen-presenting cells, naive $CD4^+$ T cells can differentiate into Th1, Th2, Th17, Treg, and Tfh cells. These differentiation programs are controlled by cytokines produced by innate immune cells, such as IL-12 and IFNγ, which are important for Th1 cell differentiation, and IL-4, which is crucial for Th2 cell differentiation. TGFβ together with IL-6 induces Th17 cell differentiation, whereas Treg differentiation is induced by TGFβ and IL-2. Tfh cell differentiation requires IL-21. Specific transcription factors that orchestrate the differentiation program of each T helper cell subset have been identified: T-bet for Th1 cells, GATA3 for Th2 cells, RORγt for Th17 cells, and Foxp3 for Treg cells. The effector T cells had been thought to be terminally differentiated lineages, but it now appears that there is considerable plasticity allowing for conversion to other phenotypes. Although Th1 and Th2 cells display more stable phenotypes, Treg cells and Th17 cells can readily switch to other T helper cell programs under certain cytokine conditions (Zhou, Chong, & Littman, 2009).

In cancer microenvironment, inflammation represents a link between the cancer cell-intrinsic (oncogenes) and -extrinsic (immune and stromal components) factors that contribute to cancer cell anchoring and tumor development (Coussens, Zitvogel, & Palucka, 2013; Grivennikov, Greten, & Karin, 2010). Polarized responses by adaptive immune cells alter the balance between pro- and anti-tumor myeloid cell bioactivities. There are two types of immune responses that have opposing effects on tumors. Chronic inflammation promotes cancer cell survival and metastasis (Condeelis & Pollard, 2006;

Coussens & Werb, 2002; Grivennikov et al., 2010; Mantovani & Sica, 2010), while acute inflammation can trigger cancer cell destruction - as illustrated by regression of bladder cancer following treatment with microbial preparations (Grivennikov et al., 2010; Medzhitov, 2009). While chronic inflammation is often linked with the presence of type-2-polarized macrophages (M2), acute inflammation (associated with cancer destruction) is linked with type-1-polarized macrophages (M1). Classically, M1 macrophages are induced by the Th1 cytokine, IFN-γ; and M2 macrophages are induced by the Th2 cytokines, IL-4 and IL-13 (DeNardo, Andreu, & Coussens, 2010; Mantovani & Sica, 2010). The immune responses elicited from tumor antigens may lead to chronic inflammation, which is a pro-tumorigenic inflammatory state. The types of immune infiltrates significantly affect the outcome of tumor progression (Arima et al., 2010; Condeelis & Pollard, 2006; Grivennikov et al., 2010). The M1 macrophages, Th1 $CD4^+$ T cells, cytotoxic $CD8^+$ T cells and NK cells are thought to be related to reduce tumor growth.

On the other hand, M2 macrophage, myeloid-derived suppressor cells, Th2 $CD4^+$ T cells and regulatory T cells are the types that can promote tumor growth (Coussens et al., 2013; DeNardo et al., 2010). In colorectal cancer for example, the clinical studies that analyzed more than 1000 patients reported the prognostic impact by immune infiltrates. The gene profiles that are related to type 1 adaptive immune responses such as antigen presentation, IFNγ and cytotoxic T cell signaling significantly influenced the prognosis of colorectal cancer patients. The Th1-attracting chemokines also contribute to positive prognosis (Fridman et al., 2011).

Fibroblasts in Cancer

More and more studies have pointed out the roles of fibroblasts in tumor progression. Fibroblasts are the key components in tumor initiation and development. Cancer cells secrete some inflammatory cytokines to educate fibroblasts and activate NF-κB in fibroblasts. Cancer-associated fibroblasts (CAF) from several kinds of tumors display proinflammatory gene signatures, promote angiogenesis and induce macrophage recruitment, which enhances tumor growth in an NF-κB-dependent pathway (Raz & Erez, 2013). Take pancreatic cancer for example, the cancer cells cross-talk with fibroblasts and the fibroblasts become CAFs and secrete TSLP, further inducing a Th2-favored immunity, which is associated with the poor survival rate of pancreatic cancer patients (De Monte et al., 2011).

Macrophages in Cancer

It is known that tumor-associated macrophages (TAM) play a notorious role in the tumor microenvironment and they are a critical component related to pro-tumoral inflammation. The chemokines such as CCL2, CCL3, CCL4, CCL8 and CXCL12 produced by tumor cells may recruit monocytes into tumors and maintain the level of infiltrating TAMs. The cytokines from TAMs promote the proliferation and survival of malignant cells (Hao et al., 2012). They also secrete some angiogenic factors and growth factors to facilitate tumor cell growth. Taken these together, the infiltration of TAMs correlate to poor prognosis (Condeelis & Pollard, 2006). A study showed that $CCR2^{+}$ monocytes are recruited to the lung, becoming metastasis-associated macrophages and secreting VEGF to enable the extravasation of tumor cells from circulation and establish metastatic tumors in the lung (Qian et al., 2011). In hepatocellular carcinoma (HCC)

studies, the peritumoral liver tissue highly expresses macrophage-colony stimulating factor (M-CSF) and it positively correlates with macrophage infiltration in HCC. The higher density of macrophages is associated with a poor survival rate for HCC patients. These TAMs exhibit similar molecular and functional profiles to M2, which expresses immune suppressive cytokines. Chemokines such as CCL17 and CCL22 are secreted by TAMs, which attracts Th2 cells. The IL-6 secreted from TAMs was shown to have an antiapoptotic effect on HCC by activating the STAT3 signaling pathway. TAMs produce VEGF, thymidine phosphorylase and several matrix metalloproteinases (MMPs) to help angiogenesis in HCC (Ken Shirabe, 1998). The immune suppressive microenvironment is also known to be controlled by TAMs. Tumor regions are often defined by the regions of hypoxia with increasing oxygen tension in macrophages. Hypoxia-inducible factor-1α (HIF-1α) constitutively expresses in almost all kinds of mammalian cell types, including macrophages. The level of HIF-1α represents the cellular hypoxic response. It is proved that loss of HIF-1α inhibits the suppressive immune responses mediated by macrophages. The T cells isolated from tumors in myeloid HIF-1α-null mice are more responsive to stimulation (Doedens et al., 2010). The cytokines such as IL-4 in breast tumors may programs TAMs secreting epidermal growth factor (EGF) to help tumor growth and metastasis (Ruffell, Affara, & Coussens, 2012).

Lymphocytes in Cancer

Tumor infiltrating lymphocytes (TIL) are also commonly associated with tumor development. The flow cytometry analysis from 30 human primary breast tumors shows that if CD4/CD8 ratios are greater than one, then they correlate to tumor size. In these patients, it also is an indicator of lymph node metastasis –indicating formation of more

aggressive breast tumors (Georgiannos, Renaut, Goode, & Sheaff, 2003). The regulatory T cells (Treg) are thought to suppress immune responses, thus resulting in immune tolerance in tumors. The tumor-infiltrating $Foxp3^+$ Treg cells are assessed in breast tumors from patients. Treg numbers are higher in breast carcinomas than in normal breasts; and when the number is positive, it correlates to the stage of breast cancer and the risk of relapse (Bates et al., 2008). The cytokines from Th2 cells can program macrophages into TAMs and induce EGF which promote tumor metastasis (Ruffell et al., 2012). The genomic analysis of cohort of breast cancer patients from different stages reveals that the ratio between Th1 and Th2 can be a predictor of overall survival. The highest Th2 signaling correlates to worst outcome (Vessela N. Kristensen, Ravi Sachidanandam, & Charles M. Perou, 2012).

Dendritic Cell and Immune Microenvironment in Breast Cancer

Dendritic Cell

Dendritic cells (DC) are professional antigen presenting cells (APCs). There are several subsets of DCs, which are classified into myeloid DCs (mDC) and plasmacytoid DCs (pDC).

In the human immune system, pDCs ($BDCA2^+$ DCs) secrete a high amount of IFNα in response to viral infection, which is thought to be the first line of barrier. The ways pDCs regulate the immune system are by producing type I interferon, inducing cytotoxic $CD8^+$ T cells through MHC class I in the early endosome, and enhancing CD4 T cell responses through MHC class II in the late endosome. pDCs may also play a role in the generation of plasma cells and antibody responses by the cytokines they secrete (such as type I interferon and IL-6). The mDCs include BDCA1 (CD1c) and BDCA3 (CD141) DCs.

The blood mDCs are over 90% BDCA1$^+$ DCs and the rest are BDCA3$^+$ DCs. BDCA1$^+$ DCs have the ability to cross-present antigens and secrete IL-12 (Stenger, Turnquist, Mapara, & Thomson, 2012). Langerhans cells are another subset of DCs that resides in the epithelia, and they are thought to be responsible for mucosal immunity. DCs express several pattern recognition receptors including Toll-like receptors (TLR), nucleotide-binding oligomerization domain-like receptors (NLR), retinoic-acid inducible gene (RIG)-like receptors (RLR) that recognize pathogen-related structures and certain RLR that recognize carbohydrate structures (Unger & van Kooyk, 2011). pDCs recognize viral antigens through TLR7 and TLR9 and produce type I interferon. BDCA3$^+$ mDCs express TLR3 and TLR8 and respond to poly I:C and poly U for maturation and cytokine production. BDCA1$^+$ mDCs express TLR4, TLR5 and TLR7. C-type lectins contain a carbohydrate-recognition domain (CRD), which is the region that binds to carbohydrates. C-type lectins include dendritic cell immunoreceptor (DCIR), dendritic-cell specific ICAM-3 grabbing non-integrin (DC-SIGN), dendritic cell lectin (DLEC), DEC-205, Langerin, Dectin-1 and Dectin-2. Type I C-type lectins (MMR and DEC-205) contain an amino-terminal cysteine-rich repeat (S–S), a fibronectin type II repeat (FN) and 8–10 carbohydrate-recognition domains (CRDs), which bind ligand in a $Ca2^+$-dependent manner. Type II C-type lectins contain only one CRD at their carboxy-terminal extracellular domain. The cytoplasmic domains of the C-type lectins are diverse and contain several conserved motifs that are important for antigen uptake: a tyrosine-containing coated-pit intracellular targeting motif, a triad of acidic amino acids and a dileucine motif. Other type II C-type lectins contain other potential signaling motifs (Carl

G. Figdor, 2002). The signals through these CLRs may lead to immune activation or tolerance; therefore, they can be used as targets to modulate immune responses.

The different maturation signals from several cytokines contribute to the plasticity of DCs, which are the major cell type to determine the activating or suppressive immune responses that guide the direction of T cell development and polarization (Figure 1).

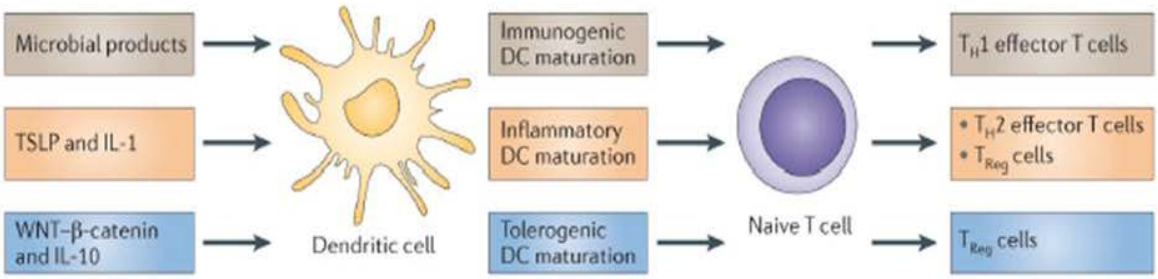

Figure 1. DC maturation (from Karolina Palucka *et al.* 2013). Dendritic cell (DC) maturation is a simple concept that is rendered complex by the likelihood that not all mature (or activated) DCs are equivalently immunogenic. For example, under steady-state conditions, particularly in lymphoid tissue, DC populations that display at least some of the features of mature DCs (for example, elevated expression of surface co-stimulatory molecules) can be found despite the absence of overt inflammation or infection. The functional importance of these cells is unknown but it is not unreasonable to suspect that tolerogenic DCs may have to acquire the capacity to present antigen, migrate and interact with T cells (characteristics of mature DCs) in order to induce antigen-specific regulatory T (Treg) cells or to induce anergy or T cell apoptosis at high efficiency. The priming of Treg cells either in the thymus or in the periphery may require activation by endogenous mediators, such as thymic stromal lymphopoietin (TSLP) or WNT, respectively. Whether these mediators induce morphologically recognizable maturation in vivo is likely but not known. However, it is clear that resting or immature DCs can or must be activated in some way to induce T cell tolerance; thus, it is inaccurate to assume that the relevant steady-state DCs are 'immature' or resting.

Some stimulation signals such as CD40L can mature DCs and induce IL-12 secretion in the early maturation stage. IL-12 is believed to be a critical factor that polarizes T cells into IFN-γ-producing Th1 cells (Palucka & Banchereau, 2012). STAT4 activation

can regulate IFN-γ production, resulting in Th1 cell polarization. However, the IL-4 from DCs induces expression the transcription factor, GATA3, leading to Th2 polarization.

Immune Microenvironment in Breast Cancer

Our earlier studies have demonstrated that more than 90% of primary breast tumors with $CD1a^+$ immature DCs infiltration. Around 60% of the tumors show the presence of DC-$lamp^+$ mature DCs in peritumoral areas (Diana Bell, Ghada Moumneh Harb, Jenny Valladeau, & Jean Davoust, 1999). In some cases, $CD4^+$ T cells cluster around mature DCs, thus resembling the DC/T cell clusters of secondary lymphoid organs that we have shown earlier. The presence of mature DCs outside lymphoid organs (where they normally reside) is linked with ongoing immune responses occurred in breast cancers.

Immature DCs residing in peripheral tissues can sense pathogens or other antigens in combination with TLR signals, tissue damage, or inflammatory cytokines to become mature DCs. The maturation of DCs leads to alteration of adhesion molecules, and the expression of co-stimulatory molecules on DCs would be up-regulated. These mature DCs, along with processed antigens, migrate to lymph nodes. There, they initiate clonal expansion of T cells and differentiate naïve T cells into different subsets of effector T cells (Figure2) (Ueno et al., 2010).

In breast tumors, TAMs produce VEGFA, which is known to be associated with the vasculature. Epithelial cells secrete CSF1 to recruit macrophage infiltration into solid tumors. These infiltrating macrophages are soon educated with high level of hypoxia genes and suppress T cell proliferation and activation. The composition of leukocytes in breast tumors is evaluated in breast cancer patients. It is known that T cell infiltration increases in breast tumor tissues and shows an activated phenotype of these infiltrating T

cells. With chemotherapy, more myeloid-lineage cell infiltration is observed (Brian Ruffell, 2012). Overexpression of CSF-1 is seen in breast tumors and the high level of circulating CSF-1 correlates to breast tumor progression and metastasis.

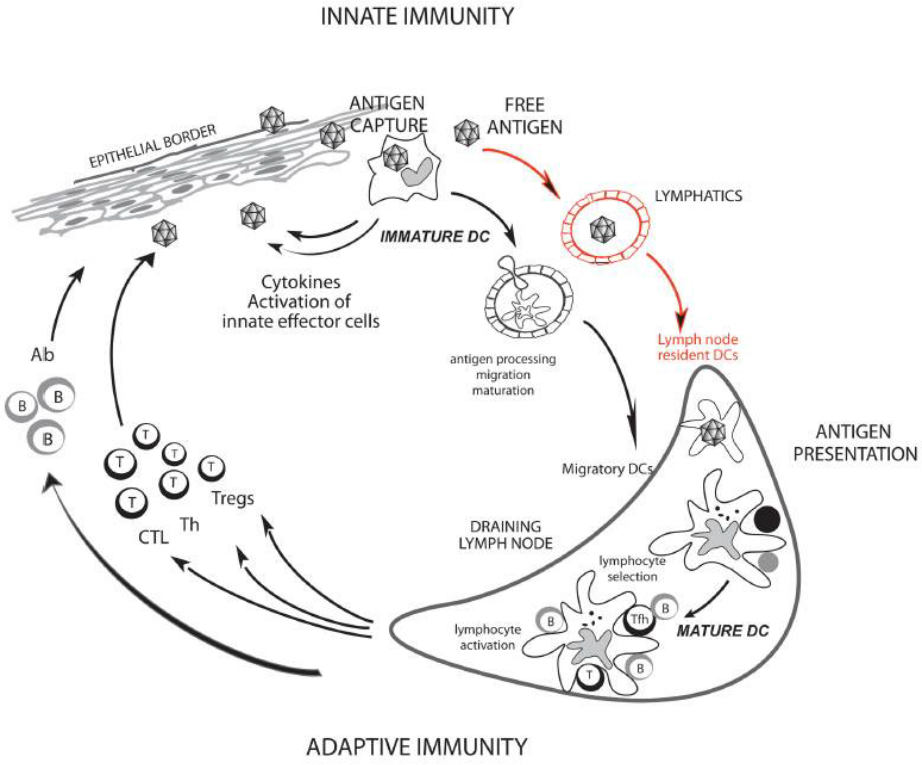

Figure 2. Dendritic cells (from Hideki Ueno *et al.* 2010). Circulating precursor DCs enter tissues as immature DCs. They can encounter pathogens (e.g. viruses) directly, which induce secretion of cytokines (e.g. IFN-a), or indirectly through the pathogen's effect on stromal cells. Cytokines secreted by DCs in turn activate effector cells of innate immunity such as eosinophils, macrophages, and NK cells. Microbe activation triggers DC migration towards secondary lymphoid organs and simultaneous activation (maturation). These activated migratory DCs that enter lymphoid organs display pMHC complexes, which allow selection of rare circulating antigen-specific T lymphocytes. Activated T cells help DCs in their terminal maturation, which allows lymphocyte expansion and differentiation. Activated T lymphocytes traverse inflamed epithelia and reach the injured tissue, where they eliminate microbes and/or microbe-infected cells. B cells, activated by DCs, and T cells migrate into various areas. B cells mature into plasma cells that produce antibodies that neutralize the initial pathogen. Antigen can also reach draining lymph nodes without the involvement of peripheral tissue DCs and can be captured by lymph node-resident DCs.

Our more recent studies have shown that in primary breast cancers upon PMA/Ionomycin stimulation, there is higher IL-13 secretion from tumor microenvironment. There are full of $CD4^+$ T cells infiltration and the cells isolated from breast tumor tissues secrete IL-13. IL-13 delivers signals into breast tumor cells to phosphorylate STAT6 (Aspord et al., 2007). In response to IL-4/IL-13, the STAT6 proteins and GATA3 are activated in T cells leading to Th2 polarization. Microarray analysis showed a high level of STAT6 in mammary glands during development. STAT6-deficient mammary glands exhibit less proliferation, suggesting that the IL-4/IL-13 from Th2 cells, which activate STAT6, are promoting factors in cell proliferation (W. J. Zhang et al., 2008). In the xenograft tumor model, these IL-13-secreting $CD4^+$ T cells accelerate the development of breast cancer tumors. Blocking IL-13 with neutralizing antibodies and soluble receptors results in inhibition of tumor progression (Aspord et al., 2007). In clinical studies, the ratio between Th1 and Th2 genomic signatures was believed to be a predictor for survival of breast cancer patients. Patients with higher Th2 signaling had a poorer outcome (Vessela N. Kristensen et al., 2012).

Immunotherapy and Immune Modulation

DC Vaccine

The ideal immunotherapy aims to harness protective and specific immune responses against tumors and also counter the immunosuppressive responses mastered by tumor cells.

There are some current immunotherapies being successfully used. The monoclonal antibody therapy, anti-CD20, can target to B-cell lymphoma cells to induce antibody-dependent cell mediated cytotoxic, complement mediated cytolysis and antiproliferation

effect (Maloney, 2012). The adoptive cell based immunotherapy which genetical engineered the receptors on T cells become chimeric antigen receptors or high affinity TCR to let the transferred T cells highly sensitive to low antigen density tumor cells and more efficiently to target to tumor cells. The ongoing clinical trials are in melanoma cancers and leukemia (Varela-Rohena et al., 2008). Another immunotherapy is checkpoint blockade therapy. It is known some co-costimulatory molecules such as CTLA4 and PD1 are negative regulators for T cells as checkpoint preventing autoimmune responses. However, for against tumor, checkpoint inhibitors can rescue those effector T cells from anergy and exhaustion to survive longer and function better to kill tumors (Ascierto, Marincola, & Ribas, 2011). DC-based vaccine for prostate cancer which is already used in clinic, which is the GM-CSF mature DCs with prostate cancer antigens and induce specific T cells responses to kill prostate cancer even functional to clear metastatic cancers (Tarassoff, Arlen, & Gulley, 2006).

For successful immunotherapy, the critical immune responses which we aimed to induce are Th1 responses, CTL responses, tumor specific antibodies, and to recruit natural killer cells and other innate immune components. Since DCs are known as potent antigen presenting cells and powerful for regulating the polarization of effector T cells, they can be good candidate for cancer immunotherapy (Palucka & Banchereau, 2012).

DCs can be used in several different ways for immunotherapy. DCs can capture endogenous antigens raised by chemotherapy, radiotherapy and some immunomodulation approaches. We can ex-vivo generate monocyte-derived DC loaded with antigens and re-infused back to patients to further induce tumor-specific T cell responses. The improved strategy is combining with TLR ligands or cytokines blocking which can reprogram the

inflammation. Furthermore, we are also expecting to use the targeting antibodies with tumor antigens to specific bring antigens to DCs and induce tumor specific immune responses (Figure3) (Palucka & Banchereau, 2012).

Identifying the correct tumor antigens for immunotherapeutic approaches is critical to achieving the goal of specific immunity induction. Numerous researchers have reported that breast cancer cells overexpress several specific antigens, such as HER2/neu, cyclin B1, survivin and MUC-1, raising the hopes of immunotherapy for breast cancer. Cyclin B1, for example, is the factor that regulates the cell cycle. Normal cells express low levels of cyclin B1 whereas tumor cells such as breast cancer, melanoma and renal cell carcinoma express high levels of cyclin B1. For anti-cancer immunotherapy, cyclin B1 peptide can be loaded on HLA-A2 and induce peptide-specific $CD8^+$ T cells responses (Saito et al., 2006). These CTL responses were observed in healthy donors as well as the patients with breast cancer, melanoma or renal cell carcinoma (Andersen et al., 2012). A study used mammaglobin-A to induce a peptide-specific $CD8^+$ T cell response in vitro. These $CD8^+$ T cells have the ability to lyse breast cancer cells (Partha P. Manna & Timothy P. Fleming, 2003).

In our previous study, we showed that DCs loaded with killed breast cancer cells are able to cross-prime $CD8^+$ T cells, which then secret IFN-γ and exhibit cytotoxic activity that eliminates breast cancer cells. These CTLs specifically respond to breast tumor antigens (cyclin B1, survivin, and MUC-1). As a result, DCs loaded with cancer antigens are able to induce tumor-specific immune responses and have the potential to be used as a therapeutic vaccine for breast cancer (Saito et al., 2006). These therapies will be tested in pre-selected patients, thereby leading to personalized therapy (Figure3).

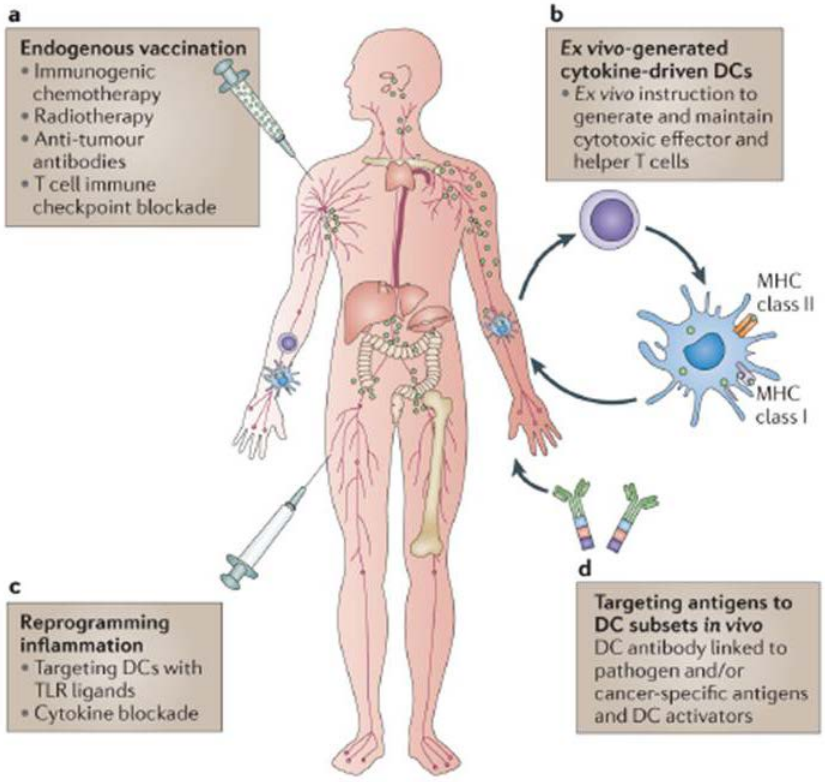

Figure 3. DCs and cancer immunotherapy (from Karolina Palucka *et al.* 2013). a. Random targeting of dendritic cells (DCs) in 'endogenous' vaccination results from in vivo antigen release owing to immunogenic cell death in response to chemotherapy, radiotherapy and immunomodulation approaches that are targeted at T cells. b. Vaccines can be based on ex vivo-generated tumor antigen-loaded DCs that are injected back into patients. c. Specific in vivo DC targeting with DC antibodies fused with antigens and with DC activators is shown. d. Targeting DCs in the tumor microenvironment to reprogram pro-tumor inflammation towards tumor rejection is shown. MHC, major histocompatibility complex; TLR, Toll-like receptor.

Immune Modulation

The goal of immunotherapy is to promote protective antitumor immunity favoring Th1 immunity. In the T helper cell differentiation program, the naïve T cells have the flexibility of committing to one of a number of specific lineages, depending on the

polarizing conditions. However, the studies in our lab show the pro-tumor Th2 immunity in breast tumor, which is polarized by the infiltrating DCs educated by breast tumor cells, results in a non-favorable environment for further immunotherapy. Therefore, we hypothesize that by utilizing DC activation signals we will be able to alter the characteristics of DCs and reprogram the functions of DCs in the breast cancer microenvironment to make them no longer induce tumor promoting Th2 immunity but rather induce tumor-rejecting Th1 immunity. This immune environment can augment the effect of immunotherapy to induce tumor-specific Th1 and cytotoxic T lymphocyte (CTL) responses.

The innate immune system recognizes antigens through different kinds of pattern recognition receptors (PRRs). There are several forms of PRRs – soluble proteins (complement), membrane bound receptors (scavenger receptors), integrins and Toll-like receptors (TLR). They respond to conserved microbial components known as pathogen associated molecular patterns (PAMPs). When the ligands bind to PRRs, the signals induce immune activation to defend against microbial infection. Besides defending infectious diseases, these signals are potent biological modifiers for activating DCs, macrophages and NK cells. Therefore, they are good candidates for controlling whether the immune system exhibits immune activation or suppression in the tumor microenvironment.

Ligands to Toll-like Receptors

There are 10 different TLR types found in human cells. TLRs can recognize PAMPs derived from bacteria, viruses, fungi or parasites. For example, TLR4 recognizes lipopolysaccharides (LPS) from Gram-negative bacteria, and TLR3 recognizes double-

stranded RNA from virus replication. Consequently, these TLR ligands would trigger several transcription factors, including NF-κB and AP-1. These would further regulate cell-surface protein expression and cytokine production. When DCs are stimulated through TLRs, the chemokine receptors and adhesion molecules undergo dramatic changes, resulting in DC trafficking to the lymph nodes. These DCs can prime antigen-specific naïve T cells to differentiate into effector T cells. It is known that DCs are responsible for orchestrating Th1/Th2/Treg balance. Besides MHC molecule and co-stimulatory molecule signals, the polarization of T cells depends on a third signal – DC-derived cytokines. IL-12, IL-27 and IFN-γ promote T cells to become Th1 cells while IL-4, IL-5 and IL-10 polarize T cells to Th2 (Murphy & Reiner, 2002). Thus, if we aim to reprogram Th2 into Th1 in tumors, we need to activate DCs to produce IL-12 or IFN-γ. TLR7 ligands – imidazoquinoline compounds and imiquimod and its derivative (R-848) – are widely used for antiviral and antitumor treatment. TLR7 ligand administration enhances DC survival, up-regulates their co-stimulatory molecules, and promotes Th1 cell polarization, which is due to IL-12 and IFN-α secretion from mDCs and pDCs, respectively (Ito, 2002). Poly I:C and dsRNA are ligands for TLR3. When they bind to TLR3 on DCs, these activated DCs may release IFN-α, resulting in a Th1 response. LPS also can induce Th1 immunity because it interacts with TLR4 on DCs causing IL-12 release (Mazzoni & Segal, 2004; Pulendran, 2005). The DCs which fused with tumors cells as vaccine combine with ligands of TLR2 and TLR4 show upregulated CD86 and MHC class II and enhanced IL-12 production resulting in effectively CTL induction (Koido et al., 2013). Taken together, ligands for TLR3, 4, 7, 8 and 9 are potent activators that skew DCs toward Th1.

A DC vaccine study that targeted the DCIR molecule shows anti-DCIR conjugates allow cross-priming and induce antigen-specific CD8 responses. After comparing several TLR ligands such as agonists for TLR3 (poly I:C), TLR4 (LPS) or TLR7/8 (CL-075), it was found that CL-075 is the most potent activator to enhance cross priming and increase cytotoxic enzymes including Granzyme B and perforin. The production of type 2 cytokines is also inhibited by CL-075 (Klechevsky et al., 2009). CL-075 has the capacity to help monocytes differentiate into potent DCs that express CD40L, CD80, CD86 and CD83. These DCs that have been conditioned with CL-075 are potent to secrete IL-12, which is known to be a Th1-favored cytokine (Du et al., 2010). These DCs are $CCR7^{+}$. They can respond to CCL19, which is expressed in lymph nodes, therefore, enhancing DC migration (Humrich et al., 2006).

β-glucan to Dectin-1

β-glucan was firstly identified 40 years ago. It is a form of polysaccharide, the cell wall components derived from fungi, yeast and some bacteria. β-glucan contains mainly a β-glycosidic chain core; and it has different lengths and branching structures, resulting in conformational complexity. It is believed that the higher the complexity of the structure, the more potent ability it has for immunomodulation (Chan, Chan, & Sze, 2009). When the β-glucan is orally administrated into animal models, β-glucan enters the proximal small intestine rapidly and can be taken up by phagocytes such as macrophages and dendritic cells and further degraded into small fragments. The small fragments bind to the complement receptor 3 (CR3) and induce the killing activity toward inactivated complement 3b (iC3b)-opsonized antigens (Figure4) (Bing Li & L. Harris, 2007).

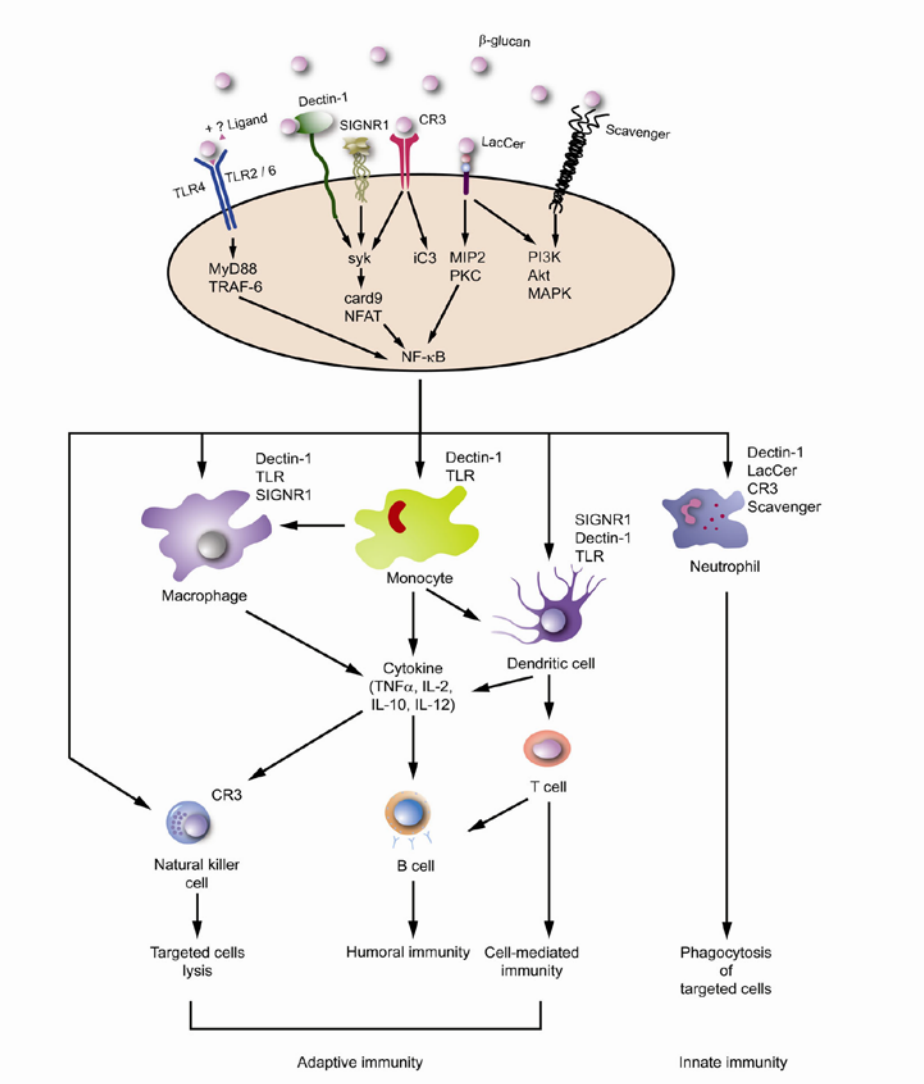

Figure 4. Immune activation induced by β-glucans (from Godfrey Chi-Fung Chan *et al.* 2009). β-glucans can act on a variety of membrane receptors found on the immune cells. They may act singly or in combination with other ligands. Various signaling pathways are activated, and their respective simplified downstream signaling molecules are shown. The reacting cells include monocytes, macrophages, dendritic cells, natural killer cells and neutrophils. Their corresponding surface receptors are listed. The immunomodulatory functions induced by β-glucans involve both innate and adaptive immune responses. β-glucans also enhance opsonic and non-opsonic phagocytosis and trigger a cascade of cytokine release, such as tumor necrosis factor (TNF)-α and various types of interleukins (ILs).

Besides the CR3 receptor, further receptors for β-glucan were found such as dectin-1.

Dectin-1 was discovered from a cDNA library screening on macrophage cell line

RAW264.7. Dectin-1 contains a cytoplasmic domain that is an unpaired immunoreceptor tyrosine-based activation motif (ITAM), a transmembrane domain, a stalk and a C-type lectin-like extracytoplasmic domain. Phosphorylation of the second tyrosine residue in its cytoplasmic domain is known to induce further activation effects, such as activation of antigen presenting cells, induction of phagocytosis, production of reactive oxygen species (ROS), and NF-κB-mediated cytokine secretion (Kanazawa, 2007). Dectin-1 expression on DCs would be induced after infection, suggesting an immune activation state. It has been proposed that dectin-1 can act as a co-stimulatory molecule for T lymphocytes. It has been shown that DCs binding to T cells through dectin-1 lead to up-regulation of activation markers on T cells (including CD25, CD69 and CD154), IFN-γ production, and proliferation of both $CD4^+$ and $CD8^+$ T cells. It has been shown that the expression of dectin-1 in RAW264.7 cells correlates with proinflammatory cytokine production after responding to β-glucan (Chan et al., 2009; Gordon D. Brown, 2001). The agonist for dectin-1, curdlan, was proved to activate dendritic cells and primed $CD4^+$ T cells promoting the antibodies production from B cells. The dendritic cells that are treated with curdlan also induce higher Granzyme B and perforin, producing $CD8^+$ T cells (Salomé LeibundGut-Landmann, 2008; Sudhanshu Agrawal, 2010). In order to confirm the effect of binding to dectin-1, different types of carbohydrates were used to block the binding of β-glucan (zymosan). It is shown that laminarin and glucan phosphate were the most effective inhibitors of binding activity (Gordon D. Brown, 2001). For the effect of immunomodulation, engagement of dectin-1 by β-glucan leads to NF-κB activation through the Raf-1 or Syk pathway. In response to β-glucan (curdlan), the dectin-1-induced Raf-1 signaling induces Th1 and Th17 polarization. Raf-1

activation regulates IL-1β, IL-6, IL-10 and IL-12 production. Blocking of dectin-1 with anti-dectin-1 antibody can abrogate the cytokine production induced by curdlan via a Raf-1-dependent pathway (Gringhuis et al., 2009). The main effect of β-glucan is on phagocytes such as macrophages and dendritic cells promoting phagocytic ability. The activation of phagocytes by β-glucan treatment also increases chemokinesis, chemotaxis, the expression of adhesive molecules, and adhesion to the endothelial cells.

Because of the immunomodulatory effects, β-glucan is considered as a possible anti-cancer agent. It has been shown that β-glucan has no direct cytotoxic effect on tumor cells and does not induce apoptosis pathways on tumor cells. β-glucan promotes proliferation of monocytic cells and stimulates the maturation of dendritic cells, which is considered that β-glucan is helpful in inducing protective immune responses. However, the exact immunological effects modulated by β-glucan are not yet clear.

CHAPTER TWO

Objectives

Rationale

We have shown that a Th2-favored microenvironment is good for breast tumor growth but detrimental for the function of anti-tumor immunity. The tumor-educated microenvironment impaired the capacity of immune cells to induce protective immunity such as Th1 responses and CTL function, which may be due to the poor function of DCs. This would hinder the efficacy of DC vaccines. Therefore, it is very important to first understand how DCs behave and how is the immune microenvironment regulated in breast cancer to determine how it could be modulated for therapy.

Furthermore, to facilitate the capacity of anti-tumor immunity, it is critical for modulating the function of DCs to promote them to be potent in protective immune induction. Signals through TLR or other surface molecules on DCs are reported to induce type 1 cytokine production. We propose to analyze BrCa-mDC responses to activation signals.

Aims

Aim 1. To determine the role of breast cancer-derived factors in mDCs and T cells polarization.

The infiltrating DCs were educated by tumor-derived factors and polarized into pro-tumoral immune responses. The molecules and cytokines that are involved in the regulation will be considered as novel therapeutic targets for immunotherapy.

Aim 2. To identify TLR ligands and/or DC activators that are able to reprogram Th1/Th2 polarization in breast cancer.

The IL-13-secreting $CD4^+$ T cells (a Th2-permissive microenvironment) accelerate breast tumor growth in vivo. We hypothesize that when we treat mice with single or combinatorial DC activators to stimulate DCs in breast tumors, we can alter tumor immunology and block tumor development in vivo. In clinical breast tumor samples, we hypothesized that we can use the DC activators to alter the cytokines profile.

Aim 3. To understand mechanisms that are involved in immune regulation in breast tumor microenvironment.

Determine the phenotype and function of mDCs treated with TLR signals or other activation signals and evaluate T cell polarization.

CHAPTER THREE

Materials and Methods

Cell Line and Reagent

Breast tumor cell lines (MDA-MB-231, Hs578T and MCF) were cultured in medium (RPMI supplemented with glutamine 2 mM, penicillin 50 U/ml, streptomycin 50 µg/ml, MEM non-essential amino acids 0.1 mM, HEPES buffer 10 mM, sodium pyruvate 0.1 mM and 10% of fetal calf serum). β-glucan, curdlan (Wako), was resuspended in PBS and working concentration is 100 ug/ml. The working concentration of the neutralization antibodies were 20 ug/ml antibody to dectin-1 (R&D), 10 ug/ml antibody to IL-12 (R&D), 100 ug/ml antibody to TGFb (R&D), 50 ug/ml antibody to CD103 (Biolegend) 100 ug/ml antibody to ITG β 8 (clone 37E1). 5-(4,6-Dichlorotriazinyl) Aminofluorescein (5-DTAF) (Molecular Probes-Invitrogen) is used for curdlan labeling.

Tumor Factors Preparation

Cell lines were culture in medium (RPMI supplemented with glutamine 2mM, penicillin 50 U/ml, streptomycin 50 µg/ml, MEM non-essential amino acids 0.1 mM, HEPES buffer 10 mM, sodium pyruvate 0.1 mM and 10% of fetal calf serum), and when the cells reached 90% of confluence fresh medium was added and left the cells in culture for additional 48 hrs. Cellular debris was removed by centrifugation and the supernatant was collected and stored at -80 °C.

Isolation and Culture of Myeloid Dendritic Cells

DCs were purified from buffy coat of blood from healthy donors. Briefly, DCs were enriched from mononuclear cells by negative selection using a mixture of antibodies against linage markers for CD3, CD9, CD14, CD16, CD19, CD34, CD56, CD66b and glycophorin A (EasySep, human pan-DC pre-enrichment kit). Cells from negative fraction were immuno-labeled with anti-human FITC-labeled linage cocktail (CD3, CD14, CD16, CD19, CD20 and CD56, BD biosciences); PE-labeled CD123 (mIgG1, clone 9F5, BD biosciences), APC-eflour780-labeled HLA-DR (mIgG2b, clone LN3, Sigma-Aldrich) and APC-labeled CD11c (mIgG2b, clone S-HCL-3, BD biosciences). DCs (lin -, CD123-, HLA-DR+, CD11c+) were sorted in a FACS Aria cytometer (BD Bioscience). DCs were seeded at 100 x 10^3 cells/well in 200 µl of medium (RPMI supplemented with glutamine 2 mM, penicillin 50 U/ml, streptomycin 50 µg/ml, MEM non-essential amino acids 0.1 mM, HEPES buffer 10 mM, sodium pyruvate 0.1 mM and 10 % of human AB serum). DCs were cultured with medium alone or in the presence of 20 ng/ml of TSLP, or different tumor derived products. After 48 hrs DCs were harvested and washed. The stimulated cells were staining for phenotype analysis or co-culture with allogeneic naïve T cells.

Immunofluorescence

Frozen sections (6 µm) from tissues were fixed with cold acetone for 10 minutes. Dectin-1 was stained with monoclonal antibody prepared in-house (mouse IgG1, clone12.2D8.2D4), followed by Alexa Flour488 or Alexa Flour568 goat anti-mouse IgG1 (Invitrogen). Cytokeratin 19 was labeled with monoclonal antibody clone A53-BA2 (IgG2a, Abcam), following by Alexa Fluor 568 goat anti-mouse IgG2a (Invitrogen).

CD83 was stained with monoclonal antibody clone HB15a (IgG2b, Immunotech) followed by Alexa Fluor 568 goat anti-mouse IgG2b (Invitrogen). CD20 was stained with monoclonal antibody clone L26 (mIgG2a, DAKO) followed by Alexa Fluor 488 goat anti-mouse IgG2a (Invitrogen). Direct labeled antibodies used were FITC anti-HLA-DR (mouse IgG2a, L243, BD Biosciences), FITC anti-CD11c (clone, KB 90, DAKO) and Alexa-Flour 488 anti-CD3 (mIgG1, UCHT1, BD Bioscience). Finally, sections were counterstained for 2 minutes with the nuclear stain DAPI (3 μM in PBS. Invitrogen, Molecular Probes).

Flow Cytometry Analysis

The anti-human antibodies used were FITC-labeled linage cocktail (CD3, CD14, CD16, CD19, CD20 and CD56, BD Biosciences); PE-labeled OX40L (mIgG1, clone Ik-1, BD biosciences); APC-labeled HLA-DR (mIgG2a, clone L243, BD); APC-labeled CD11c (mIgG2b, clone S-HCL-3, BD Biosciences); PerCP-labeled CD3 (mIgG1, clone SK7, BD Biosciences); PECy7-labeled CD4 (mIgG1, clone SK3, BD biosciences); APCCy7-labeled CD8 (mIgG1, clone SK1, BD biosciences); PE-labeled CD80 (mIGg1; L307.4, BD biosciences); FITC-labeled CD86 (mIgG1, clone 2331(FUN-1), BD biosciences); PE-labeled CD70 (mIgG3; clone Ki-24, BD biosciences); PE-labeled MHC classI (mIgG2a; clone W6/32; Dako); FITC-labeled CD83 (mIgG1; clone HB15e; BD biosciences); Pacific blue labeled IL-10 (rat IgG1, clone JES3-9D7, e-biosciences); PE-labeled IL-13 (rat IgG1, clone JES10-5A2 BD biosciences); PECy7-labeled TNF-α (mIgG1, clone mAb11, BD biosciences); Alexa Flour 700 labeled IFN-γ (mIgG1, clone B27, BD biosciences); PerCP Cy5.5 labeled IL-17A (mIgG1, clone BL168, Biolegend); Alexa Flour 647 labeled CD103 (mIgG1, clone Ber-act8, Biolegend); pacific blue labeled

GranzymeA (mIgG1, clone GB9, Biolegend); Alexa Flour 700 labeled GranzymeB (mIgG1, clone GB11, Biolegend); PE labeled perforin (mIgG2b, clone dG9, eBioscience); FITC labeled pSTAT4 (mIgG2b, clone 38/p-stat4, BD Pharmingen) PE labeled pSTAT6 (mIgG1, clone J91-99358.11, BD Pharmingen); AF647 labeled pSTAT3 (mIgG2a, clone 4/pStat3), AF647 labeled pSTAT5 (mIgG1, clone 47), anti-ITG β 8 (mIgG1, clone 14E5) conjugated with AF488. For surface staining, cells were incubated with the antibodies for 30 minutes at 4 ºC in the dark, then washed three times and fixed with 1% paraformaldehyde to be analyzed in a FACS Canto or LSR-II cytometer (Becton Dickinson). For intracellular cytokines, cells were stained using BD cytofix/cytoperm fixation/permeabilization kit according to the manufacturer directions. For pSTATs staining, cells were fixed with 2-4% formaldehyde for 10 minutes at 37ºC and permeabilized with ice-cold methanol for 30 minutes at 4ºC. Cells were washed and stained with pSTAT3, pSTAT4, pSTAT5 and pSTAT6 antibodies for 30 minutes at room temperature.

Cytokine Analysis

T cells were harvested from DC-T co-culture system. For intracellular staining, cells were resuspended at a concentration of 10^6 cells/ml in medium and activated for 5 h with PMA and ionomycin, Brefeldin A (Golgiplug, BD biosciences) and monensin (Golgistop BD biosciences) were added for the last 2.5 h. Cells were stained using BD cytofix/cytoperm fixation/permeabilization kit according to the manufacturer directions and be analyzed in a FACS Canto or LSR-II cytometer (Becton Dickinson). Tumors from humanized mice implanted with breast cancer cell line Hs578T were also analyzed. Whole-tissue fragments (4 x 4 x 4 mm, 0.015-0.030 g, approximately), were placed in

culture medium with 50 ng/ml of PMA (Sigma-Aldrich), and 1 μg/ml of ionomycin (Sigma-Aldrich) for 18 h. Cytokine production was analyzed in the culture supernatant by Luminex.

DC-T Cell Co-cultures

Total T cells were enriched from fraction2/3 of healthy donors using magnetic depletion of other leukocytes (EasySep® Human T Cell Enrichment Kit, Stemcell technologies). Activated mDCs with medium, TSLP or tumor derived factors were co-cultured with naïve T cells in a ratio 1:5 during 7 days. After that the cells were washed and re-stimulated 5 hrs with PMA (50 ng/ml) and Ionomycin (1 μl/ml), Brefeldin A and monensin were added for the last 2.5 hrs. Followed by surface and intracellular staining. For curdlan treatment, DCs were pre-incubated with curdlan for 3 min at room temperature.

Tumor Bearing Humanized Mice

For experiments with NOD/SCID/β2m−/− mice, they were irradiated the day before tumor implantation. Then mice were reconstituted with 1 million of monocyte derived DCs (MDDCs), 10 million $CD4^+$ T cells and 10 million CD8+ T cells autologous T cells. MDDCs were generated from the adherent fraction of PBMCs by culturing with 100 ng/ml GM-CSF (Immunex) and 10 ng/ml IL-4 (R&D Systems). CD4+ and CD8+ T cells were positively selected from thawed PBMCs using magnetic selection according to the manufacturer's instructions (Miltenyi Biotec). The purity was routinely >90%. Tumor size was monitored every 2–3 d. Tumor volume (ellipsoid) was calculated as follows: $[(\text{short diameter})^2 \times \text{long diameter}]/2$. Tumor bearing humanized mice transferred with

autologous T cells, were injected intra-tumor with 100 μg/ml of curdlan at days 3, 6 and 9 post tumor implantation.

Binding Assay

CD8 T cells were sorted from DC-T co-culture and labeled with CFSE. Twenty thousand cells were put on acetone-fixed breast tumor sections and incubated at 37℃. After 1hr, the unbound cells were washed and fixed with 4% PFA for 10 min. The slides were treated with background buster for 30 min at RT, and then the sections were stained with cytokeratin and finally counterstained for 2 minutes with the nuclear stain DAPI.

T Cell Retention

The NOD/SCID/β2m−/− mice were subcutaneously injected with 10 million MDA-MB231 cells. CD8 T cells were sorted from DC-T co-culture and labeled with CFSE. Five hundred thousand cells were intra-tumoral injected into mice. After 3 days, the tumors were harvested freezing with OCT or homogenized with collagenase (2.5 mg/ml) digestion. Some groups of mice were left for tumor growth monitoring.

Microarray Analysis

Total RNA was purified using mirVana miRNA Isolation Kit (Invitrogen). RNA integrity was assessed using the Bioanalyzer 2000 (Agilent). Target labeling was carried out using the TargetAmp Nano-g Biotin-aRNA Labeling Kit for the Illumina System (Epicentre). Labeled RNA was hybridized onto HumanHT-12 v4 Expression BeadChips (Illumina). Illumina GenomeStudio version 1.9.0 software was used to subtract background and scale samples to the global average signal intensity.

CHAPTER FOUR

Results

Inflammatory Th2 Microenvironment in Breast Tumors

Earlier work from our lab found that breast cancer tumors are infiltrated with mature DCs. Mature DCs are often found in clusters with $CD4^+$ T cells, suggesting an ongoing immune response (Diana Bell et al., 1999). To understand the impact of these infiltrates on tumor biology, we are using a pilot cohort of 19 samples of primary breast cancer tumors revealed the secretion, upon activation with PMA and Ionomycin, of both type 1 (IFN-γ) and type 2 (IL-4 and IL-13) cytokines (Aspord et al., 2007). The current study extends the analysis to a total of 99 consecutive samples. As shown in figure 5, we found supernatants from tumor sites contained significantly higher levels of IL-2, type 2 (IL-4 and IL-13) and inflammatory (TNF-α) cytokines than those from macroscopically uninvolved surrounding tissue (Figure 5A).

To identify the cells producing these cytokines, analysis of single cell suspensions prepared from primary tumors demonstrated the presence of $CD4^+$ T cells that secrete IL-13 (Figure 5B), most of them co-expressing IFN-γ and TNF-α. A small fraction of $IL\text{-}13^+CD4^+$ T cells co-expressed IL-4 but none expressed IL-10. Through immunofluorescence staining on primary breast tumors, we confirmed that IL-13 was secreted by infiltrating $CD3^+$ T cells (Figure 5C). The Th2 responses can be subdivided into inflammatory Th2 cells that produce high levels of TNF but little IL-10, and conventional Th2 cells that produce little TNF but high levels of IL-10 (Liu et al., 2007).

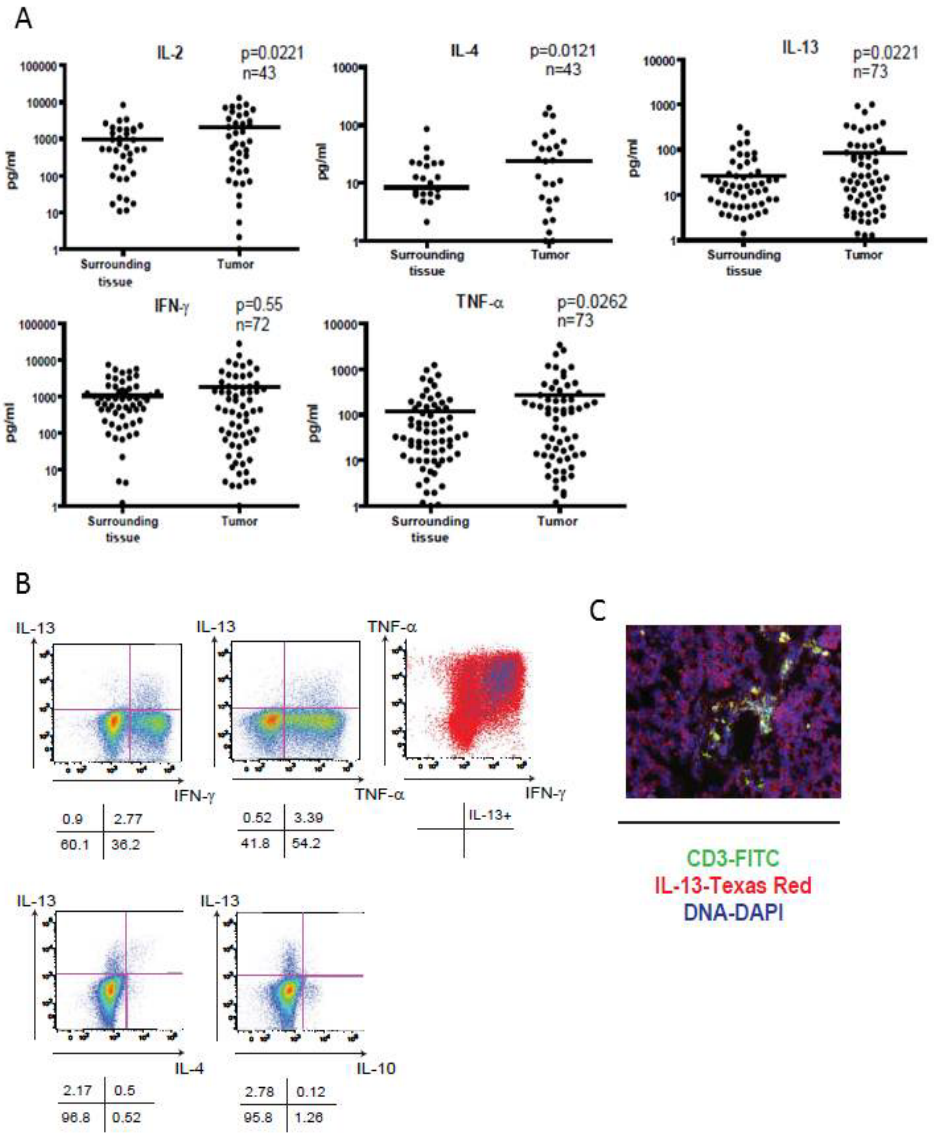

Figure 5. Inflammatory Th2 in breast cancer immune environment. (A) Primary breast tumor samples were received from Baylor University Medical Center. Cytokine profiles as determined by Luminex in supernatants of human breast tumor fragments stimulated for 16 h with PMA and ionomycin. Single points indicate the value of cytokine in the tumor supernatant from each patient. (B) Single-cell suspensions from tumor samples were stimulated for 5 h with PMA and ionomycin. Cytokine production was measured by flow cytometry. Dot plots are gated on viable $CD3^{+}CD4^{+}$ T cells. (top right dot plot) Blue indicates gate on CD3+CD4+IL-13+ T cells that coexpress IFN-γ and TNFα. Representative of four different patients from whom we have been able to obtain sufficient numbers of cells for 10-color analysis. (C) Frozen tissue sections from the same patient as in D were analyzed by immunofluorescence. Triple staining with anti-CD3 FITC (green), anti– IL-13–Texas red (red), and DAPI nuclear staining (blue). Bar, 90 μm.

Earlier studies have suggested that such T cells are driven by OX40L-expressing DCs that were exposed to TSLP.

TSLP is Expressed in Breat Cancer and Contributes to OX40L Induction on DCs and Th2 Cells Polarization Resulting in Tumor Progression

We further investigated the molecules which are involved in breast tumor progression. Microarray analysis of transcriptional profiles of mDCs exposed to breast cancer cell line supernatants demonstrated the upregulation of genes from the TNF family, including OX40L. OX40L signaling is known to induce inflammatory Th2 responses (Ito et al., 2005). We analyzed the presence of OX40L in primary breast cancers. Immunofluorescence staining of frozen tissue sections of primary breast cancer tumors showed the expression, in 57 out of 60 analyzed tumors, of OX40L by a majority of HLA-DR^{high} cells (Figure 6A). Flow cytometry analysis of single cell suspensions further confirmed the expression of OX40L by a fraction of HLA-DR^{high} CD14^{neg} CD11c^{high} mDCs (Figure 6B). Paired analysis demonstrated that the tumor beds express higher percentages of OX40L^{+} mDCs than the surrounding tissue ($p=0.0156$, $n=7$ paired samples, mean ± SE for surrounding tissue = 1.5% ± 0.8, $n=7$; and for breast cancer tumors 11% ± 1.67, $n=12$, respectively). Thus, breast cancer tumors are infiltrated with OX40L^{+} mDCs.

To identify the breast cancer tumor factor(s) which induce(s) OX40L on mDCs, LIN^{neg}HLA-DR^{+} CD123^{-}CD11c^{+} mDCs were sorted from blood of healthy volunteers and exposed to breast cancer supernatants. Fragments of primary tumors were sonicated, centrifuged, filtered and used in cultures with blood mDCs. As illustrated in Figure 6C**,** mDCs acquired OX40L. To determine the impact of OX40L on the generation of

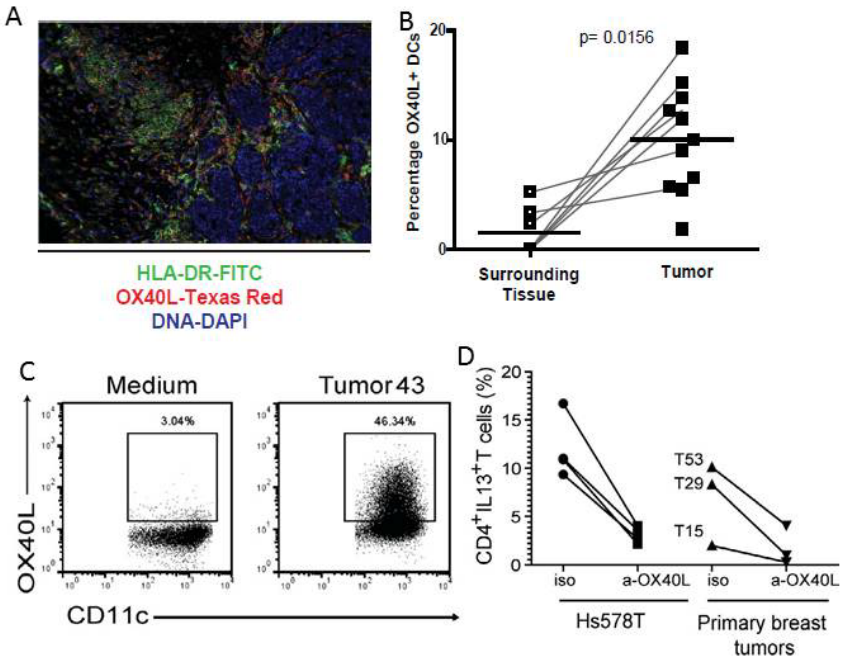

Figure 6. Breast cancer tumors produce soluble factors that induce functional OX40L expression on DCs. (A) Immunofluorescence of primary breast tumor with indicated antibodies. Bar, 180 µm. Representative of 57/60 tumors analyzed. (B) Primary breast tumors were digested with collagenase and single cells suspension were prepared for polychromatic flow cytometry analyzing $OX40L^+$ DCs. Single points indicate the percentage of OX40L+ cells in the cell suspension from each patient. (C) Myeloid DCs were purified from buffy coat of blood from healthy donors. DCs were cultured in medium or the presence of breast tumor (Tumor 43) sonicate supernatant. After 48 hrs, DCs were harvested to stain with OX40L. (D) mDCs were exposed for 48 h to supernatants of breast cancer cells Hs578T, and then co-cultured with allogeneic naive $CD4^+$ T cells in the presence of 40 µg/ml of anti-OX40L (Ik-5 clone) or isotype control antibody. After 1 wk, cells were collected and restimulated for 5 h with PMA/ionomycin for intracellular cytokine staining.

inflammatory Th2 responses in breast cancer, blood mDCs were first exposed for 48 hours to breast tumor soluble fractions. Exposed mDCs were then used to stimulate naïve allogeneic $CD4^+$ T cells with either the anti-OX40L antibody or a relevant isotype control. Blocking OX40L prevented the expansion of $IL13^+CD4^+$ or TNF^+CD4^+ T cells by 1) mDCs exposed to Hs578T breast cancer cells (n=4, median inhibition of $IL13^+CD4^+$ cells = 74%, range: 67-80%; Figure 6D), and 2) mDCs exposed to sonicates

of randomly selected primary breast cancer tumors. Breast cancer cells produce (a) factor(s) that activate mDCs and induce them to express OX40L and to elicit inflammatoryTh2 cells.

OX40L expression on mDCs can be induced by breast cancer cell-derived soluble factors. Studies have demonstrated that interaction between thymic stromal lymphopoietin (TSLP) and human DCs plays an essential role in evoking inflammatory Th2 responses through OX40 ligand expression on mDCs (Ito et al., 2005; Ziegler & Liu, 2006). TSLP, first isolated from a mouse thymic stromal cell line, is an IL-7-like cytokine (Liu et al., 2007; Ziegler & Liu, 2006). It is mainly secreted by fibroblasts, epithelial cells and stromal cells. The receptor for TSLP consists of 2 chains which are TSLPR and IL-7Ra chain.

All tested breast cancer cell lines expressed and secreted TSLP Supernatants of some primary breast cancer tumors stimulated with PMA and Ionomycin displayed up to 300 pg/ml TSLP (Appedix A). Importantly, TSLP is expressed in 35 out of 38 analyzed primary breast cancer tumors obtained from patients regardless of grade, histology or stage of analyzed tumors (Figure 7A). TSLP is also expressed in lung and kidney metastasis of MDA-MB-231 tumors in humanized mice (Figure 7B).

To determine the impact of blocking TSLP on the generation of inflammatory Th2 responses in breast cancer, anti-TSLP neutralizing antibodies to breast cancer tumor sonicate supernatant inhibited their ability to induce OX40L on mDCs (Figure 7C). Such mDCs displayed a diminished capacity to expand $IL13^{+}CD4^{+}$ or $TNF^{+}CD4^{+}$ T cells (n=3; median inhibition=73%, range: 72-77%) (Figure 7D and 8A). When anti-TSLP receptor

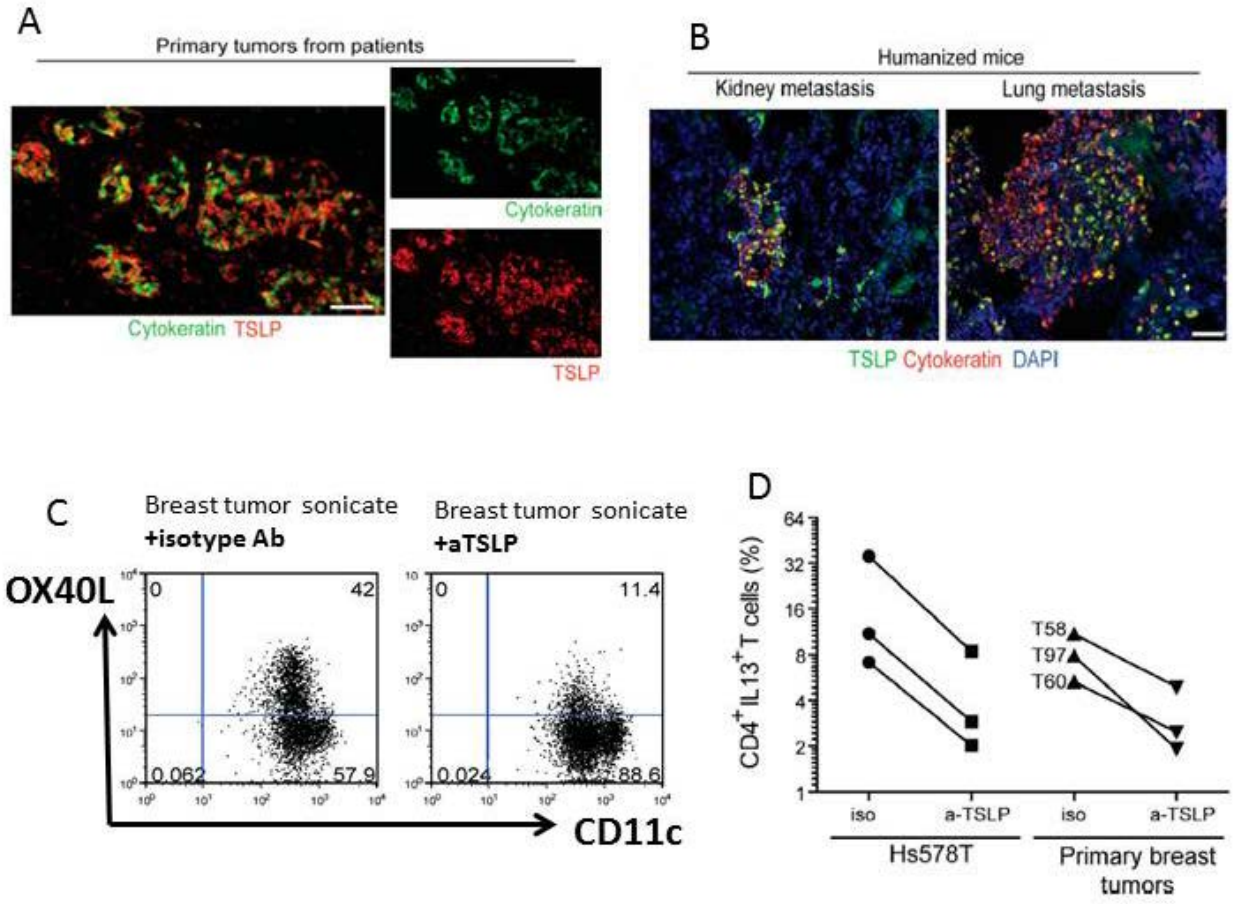

Figure 7. TSLP in breast cancer environment which contribute to OX40L and Th2 responses induction. (A) Frozen tissue sections from primary breast tumors from patients (38 patient samples) were analyzed by immunofluorescence for expression of TSLP. Staining pattern is representative of 35 out of 38 analyzed tumor samples from different patients. Bars:180 μm (B) NOD/SCID/β2m$^{-/-}$ mice were sublethally irradiated and transplanted with human CD34^{+} HPCs by intravenous injection. 4 wk after HPC transplant, 5 × 106 MDA-MB-231 breast cancer cells were implanted subcutaneously. Tumors at the site of implantation, as well as lungs and kidneys, were harvested at 3 mo after implant. Frozen tissue sections were analyzed by immunofluorescence for expression of TSLP (green) and cytokeratin (red). Staining pattern is representative of tumors from three different mice. Bar, 90 μm. (C) mDCs were incubated with soluble factors from sonicated human breast tumors in the presence or absence of 20 μg/ml of anti-TSLP (AB 19024; rabbit IgG). OX40L expression was measured by flow cytometry after 48 h of incubation. (D) mDCs treated as in C were co-cultured with naive allogeneic CD4+ T cells for 7 d. IL-13 production was measured by intracellular cytokine staining and flow cytometry after cells were restimulated for 5 h with PMA and ionomycin. Graph shows data from three independent experiments.

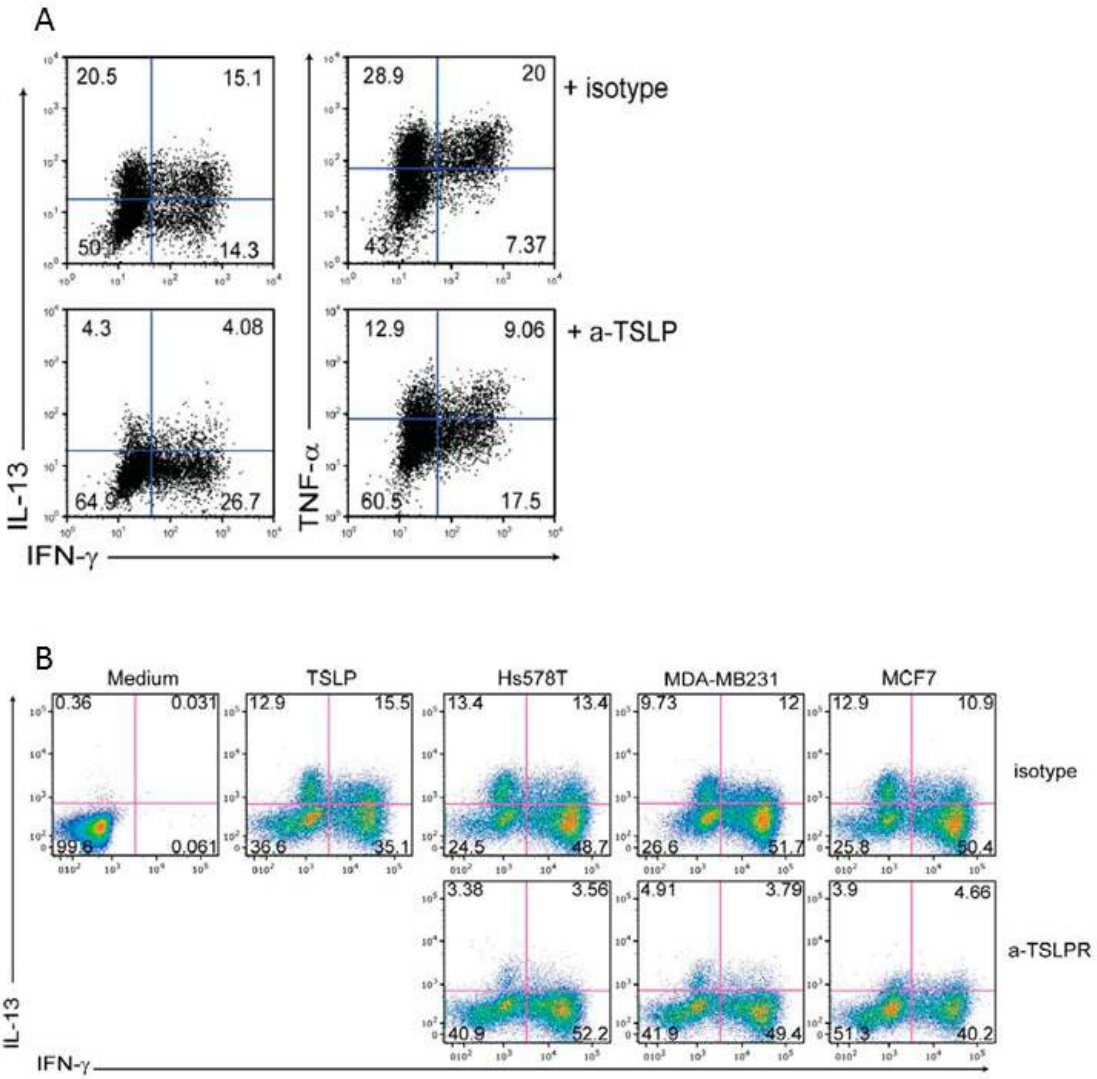

Figure 8. Blocking TSLP and TSLP-R in vitro. (A) mDCs treated as in A were cocultured with naive allogeneic $CD4^+$ T cells for 7 d. IL-13 production was measured by intracellular cytokine staining and flow cytometry after cells were restimulated for 5 h with PMA and ionomycin. Data are representative of three experiments. (B) mDCs were treated with anti TSLP-R (clone AB81_85.1F11, mouse IgG1), media or control antibody during activation with TSLP or with supernatant of one of the three different breast cancer cell lines (Hs578T, MDA-MB-231, and MCF7). mDCs were then cocultured with allogeneic naive $CD4^+$ T cells. After 1 wk, cells were collected, restimulated for 5 h with PMA and ionomycin, and analyzed by flow cytometry.

β chain (TSLPR) antibody was added to mDCs during their exposure to the supernatant

of three different breast cancer cell lines (Hs578T, MDA-MB231 and MCF7), resulting

mDCs showed a much diminished expansion of $IL13^+CD4^+$ T cells (Figure 8B). Thus, TSLP is the factor secreted by breast cancer cells which contributes to generation of inflammatory Th2 responses.

Our results thus far suggest a role for the TSLP-OX40L axis in generation of $IL13^+TNF^+CD4^+$ T cells but do not establish whether this axis might actually contribute to breast cancer tumor development. To address this question, humanized mice were reconstituted with both Hs578T cells, and T cells with or without anti-OX40L, anti-TSLPR and anti-TSLP neutralizing antibodies. As shown in Figure 9A, the administration of neutralizing anti-OX40L antibodies leads to significant inhibition of tumor development.

The administration of a neutralizing anti-TSLP antibody also results in the inhibition of tumor development (Figure 9B). TSLP blockade also leads to decreased secretion of IL-4 and IL-13 by tumor infiltrating T cells upon PMA and Ionomycin activation (APPENDIX). Finally, the administration of antibody blocking TSLPR nearly completely blocks tumor development driven by $CD4^+$ T cells (Figure 9C). These results indicate that the TSLP contributes to breast cancer pathogenesis.

Curdlan Dampens Inflammatory Th2 Response in Tumor Microenvironment and Inhibits Tumor Growth in vivo

The ideal immunotherapy aims to counter the immunosuppressive responses mastered by tumor cells, overcome protumoral immunity, induce specific immune responses such as Th1 responses and CTL mobilization, and to recruit natural killer cells

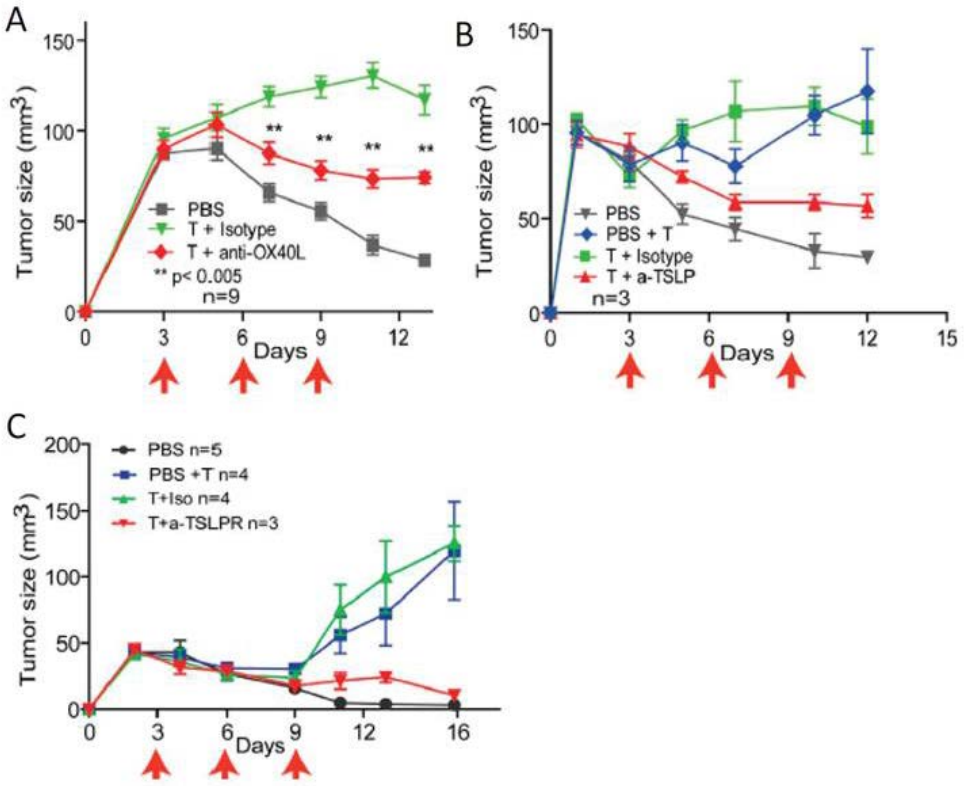

Figure 9. Blocking OX40L-TSLP in vivo. (A) NOD/SCID/β2m-/- mice were sublethally irradiated and transplanted with human CD34+ HPCs by intravenous injection. 4 wk after HPC transplant, 10×10^6 Hs578T breast cancer cells were implanted subcutaneously. 3, 6, and 9 d after, mice were reconstituted with autologous total T cells together with 200 μg per injection of blocking anti-OX40L or isotype control antibody (mouse Ig; red arrows). PBS group was injected with tumor cells but not with T cells (gray line). Tumor size was measured at indicated times. Mean values from three experiments representing nine mice per each condition. Anti-OX40L and isotype-treated cohorts were compared statistically. (B) NOD/SCID/β2m-/- mice were irradiated and implanted with 10×10^6 Hs578T breast cancer cells together with 200 μg per injection of neutralizing anti-TSLP (rabbit), rabbit isotype control antibody, or PBS. 3, 6, and 9 d after, mice were reconstituted with immature DCs and autologous total T cells together with 200 μg per injection of neutralizing anti-TSLP (rabbit), rabbit isotype control antibody or PBS. Representative of three indeendent experiments with a total of nine mice in TSLP blockade group. (C) Same as in B, but mice were injected with anti-TSLPR or isotype control at days 3, 6, and 9. Representative of two independent experiments. *n* indicates number of mice per cohort in this representative experiment.

and other innate immune components. Since DCs are known to drive the polarization of effector T cells, they may also serve as vectors to deliver tumor antigens that elicit

antitumor immune responses. Utilizing the DC activators to modulate the function of infiltrating DCs can give the potential to induce anti-tumor immune responses. β-glucan is reported as an immunomodulator which can induce both Th1 and Th17 responses against fungi. In the mammary tumor-bearing mice model, administration of anti-tumor monoclonal antibodies gives partial inhibition of tumor progression.

Combined with β-glucan administration could enhance the immunotherapy effect from monoclonal antibody and blocks tumors formation. The $CD4^+$ T cells from tumors treated with β-glucan show low IL-4 production and increase the $IFN\gamma^+$ CD4 T cells which indicates that β-glucan administration converts non-protective Th2 response to protective Th1 immunity and this may benefit to immunotherapy (Jarek Baran, 2007). The particulate form of β-glucan binds to dectin-1 on DCs and activates DCs through dectin-1 leading to enhance Th1 prolarization and the effector function of cytotoxic T lymphocytes (Kaoru Morikawa, 1985; B. Li et al., 2010; Salomé LeibundGut-Landmann, 2008; Sudhanshu Agrawal, 2010). The proliferation of antigen-specific T cells is also promoted by β-glucan administration (Qi et al., 2011).

We first evaluate whether β-glucan (curdlan) would affect breast tumor progression using our humanized mouse model bearing human breast cancer. The NOD/SCID/$\beta 2m^{-/-}$ mice were implanted with Hs578T breast tumor and reconstituted the immune cells with human monocyte-derived DCs, $CD4^+$ T cells and $CD8^+$ T cells with or without curdlan at 3, 6 and 9 days after tumor inoculation (Figure 10A). The tumor size was monitored. The tumors with human DCs and T cells injection grow larger indicating the breast tumor growth dependent on immune microenvironment, whereas with curdlan treatment inhibited tumor progression. (Figure 10B) The results were consistent in different donors

which we used for DC and T cells purification. For analyzing cytokine profile upon PMA/Ionomycin activation, the T cells in the tumor microenvironment secreted significantly lower IL-13 (DC+T: 1038±114.8 pg/ml; DC+T+curdlan: 361.1±62.22 pg/ml; n=23; $p<0.0001$) but similar levels of IFNγ (DC+T: 6880±1796 pg/ml; DC+T+curdlan:10669±2081 pg/ml; n=23; $p=0.1740$) And TNFα, IL-10 and IP-10 were also examined, whereas showing no significant differences between with or without curdlan treatment. The higher IL-17A (mean of DC+T group=104.1pg/ml; mean of DC+T+curdlan group=482.4pg/ml; $P<0.0001$) secretion from curdlan group was observed. (Figure 10C) These results demonstrated that curdlan treatment inhibits breast tumor growth in vivo which is due to diminishing Th2 responses.

Expansion of Inflammatory Th2 Cells were Diminished by Curdlan

To determine whether the modulation on DCs by curdlan reprograms T cells polarization, the blood sorted mDCs were first expose to curdlan and breast tumor (MDA-MB231) supernatant. These exposed DCs were harvested and co-cultured with allogenic naïve $CD4^+$ T cells for seven days. The cultured T cells were activated for 5 hrs with PMA/Iono and their cytokine profile was analyzed using intracellular cytokine staining (ICS) and flow cytometry. As expected, $CD4^+$ T cells exposed to DCs that had been pretreated with BCsups alone produced both IL-13 and TNF-α (22+3% of $CD4^+$ T cells). In contrast, T cells exposed to DCs treated with both BCsups and curdlan produced less IL-13 (6±0.3% of $CD4^+$ T cells; n=13; $p<0.0001$) (Figure 11A**)**. In both cases, CD4+ T cells produced IFN-γ (Figure 11A). Curdlan-treated DCs perform less capacity to expand IL-13^+TNFα^+ $CD4^+$ T cells but induce IL-17^+ T cells (Figure 11C). The secreted cytokines in the supernatant from DC-T co-culture were analyzed. $CD4^+$ T

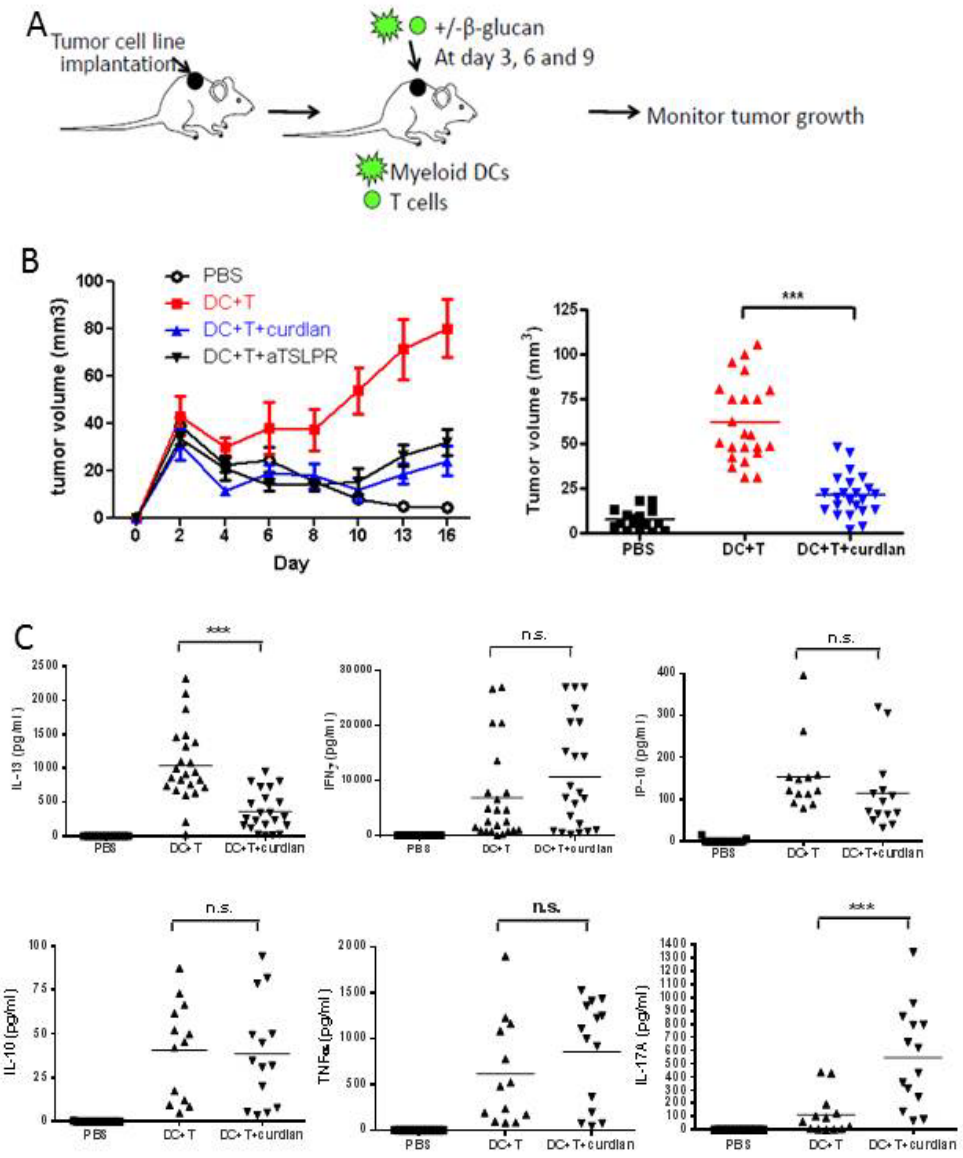

Figure 10. Curdlan blocks iTh2 in human breast cancer. (A) Scheme of in vivo experiment. (B) NOD/SCID/β2m$^{-/-}$ mice were irradiated the day before tumor implantation. Then mice were reconstituted with 1 million of monocyte derived DCs (MDDCs) and autologous T cells. β-glucan (Curdlan) (100ug/ml) or anti-TSLPR (200ug/mouse) was co-injected with DCs and T cells at days 3, 6 and 9 post tumor implantation. Tumor size was monitored every 2–3 d. Tumor volume (ellipsoid) was calculated as follows: [(short diameter)^2 × long diameter]/2. White circle: PBS, red: DC+T, blue: DC+T+curdlan, black: DC+T+aTSLPR. Mean value from five independent experiments representing 23 mice in each group. (C) Tumors were harvested on day 16 and stimulated with PMA/Ionomycin for 18 hrs. Supernatant was harvested and cytokines were detected by Luminex. Single points indicate the value of cytokine in the tumor supernatant from each mouse.

cells which co-culture with curdlan-treated DCs secrete less IL-13 but higher IL-17. The TNFα, IFNγ, IL-10 and IP-10 show no significantly differences (Figure 11B). The inflammatory Th2 microenvironment is proved that it can foster breast tumor growth (Pedroza-Gonzalez et al., 2011). The Th2 cytokines also promote the tumor growth of colorectal cancers. The colorectal cancer (CRC) cell line which express $STAT6^{high}$ show pro-Th2 cytokine profile and overgrow in xenograft in vivo model (B. H. Li et al., 2008).

It is known curdlan is a cell wall component derived from fungi or some kind of bacteria. It serves as a natural ligand for dectin-1. Dectin-1 is a C-type lectin and the phosphorylation of the second tyrosine residue in its cytoplasmic domain is known to induce further activation effects, such as activation of antigen presenting cells, induction of phagocytosis. It has been proposed that dectin-1 can act as a co-stimulatory molecule for T lymphocytes. It has been shown that DCs binding to T cells through dectin-1 lead to up-regulation of activation markers on T cells, IFN-γ production, and proliferation of both $CD4^+$ and $CD8^+$ T cells (Kaoru Morikawa, 1985; Sudhanshu Agrawal, 2010). Dectin-1 represents an ideal candidate for our approach. To assess the presence of dectin-1 in breast cancer microenvironment, the immunofluorescense staining analysis on breast tumor tissues revealed the presence of dectin-1^+ infiltrating cells which are mainly $CD11c^+CD20^-$HLA-DR^+CD83^+ mature DCs in peritumoral regions (Figure 12). It indicates that signaling immune cells through dectin-1 allows us to approach reprogramming in breast tumors.

Curdlan Inhibits OX40L Induction

In order to determine the mechanisms how curdlan modulates the immune microenviroment in breast tumors and inhibits breast tumor growth, we examined the

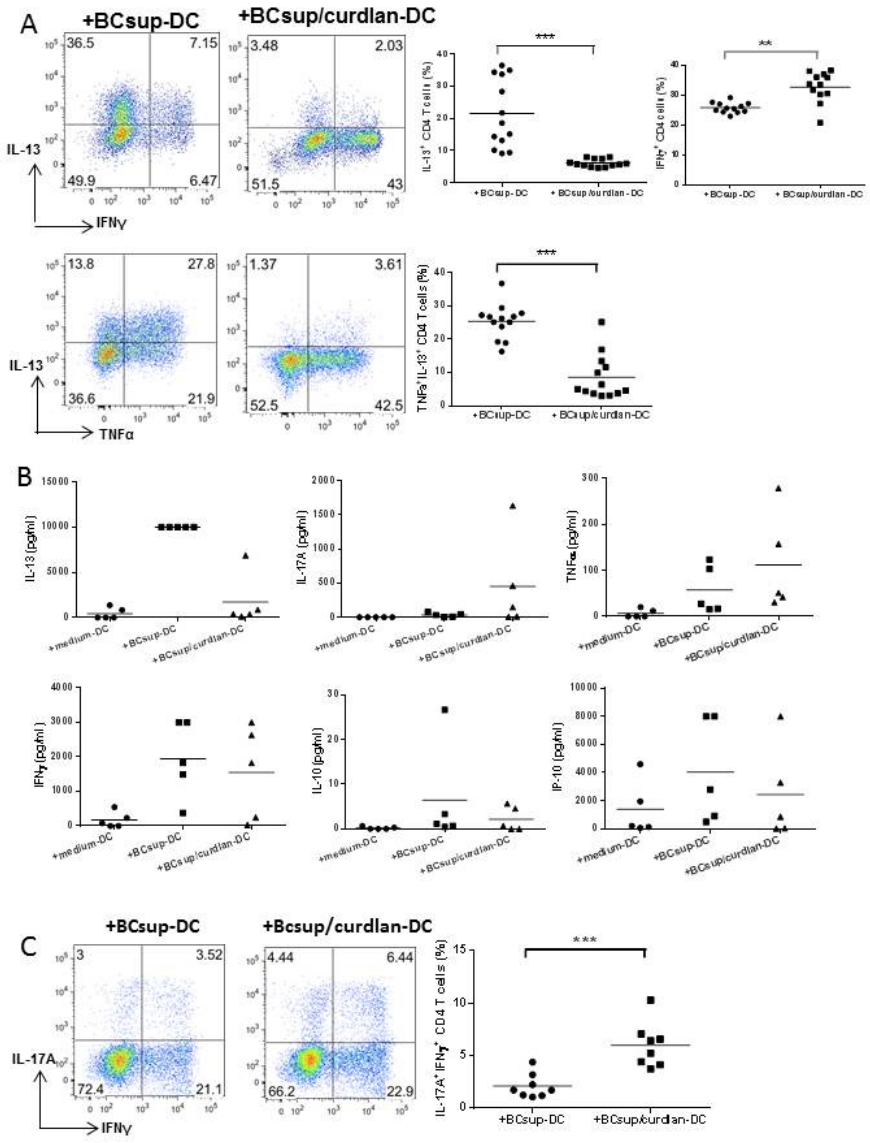

Figure 11. Curdlan blocks iTh2 in vitro. (A) Blood sorted mDCs (HLA-$DR^+/CD11c^+/CD123^-/Lin^-$) were pre-treated with 100ug/ml curdlan and activated by supernatant of a breast cancer cell line (MDA-MB231) for 48 hrs and then co-culture with allogenic naive $CD4^+$ T cells. After 7-day culture, cells were collected and re-stimulated for intracellular cytokines analysis. Summary of different experiments showing the effect of curdlan treatment in the induction of $IL\text{-}13^+$ or $TNFa^+IL\text{-}13^+$ secreting cells. Single points represent the percentage from individual experiment with mDCs from 13 different healthy donors. (B) Supernatant were harvested and analyzed cytokines secretion with Luminex. (C) Summary of different experiments showing the effect of curdlan treatment in the induction of $IL\text{-}17A^+IFN\gamma^+$ secreting cells. Single points represent the percentage from individual experiment with mDCs from 7 different healthy donors. Dot plot is the representative plot from 7 experiments.

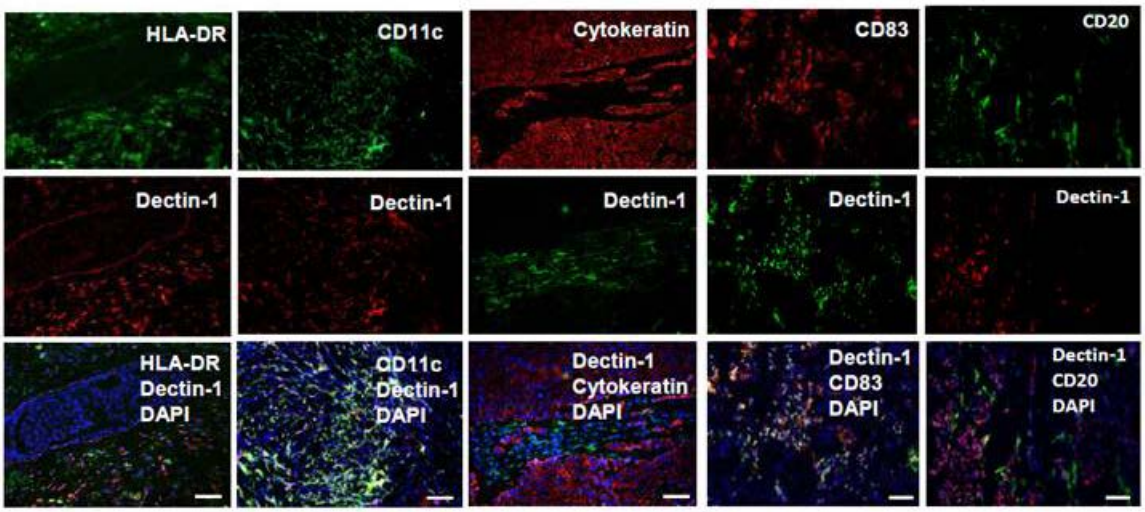

Figure 12. Immunofluorescence staining of dectin-1 on primary breast tumors. Immunofluorescence on frozen breast tumor tissue sections and stained with (left to right) Dectin-1 (red) and HLA-DR (green); Dectin-1 (red) and CD11c (green), Cytokeratin (red) and Dectin-1 (green); CD83 (red) and Dectin-1 (green). CD20 (green) and Dectin-1 (red). Representative of 27/27 tumors analyzed. Bar: 90µm.

Table 1. Breast tumor tissue for Dectin-1 staining.

	Diagnosis	Cancer grade	Cancer stage	ER	PR	Her2/ neu
T107	Invasive duct carcinoma, grade III	III		Not test		
T127	Infiltrating ductal carcinoma. Grade III. Stage IIB	III	IIB	diffuse, 3(+)	60%,3(+)	(-)
T135	In situ and invasive ductal carcinoma	III	IIA	Not test		
T151	Invasive ductal carcinoma w/ lobular features. Diagnosis	III	IIB	diffuse, 2(+)	50%, 2-3(+)	(-)
T153	Invasive ductal carcinoma.	III		diffuse, 2-3(+)	30%, 3(+)	(-)

Table Continues

	Diagnosis	Cancer grade	Cancer stage	ER	PR	Her2/ neu
T182	Invasive ductal carcinoma w/ focal lobular	II	IIB	2-3 (+), 100%	2-3 (+) 10% cancer	(-)
T195	Infiltrating ductal carcinoma	III	IIA	1-2(+), 10-15%	(-)	2(+), in 20% of cell
T241	Infiltrating ductal carcinoma, grade II, stage IIIA	II	IIIA	>95%, 2-3 (+)	>90%, 2-3 (+)	3 (+)
T254	Invasive ductal carcinoma	III	I	Not test		
T255	Invasive lobular carcinoma	II	IIA	3 (+), > 90%	(-)	(-)
T256	Invasive ductal carcinoma	III	IIA	3 (+)in>80% of tumor	2-3(+) in 60% cancer	2 (+) membran stain
T260	breast, Invasive ductal carcinoma,	III		(-)	(-)	1(+)
T261	breast, Invasive carcinoma of the breast ductal type	III		>75%, 3 (+)	(-)	1(+) 25-50% tumor
T264	breast, invasive ductal and lobular carcinoma	III	I	Not test		
T266	breast, Invisive ductal carcinoma, DCIS	III	I	Not test		
T270	sarcomatoid metaplastic carcinoma	III	IIB	(-)	(-)	(-)
T276	Breast: Invasive carcinoma of the breast, ductal type,	III	I	75%, 3(+)	>75%, 2-3(+)	high, (>20%,up to75%)
T279	Breast: Invasive carcinoma of the	II	IIB	Not test		
T281	Invasive carcinoma of the breast, ductal type;	II	IIB	>75%, 3(+)	25-50%, 2-3(+)	(-), focal 1(+)

Table Continues

	Diagnosis	Cancer grade	Cancer stage	ER	PR	Her2/ neu
T282	Multifocal invasive carcinoma of the breast		IIIA	Not test		
T286	In situ and invasive lobular carcinoma	III	I	Strong, >85%	(-) in most area	(-)
T288	Invasive carcinoma of the breast, ductal type	III	IIA	(-)	(-)	Not test
T291	Invasive carcinoma of the breast, ductal type	II	IIA	(-)	(-)	(-)
T294	Invasive ductal carcinoma	III	IIA	3(+), 80%	3(+), <1%	3(+), 90%
T296	Invasive ductal carcinoma	III	IIA	3(+), >75%	(-)	(-)
T298	Invasive carcinoma of the breast, ductal type	III	IIA	>75%, 3(+)	25-50%, 2-3 (+)	(-)

Table 2. Primary breast tumor samples were received from Baylor University Medical Center. The combined histologic grading system, including nuclear grade, tubule formation and mitotic rate, and staging system (according to tumor size, invasive or not, lymphoid node involvement, and spread out or not) were applied according to pathologist's report after surgery. Receptor status: ER/PR positivity, HER2 overexpression is indicated. NA, not available. NT, not tested.

effects on mDCs by curdlan. Because inflammatory Th2 response is generated from OX40L signal, the impact of OX40L expression after curdlan treatment is examined. The human myeloid DCs were purified from healthy donors and treated with curdlan in prior to activation by breast tumor (MDA-MB231) supernatant. The DCs after 48hrs activation in breast tumor supernatant express OX40L and the OX40L induction is inhibited by curdlan treatment (breast tumor-treated DCs=25±2%; n=10; breast tumor-treated DCs+curdlan=6±1.1%, n=10; $P<0.0001$) (Figure 13A). In order to confirm if the curdlan indeed inhibits TSLP-mediated OX40L induction, the sorted mDCs were treated

with TSLP (20ng/ml) and the DCs expressed OX40L but inhibited by curdlan pre-treatment (Figure 13B). The addition of anti-dectin-1 antibodies to DCs before curdlan treatment allowed OX40L expression by DCs exposed to breast cancer supernatant. (Figure 13C) The role of dectin-1 in curdlan mediated prevention of tumor development is further demonstrated by experiments in vivo. There, adding anti-dectin-1 antibodies to developing breast cancer tumors blocks the protective effect of curdlan (Figure 13D). Thus, curdlan acts via dectin-1 in this system. Blood DCs express dectin-1 and accumulate dectin-1 at the sites of binding to fluorescence-labeled curdlan (Figure 13E). These results further corroborate the finding that curdlan acts through dectin-1 in breast cancer.

To see the reprogramming effect, the $OX40L^+$ DCs and $OX40L^-$ DCs were sorted separately. The $OX40L^+$ DCs were further treated with or without curdlan for 24hrs. The DCs were harvested to co-culture with allogenic total T cells and the ICS was performed to determine the T cell polarization. As expected, $OX40L^+$ DCs induced T cells to express IL-13 while $OX40L^-$ DCs did not. Treatment of $OX40L^+$ DCs with curdlan altered their T cells polarization pattern as no IL-13 production was induced (Figure 14). Thus, curdlan blocks the development of human breast cancer by altering $CD4^+$ T cell immunity via modification of the phenotype and function of tumor-conditioned DCs.

Curdlan Modulates the Phenotype and Function of mDCs in Breast Tumor Microenvironment

The phenotypes and cytokines secretion were examined. DCs treated with breast cancer supernatant and curdlan express high levels of maturation and activation markers such as CD83, CD80, CD86, CD70 and MHC class I indicating that curdlan does not block DC maturation (Figure15A).

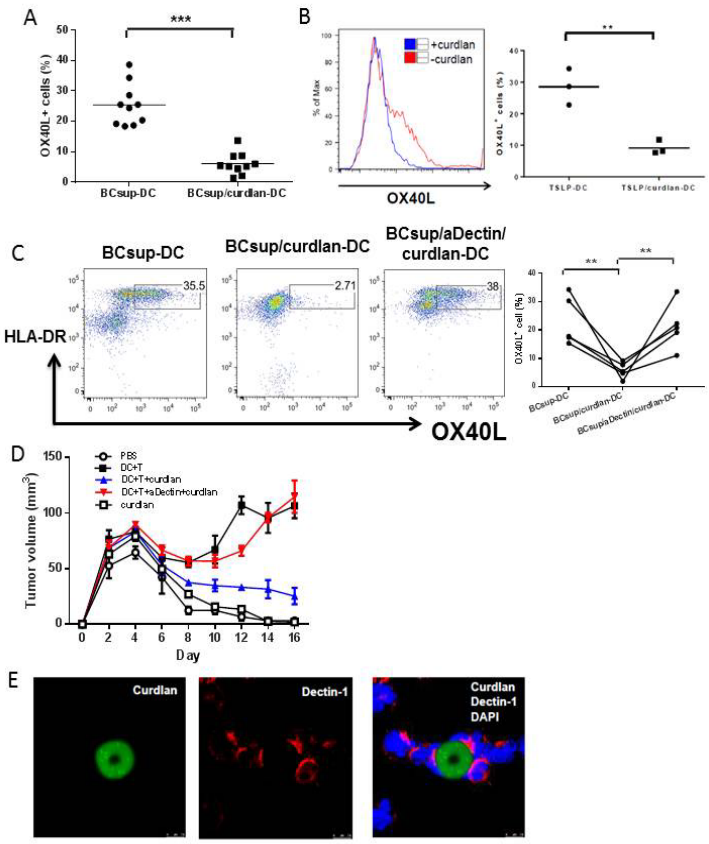

Figure 13. Curdlan modulates mDCs maturation in breast cancer via dectin 1. (A) Myeloid DCs were purified from buffy coat of blood from healthy donors. DCs were cultured in the presence of tumor derived products. The curdlan (100ug/ml) treatment is 3min at room temperature prior to adding tumor supernatant. After 48 hrs, DCs were harvested to stain with OX40L. The percentage of $OX40L^+$ cells was summarized. Single point indicates the percentage of $OX40L^+$ cells from 10 individual experiments. (B) Myeloid DCs were purified from buffy coat of blood from healthy donors. DCs were cultured in the presence of TSLP (20ng/ml). The curdlan (100ug/ml) treatment is 3min at room temperature prior to adding tumor supernatant. After 48 hrs, DCs were harvested to stain with OX40L. The percentage of $OX40L^+$ cells was summarized. Single point indicates the percentage of $OX40L^+$ cells from 3 individual experiments. (C) mDCs were pre-treated with anti-Dectin1 neutralizing antibody, following by curdlan and tumor supernatant. OX40L expression on DCs was analyzed. Representative dot plot of 4 individual experiments. Each curve indicates individual experiment. (D) Hs578T-bearing NOD/SCID/β2m−/− mice were reconstituted with monocyte derived DCs (MDDCs) and autologous T cells. β-glucan (Curdlan) (100ug/ml) or aDectin plus curdlan was co-injected with DCs and T cells. Tumor size was monitored. White circle: PBS, black: DC+T, blue: DC+T+curdlan, red: DC+T+aDectin+curdlan, white square: curdlan. (E) Blood sorted DCs were treated with DTAF-curdlan for 30min. The DCs were harvested and put on slides with cytospin fixing with cold methanol. Dectin1 was stained and conterstained with DAPI and acquired with confocal microscope. Green: curdlan; Red: Dectin1; Blue:DAPI.

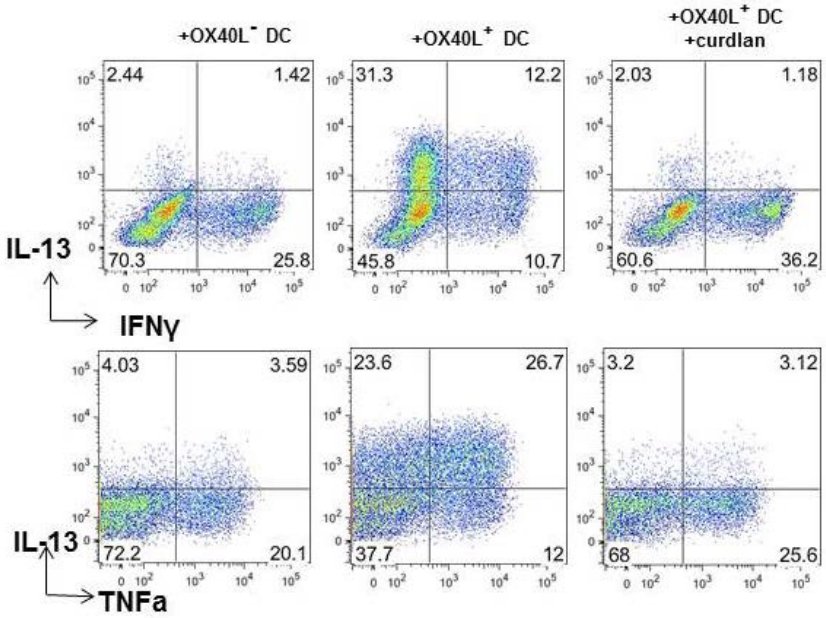

Figure 14. . Curdlan reprograms OX40L expression on mDCs. Blood sorted mDCs were 48hr exposed to BCsup. $OX40L^+$ or $OX40L^-$ DCs were sorted. $OX40L^+$ DCs were treated with/without curdlan for 24 hrs and co-culture with allogenic naïve total T cells. After 7-day culture, cells were collected and re-stimulated for intracellular cytokines analysis.

Signal transducers and activators of transcription (STAT) proteins are cytoplasmic transcription factors which are involved in the signal transduction in regulation the production of cytokines, hormones and growth factors. Cell survival, proliferation and differentiation are also the cellular processes that can be controlled by the activation status of STATs. It is believed that modification of STAT proteins could have the therapeutic effect on tumors. In the breast tumor microenvironment, it is proved that the infiltrating $CD4^+$ T cells mainly polarize toward Th2 responses. OX40L is transcribed in DCs upon STAT5 and STAT6 phosphorylation. Furthermore, we have shown that STAT6 is activated in breast cancer microenvironment, both in the leukocyte infiltrate and in cancer cells (Aspord et al., 2007). STAT6 is known as a key factor in Th2 cell polarization. Phosphorylation of STAT6 can lead to enhance the production of type 2 cytokines, IL-4 and IL-13. However, phosphorylation of STAT4 is critical in Th1 cell

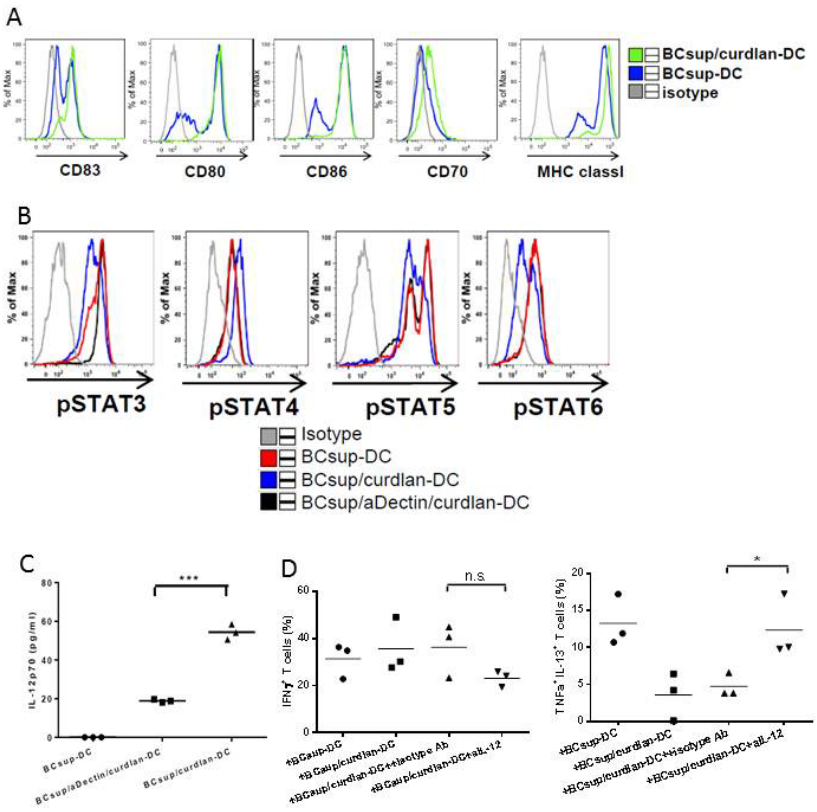

Figure 15. Curdlan modulates mDCs phenotype in breast cancer. (A) DCs were purified from buffy coat of blood from healthy donors. DCs were cultured with medium alone or in the presence of tumor derived products. The curdlan treatment is 3min at room temperature prior to adding tumor supernatant. After 48 hrs, DCs were harvested and washed. The stimulated cells were staining for phenotype (CD83, CD80, CD86, CD70, MHC classI). Grey: isotype; blue: BCsup-DC; green: BCsup/curdlan-DC (B) Blood sorted mDCs were harvested after 1 hr incubation with curdlan, stained as indicated and analyzed with flow cytometry. Grey: isotype; red: BCsup-DC; blue: BCsup/curdlan-DC; black: BCsup/aDectin/curdlan-DC. Representative histogram of 4 individual experiments. (C)The supernatant from DC culture was collected for IL-12p70 Luminex. Single points indicate individual experiment. (D) anti-IL-12 neutralizing antibody was used to pre-treat the curdlan/BCsup-DCs prior to their co-culture with allogenic naïve T cells. ICS at day 7, 3 experiments. (antibody was used to pretreat the DCs. After 48 hrs, DCs were harvested and co-culture with allogenic naïve T cells. After 7 days co-culture, intracellular cytokine staining was performed (IL-13, IFNg and TNF). The percentage of $IFNg^{+}$ T cells and $TNFa^{+}IL\text{-}13^{+}$ T cells were summarized from 3 experiments.

differentiation which may be due to pSTAT4 induce the signals for IL-12 production and increase the capacity of IFNγ secretion (Vahedi et al., 2012). Therefore, the STAT4 and STAT6 phosphorylation in DCs were examined. The mDCs were activated in breast

tumor supernatant for 1hr and harvested. The DCs treated with β-glucan increase pSTAT4 and reduce pSTAT6 which finally increase the ratio of pSTAT4/pSTAT6. (Figure 15B) It demonstrated the potential of these DCs to redirect T cells polarization. Accordingly, curdlan-treated DCs secreted substantially higher amounts of IL-12p70 which could be inhibited by adding dectin-1 neutralizing antibodies (Figure 15C). As expected, adding IL-12 neutralizing antibodies to the co-culture of DCs and naïve T cells restored generation of iTh2 cells (Figure 15D). Thus, curdlan allows reprogramming of the breast cancer microenvironment via blockade of STAT6 in tumor-conditioned DCs which enables activation of STAT4 and IL-12 production leading to Th1 response.

To further delineate the impact of dectin-1 ligation on tumor-conditioned DCs, we analyzed transcriptional profiles of BCsup-DCs that have been exposed or not to curdlan. Curdlan treated BCsup-DCs over-expressed 314 transcripts and under-expressed 873 transcripts. Ingenuity pathway analysis (IPA) of the 314 transcripts revealed abundance of transcripts forming network centered on NF-κB, IL-6 and TNF. Up-regulated genes are with TNF, JUN/IL12/IL15 and NFKB/IFN network. Curdlan-exposed DCs showed abundant transcription of DC maturation markers such as *CD86* and *TNFSF9* (4-1BBL); cytokines such as *IL-12, IL-15 and IL-23;* and several molecules possibly facilitating their migration including high transcription of matrix metalloproteinase 7 (MMP7). The latter one might facilitate DC migration to the draining lymph nodes, a feature that appears blocked in breast cancer infiltrating DCs. Conversely, curdlan-exposed DCs under-expressed *CD14* and *CD68* both of which are associated with an immature and non-committed DCs phenotype. In addition, *CCR6* which could contribute to immature DC retention at the tumor site by binding to MIP3-α as we have shown previously, was

also under-expressed consistent with DC maturation. Because in the presence of curdlan the DCs cannot any longer respond to TSLP, the maturation program is likely driven by *GM-CSF*, *IL-6* and *TNF* triggered by curdlan exposure. Whereas the molecular mechanism allowing the blockade of iTh2 will need to be confirmed, two genes stand as candidates, *Notch 2* and *IL1F9 (IL-36γ).* Indeed, in the mouse, DC-specific deletion of the Notch2 receptor causes a reduction of DC populations in the spleen (Lewis et al., 2011). Furthermore, Notch signaling plays a critical role in repressing TSLP production in keratinocytes, thereby maintaining integrity of the skin (Radtke & Raj, 2003). IL-36 receptor pathway is involved in the regulation of IFN-γ secretion by $CD4^+$ T cells and Th1 responses (Solenne Vigne, 2012) and IL-36γ has been recently shown as downstream of dectin-1/Syk signaling pathway upon exposure to *Aspergillus Fumigatus* (Gresnigt et al., 2013). Thus, curdlan exposure in the presence of soluble tumor factors leads to phenotype switch and enables DC commitment to maturation phenotype associated with enhanced capacity to leave tumor beds and migrate to lymphoid tissues as well as induce IFN-γ secreting $CD4^+$ T cells. (Appendix B)

TLR7/8 Agonists, CL-075, Modulate Function of mDCs Leading to Inhibition Inflammatory Th2 Responses in vitro and in vivo and Blocks Breast Tumor Progression

It is known several agonists against Toll-like receptors (TLR) were also immunomodulators (Medzhitov, 2009). We were interested in if the TLR ligands can perform the same effects as curdlan. Here we pre-treated sorted mDCs with TLR7/8 agonists, CL-075 (1ug/ml), and then conditioned with breast tumor (MDA-MB231). supernatant. The DC phenotype and cytokine production were examined. CL-075 treatment inhibits OX40L induction (Figure 16A) and upregulates IL-12p70 secretion (Figure 16B). The DCs were also co-cultured with allogenic naïve T cells. Cytokines

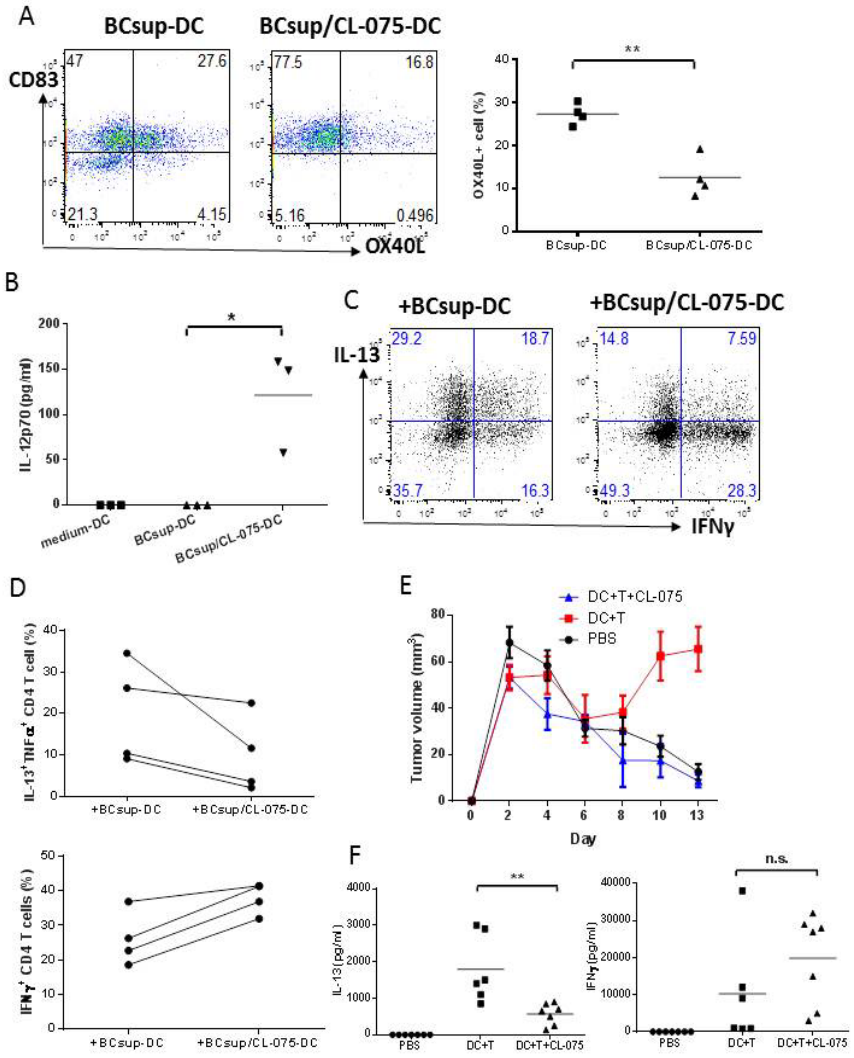

Figure 16. TLR7/8 L (CL-075) effect in vitro and in vivo. (A) Blood sorted mDCs were pretreated with CL-075 (1ug/ml) and breast tumor supernatant were added. After 48 hrs, DCs were harvested and stained with OX40L and CD83. The percentage of $OX40L^+$ cells was summarized. Single point indicates the percentage of $OX40L^+$ cells from 4 individual experiments. (B) Supernatant was harvested and IL-12p70 was analyzed. (C) DCs were harvested and co-culture with allogenic naïve T cells in 1:5 ratio. After 7 days co-culture, intracellular cytokine staining was performed (IL-13, IFNg and TNF). (D) The percentage of $IFNg^+$ T cells and $TNFa^+IL\text{-}13^+$ T cells were summarized from 4 experiments. (E) NOD/SCID/β2m−/− mice were sublethally irradiated the day before tumor implantation. Then mice were reconstituted with 1 million of monocyte derived DCs (MDDCs) and autologous T cells. CL-075 (1ug/mouse) was co-injected with DCs and T cells at days 3, 6 and 9 post tumor implantation. Tumor size was monitored every 2–3 d. Tumor volume (ellipsoid) was calculated as follows: $[(\text{short diameter})^2 \times \text{long diameter}]/2$. (F) Tumors were harvested on day 14 and stimulated with PMA/Ionomycin for 18 hrs. Supernatant was harvested and cytokines were detected by Luminex.

production from T cells was detected through intracellular cytokine staining. It shows less IL-13^{+}CD4^{+} T cells from the T cells co-cultured with CL-075-DCs. (Figure 16C and 16D)

In vivo system, NOD/SCID/β2m$^{-/-}$ mice were reconstituted the immune cell with human monocyte derived DCs and autologous CD4 and CD8 T cells. CL-075 (1ug/mouse) was co-injected with DCs and T cells. Tumor size was monitored (Figure 16E). Tumors were harvested on day 14 and stimulated with PMA/Ionomycin for 18 hrs. Supernatant was harvested and cytokines were detected by Luminex (Figure 16F). CL-075 treatment inhibits tumor progression and the tumors contain less IL-13 and more IFNγ.

Curdlan-Treated DC Promotes CD8 Function and Retention

From the microarray analysis, curdlan exposure of BCsup-DCs resulted in the enhanced transcription of *IL-15, IL15-RA* and *4-1BBL*, molecules that are known to play important role in generation of high avidity CD8^{+} effector T cells facilitating cancer rejection. It is shown that IL15-DC promote stronger CD8 T cells proliferation and membrane-bound IL-15 contribute in more efficiently CD8 T cells priming and tumor antigen-specific CTL responses (Dubsky et al., 2007). In the research of TIL therapy, with anti-4-1BB could increase the percentage of CD8 in the preparation and induced higher frequency of perforin and granzyme B suggesting the better killing activity of CD8 T cells when providing the signals through 4-1BBL/4-1BB (Chacon et al., 2013). Flow cytometry result shows the upregulated of IL-15, IL-15R and 4-1BBL expression on curdlan treated-DCs. (Figure 17A)

This led us to question whether reprogramming of the breast cancer microenvironment by curdlan could also lead to changes in the $CD8^+$ T cell compartment. As $CD8^+$ T cells are essential effectors of anti-tumor immunity, naïve allogeneic $CD8^+$ T cells were co-cultured with BCsup-DCs, exposed or not to curdlan. ICS at day 7 revealed that $CD8^+$ T cells cultured with BCsup-DCs produce, upon PMA/Iono restimulation, IL-13 (+BCsup-DC: 23±1.3%; n=9), IFN-γ and TNF (Figure 17B), indicating a partial Type 2 polarization. However, $CD8^+$ T cells cultured with curdlan-treated BCsup-DCs displayed a Type 1 phenotype with few IL-13-producing $CD8^+$ T cells (+BCsup-DC: 23±1.3%; +BCsup/curdlan-DC: 2±1%; n=9; $p<0.0001$), and predominantly IFN-γ-producing CD8+ T cells (+BCsup-DC: 53±1%; +BCsup/curdlan-DC: 68±1.6%; n=9; $p<0.001$) (Figure 17B). $CD8^+$ T cells cultured with BCsup-DCs expressed high levels of perforin but low levels of granzymes (Gzm) A and B (Figure 17C). Similarly to monocyte-derived DCs, curdlan exposed BCsup-DCs allowed the generation of $CD8^+$ T cells expressing high levels of Gzm A and B (Figure 17C). Thus, curdlan enables DCs exposed to breast cancer microenvironment to generate $CD8^+$ T cells expressing a broad array of effector molecules facilitating cancer rejection. We then wished to establish whether dectin-1 was involved in the functions of curdlan-treated DCs on $CD8^+$T cells. Thus, DCs were exposed to curdlan in the presence of anti-dectin-1 neutralizing antibody. As illustrated in Figure 17C, these DCs induced the differentiation of $CD8^+$ T cells that expressed lower levels of effector molecules.

DCs were exposed to breast cancer supernatants with and without curdlan and then co-cultured with CFSE-labeled naïve allogeneic T cells. Proliferating CFSE-negative $CD8^+$ T cells were sorted at day 6 and injected into breast cancer tumors established in

immunodeficient mice. At day 3 post-injection, $CD8^+$ T cells generated by curdlan-treated DCs persisted in the breast cancer microenvironment and could be detected in

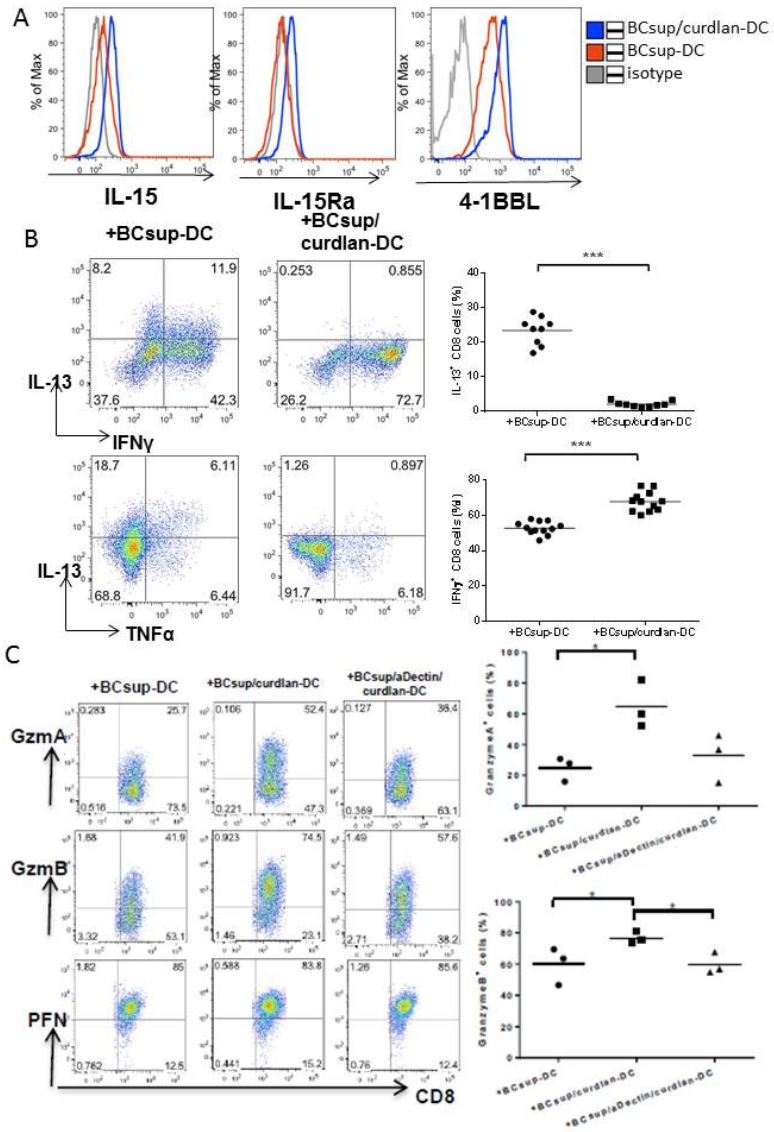

Figure 17. Curdlan enables mDCs in breast cancer to generate $CD8^+$ T cells express effector molecules. (A) Blood sorted mDCs were pre-treated with curdlan and activated by BCsup for 48 hrs. DCs were harvested and washed. The stimulated cells were stained for phenotype (IL-15, IL-15Ra and 4-1BBL) (B) Curdlan/BCsup-DCs were co-cultured with allogenic naïve T cells. ICS at day 7 on gated Aqua-CD3+CD8+ T cells. Summary of 9 individual experiments. (C) Expression of Granzyme A, Granzyme B and perforin.

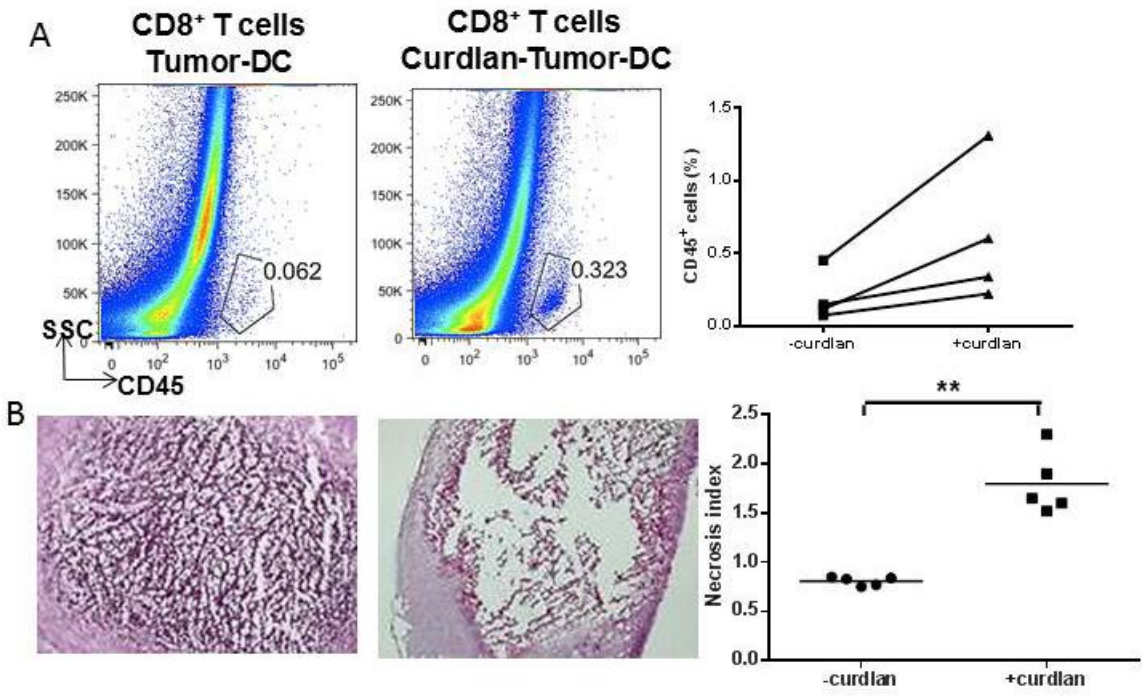

Figure 18. Curdlan enables mDCs in breast cancer to generate CD8+ T cells able to retain and reject tumors. (A) $CD8^+$ T cells were sorted from in vitro culture and intratumoral injected into NOD-SCID mice bearing breast tumor (MDA-MB231). Tumors were harveseted and the single cell suspension were stained with CD45 and analyzed by flow cytometry. The percentage of $CD45^+$ cells was summarized from 4 individual experiments. (B) Frozen sections from the tumors were used for H&E staining. The necrosis level is rated and calculated with each region. Summary of Points x areas/total area in each section=necrosis index. Necrosis index from 5 sections were summarized.

substantially higher numbers compared to $CD8^+$ T cells generated by breast cancer supernatant treated-DCs without curdlan (Figure 18A). $CD8^+$ T cell persistence was associated with tumor necrosis (Figure 18B**).**

To control tumor in vivo, the expression of effector molecules such as Gzms by $CD8^+$ T cells is necessary but not sufficient. Indeed, the accumulation and persistence of $CD8^+$ T cells in cancer nests is also critical for cancer rejection. CD103 integrins allow the

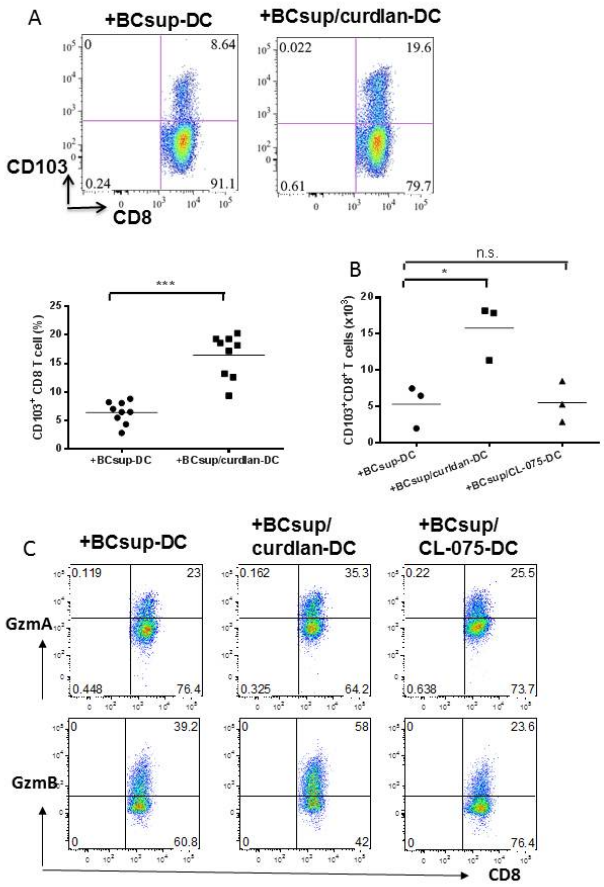

Figure 19. CD103 induction on CD8 T cell co-cultured with BCsup/curdlan-DC but not BCsup/CL-075-DC. (A) Blood sorted mDCs were pre-treated with curdlan and activated by BCsup for 48 hrs and co-culture with allogenic naïve T cells. After 6 days, cells were collected and stained with CD103. CD103 expression on CD8 T cells was summarized from 7 individual experiments. (B) Blood sorted mDCs were pre-treated with curdlan or CL-075 and activated by BCsup for 48 hrs and co-culture with allogenic naïve T cells. After 6 days, cells were collected and stained with CD103. CD103 expression on CD8 T cells was summarized from 3 individual experiments. (C) Blood sorted mDCs were pre-treated with curdlan and activated by BCsup for 48 hrs and co-culture with allogenic naïve T cells. After 7-day culture, cells were collected and stained with GranzymeA and GranzymeB.

retention of effector and memory T cells in epithelial via binding to their ligand E-cadherin on epithelial cells (Le Floc'h et al., 2011; Le Floc'h et al., 2007; Schön MP,

1999; William W Agace & Parker, 2000). DCs exposed to curdlan showed an increased ability to induce CD103 on $CD8^+$ T cells (Figure19A). However, if the DCs were treated with CL-075 but not β-glucan, they did not have the ability to induce CD103 expression on CD8 T cells. (Figure 19B) And the effector molecules, GzmA and GzmB, on CD8 T cells were not induced by CL-075 treated-DCs. (Figure 19C)

To assess whether these $CD103^+CD8^+$ T cells adhered to breast cancer cells, we used a modified Stamper-Woodruff tissue binding assay (Diana Bell et al., 1999). Proliferating CFSE-negative allogeneic $CD8^+$ T cells were sorted from co-cultures with DCs, re-labeled with CFSE (green) and overlaid on frozen breast cancer tissue sections to allow adherence. After a 60-minute contact, tissue sections were washed and counter-stained with anti-cytokeratin mAbs (red) to visualize the cancer cells. Numbers of bound T cells per 0.15 mm^2 $cytokeratin^+$ areas were assessed using a series of consecutive tissues sections. $CD8^+$ T cells exposed to curdlan-treated DCs adhered significantly more to frozen breast cancer tissue sections (Figure 20A) (+BCsup-DC: 7±1; +BCsup/curdlan-DC: 26±2; n=20; $p<0.0001$) and blocking CD103 with a monoclonal antibody decreased their numbers (Figure 20B) (+BCsup/curdlan-DC+isotype Ab: 22±3; +BCsup/curdlan-DC+aCD103: 2±0.5; n=20; $p<0.0001$). The binding of $CD8^+$ T cells to breast cancer tissue sections was also decreased when BCsup-DCs were pre-treated with anti-dectin-1 antibody prior to curdlan (Figure 20C) (+BCsup/curdlan-DC:32±4; +BCsup/aDectin/curdlan-DC: 15±3; n=10; $p=0.003$). Thus, curdlan exposure enables DCs to expand $CD103^+CD8^+$ T cells in a dectin-1-dependent manner.

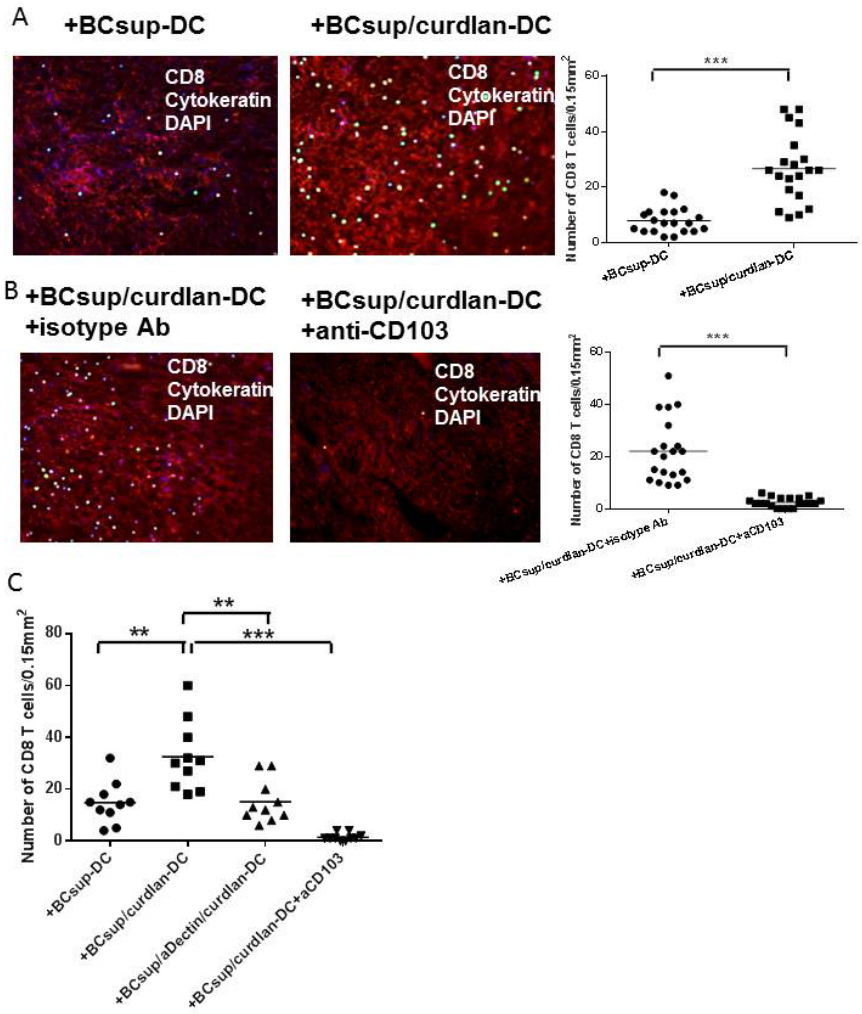

Figure 20. CD8 T cells which co-cultured with BCsup/curdlan-DC show better capacity binding to breast tumor sections. (A) CD8 T cells were sorted from DC-T coculture and labeled with CFSE for Stamper-Woodruff assays on breast tumor sections. The sections were fixed and stained with cytokeratin (red). The CD8 T cells (green) were counted in each 0.15 mm^2 $cytokeratin^+$ area. Twenty fields were counted from two individual breast tumor sections. (B) The T cells were pre-incubated with anti-CD103 or isotype antibodies and then incubated on breast tumor sections. The sections were fixed and stained with cytokeratin. The CD8 T cells (green) were counted in each 0.15 mm^2 $cytokeratin^+$ area. Twenty fields were counted from two individual breast tumor sections. (C) CD8 T cells were co-cultured with DCs which were pre-treated with anti-Dectin1 neutralizing antibody, following by curdlan and BCsup. CD8 T cells were sorted from DC-T coculture and labeled with CFSE for Stamper-Woodruff assays on breast tumor sections. The sections were fixed and stained with cytokeratin. Summary of the number of CD8 T cells each 0.15 mm^2 $cytokeratin^+$ area. Ten fields were counted from two individual breast tumor sections.

To establish how DCs enabled induction of CD103 expression in $CD8^+$ T cells, we analyzed the role of TGF-β1 as it induces CD103 expression on T cells (Parker CM, 1992). Accordingly, TGF-β1-neutralizing antibodies substantially reduced the ability of curdlan-treated DCs to induce the differentiation of $CD103^+CD8^+$ T cells (Figure 21A). The involvement of TGF-β1 was further confirmed by pharmacological blockade of TGF-β1 using TGF-β RI kinase inhibitor II (Ito et al., 2008) in DC-T cocultures (Figure 21A). Transcriptional profiling revealed that curdlan exposure enables over-expression of *ITGB8* in DCs (Figure 21B). The product of this gene is a cell surface receptor for the latent domain (LAP) of TGF-β. Through its association with LAP, TGF-β is maintained in a latent form and the binding to the integrin αvβ8 with subsequent metalloproteolytic cleavage of LAP represents a major mechanism of TGF-β activation in vivo (M. O. Li & Flavell, 2008).

Consistent with RNA expression, curdlan-treated BCsup-DCs but not CL-075-treated or polyI:C-treated BCsup-DCs showed substantially increased cell surface expression of αvβ8 (Figure 21C). Furthermore, adding antibodies neutralizing αvβ8 to $CD8^+$ T cell co-cultures with curdlan-treated BCsup-DCs resulted in the complete inhibition of CD103 expression by $CD8^+$ T cells triggered as the result of DC exposure to curdlan (Figure 21D). Thus, curdlan-treated DCs activate TGF-β1 through αvβ8 to expand $CD103^+CD8^+$ T cells that reject breast cancer cells.

Accordingly, intratumoral injection of curdlan increased the frequency of $CD103^+CD8^+$ T cells in breast cancer tumors *in vivo* (Figure 22A) (DC+T: 9±0.3; n=3; DC+T+curdlan: 31±1.2; n=4; $p<0.0001$). When sorted, these $CD8^+$ T cells triggered tumor necrosis upon transfer into tumors established in immunodeficient mice (Figure

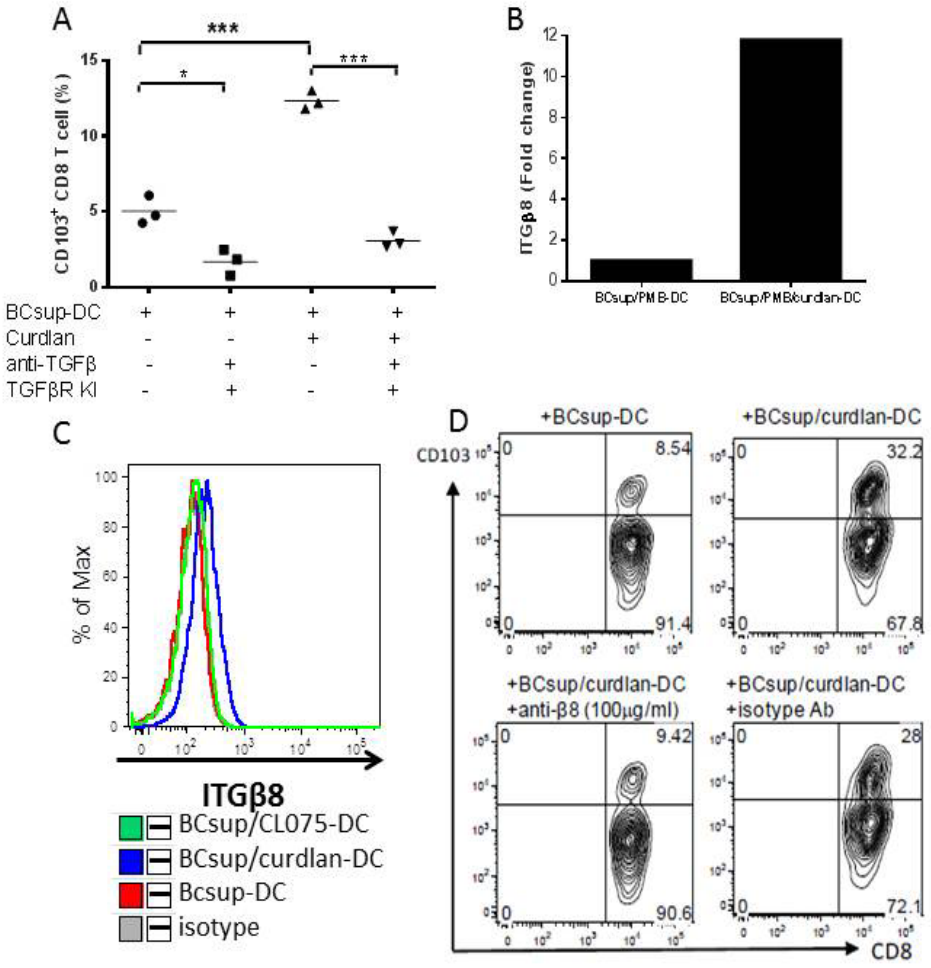

Figure 21. CD103 induction is TGFβ-mediated and ITGβ8-mediated. (A) DCs were pre-treated with anti-TGFβ and TGFβ receptor kinase inhibitor for 30 min and then co-culture these DCs with T cells, the CD103 expression was examined. Single points represent individual experiment. (B) Blood sorted mDCs were pretreated with curdlan and BCsup were added. DCs were harvested for microarray analysis. Summary of transcriptional fold change between BCsup/PMB-DC and BCsup/PMB/curdlan-DC from 3 donors. (C) ITGB8 staining. (left) Grey: isotype, red: BCsup-DC, blue: curdlan/BCsup-DC, green: CL-075/BCsup-DC. (D) Blood sorted mDCs were pre-treated with curdlan, activated by BCsup for 48 hrs, pre-treated with anti-ITGB8 mAb and co-cultured with allogenic naïve T cells. The percentage of $CD103^+CD8^+$ T cells at day 6. Single point indicates the percentage of $CD103^+CD8^+$ T cells from 3 individual DC donors.

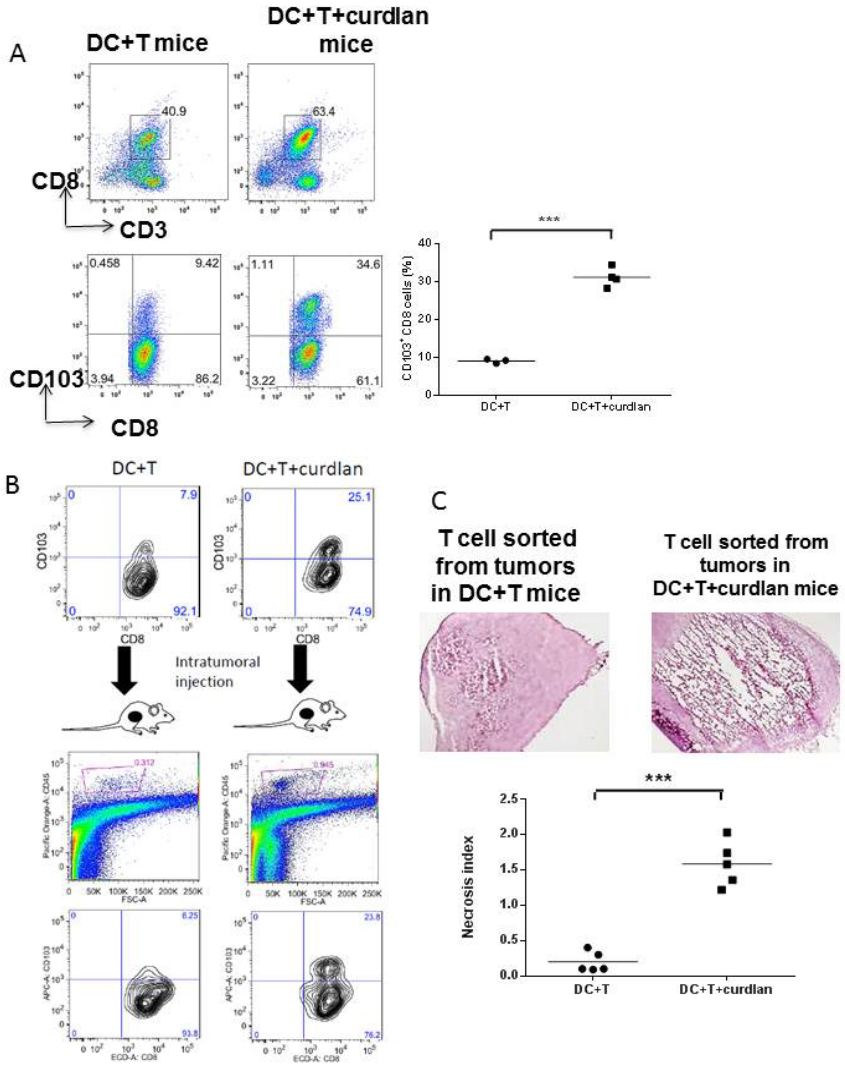

Figure 22. CD8 T cells from curdlan-treated mice are able to retain in tumors and express CD103. (A) Hs578T-bearing NOD/SCID/β2m$^{-/-}$ mice were reconstituted with monocyte derived DCs (MDDCs) and autologous T cells. β-glucan (Curdlan) (100ug/ml) was co-injected with DCs and T cells. Tumors were harvested and digested with collagenase. In CD45^{+} cells, the cell population and CD103^{+}CD8^{+} T cells were analyzed. Single dots represent the percentage of CD103^{+}CD8 cells from each mouse. (B) CD8^{+} T cells were sorted from the tumor cell suspension harvested from mice and intratumoral injected into NOD-SCID mice bearing breast tumor. After 3 days, the tumors were harvested and digested with collagenase. In CD45^{+} cells, the cell population and CD103^{+}CD8^{+} T cells were analyzed. (C) CD8^{+} T cells were sorted from the tumor cell suspension harvested from mice and intratumoral injected into NOD-SCID mice bearing breast tumor (MDA-MB231). After 3 days, the tumors were harvested. Frozen sections from the tumors were used for H&E staining. The necrosis level is rated and calculated with each region. Summary of Points x areas/total area in each section=necrosis index. Necrosis index from 5 sections were summarized.

22B and 22C). A single injection of $CD8^+$ T cells elicited by BCsup-DCs treated with curdlan completely inhibited breast cancer development in a manner dependent upon the expression of CD103 (Figure 23). Indeed, breast cancer tumors grew out in mice which received control $CD8^+$ T cells expanded by BCsup-DCs or in the presence of CD103 blocking Ab (Figure 23).

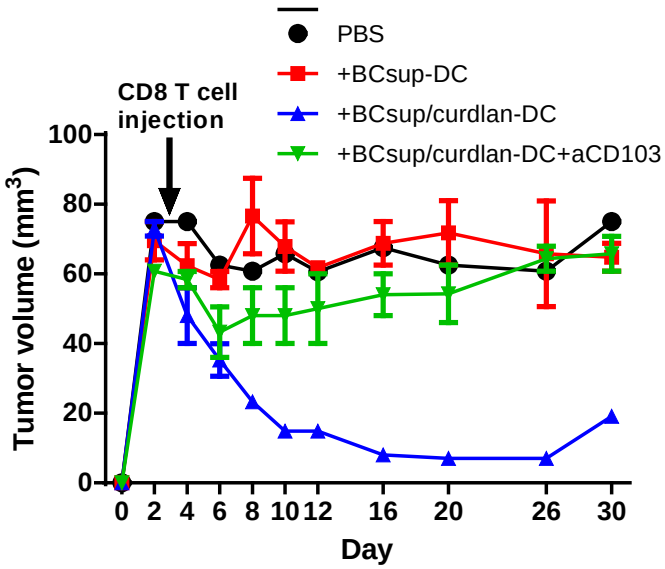

Figure 23. Tumor growth curve with CD8 injection. The NOD/SCID/β2m−/−mice were subcutaneously injected with $10x10^6$ MDA-MB231 cells. 500K sorted CD8+ T cells were injected into tumors. Black: PBS, n=6; Red: CD8+ T cells from BCsup-DC-T co-culture, n=6; Blue: CD8+ T cells from BCsup/curdlan-DC-T co-culture, n=7; Green: CD8+ T cells from BCsup/curdlan-DC-T co-culture with pre-treatment with anti-CD103 mAb, n=8.

CHAPTER FIVE

Conclusions

The studies described here have advanced the knowledge of novel therapeutic targets. It demonstrates an important concept that targeting dendritic cells in tumor microenvironment can allow reprogramming of their function leading to reprogramming of the whole tumor microenvironment which gives the significance and potentially broad clinical implication.

- In breast cancer TSLP secreted from tumor cells induces OX40L expression on mDCs and polarized T cells into inflammatory Th2 immunity which promotes tumor development.
- β-glucan (curdlan) inhibits breast tumor development in vivo which is due to the modulation of DC maturation, secretion of IL12p70 by DCs and subsequent inhibition of inflammatory Th2 responses in the tumor microenvironment. This effect is not unique and can also be triggered by TLR8 ligation or by poly I:C.
- β-glucan (curdlan) treated DCs induce $CD8^{+}$T cells with mucosal phenotype and expression of CD103, integrin which interacts with E-cadherin on epithelial cells. CD103 expression helps $CD8^{+}$ T cells retain in the tumors with superior capacity to accumulate in and to reject breast cancer in vivo. This is unique to curdlan.

Altogether, since the TSLP-OX40L-IL-13 microenvironment was observed in heterogeneous types of breast cancers which are not correlated with grade, stage and expression of hormone receptors, we are expecting to apply these approaches on all kinds of breast cancers. Our studies have identified a number of targets generated by tumor-infiltrating DCs and T cells the ligation of which results in tumor destruction in vivo by the human immune system in humanized mice. These include OX40L, IL-13 and now dectin-1. All these agents act in a unique pathway that we have characterized. It is likely that a combination of antagonists to independent pathway will synergize for tumor eradication which always proves to be more challenging in patients that it is in mouse models.

CHAPTER SIX

Discussion

Based on our results presented herein and in our earlier studies we propose a vicious circle of smoldering type 2 pro-cancer immnuty that perpetuates breast cancer and which is maintained by TSLP. There, breast cancer attracts DCs possibly through macrophage inflammatory protein 3 alpha (MIP3-α) (Diana Bell et al., 1999). Tumor infiltrating DCs are then exposed to TSLP secreted by breast cancer cells which triggers their maturation and OX40L expression. This might explain the aseptic mDC maturation as we found in breast cancer (Aspord et al., 2007; Diana Bell et al., 1999). $OX40L^+$ mDCs induce $CD4^+$ T cells to secrete IL-13, as well as TNF-α. These inflammatory $CD4^+$ T cells contribute to tumor development in an IL13-dependent pathway (Aspord et al., 2007). Thus far, TSLP represents the only factor that activates mDCs without inducing them to produce Th1-polarizing cytokines (Liu et al., 2007). Under normal physiological conditions, TSLP appears to play a critical role in $CD4^+$ T cell homeostasis in the peripheral mucosa-associated lymphoid tissues and in the positive selection and/or expansion of Tregs in the thymus. In inflammatory conditions, such as atopic dermatitis and asthma, epithelial cells markedly increase TSLP expression (Liu et al., 2007). The TSLP-activated DCs migrate to the draining lymph nodes, prime $CD4^+$ T cells via OX40L to differentiate into inflammatory Th2 effector and memory cells and therefore initiate the adaptive phase of allergic immune responses. Interestingly, in breast cancer $OX40L^+$ mDCs are present in the tumor. It remains to be determined whether this reflects their inability to migrate from

the tumor to draining lymph nodes. Indeed, such evasion mechanism has been documented recently in human and mouse tumors showing an inhibition of DC migration from tumors to tumor-draining lymph nodes (Villablanca et al., 2010). This effect depends on tumor-derived ligands of the liver X receptors (LXRs) (Villablanca et al., 2010). It also remains to be determined whether these DCs are able to prime Th2 immunity in situ in tertiary lymphoid structures or whether their main role is to maintain the activation and survival of Th2 cells at the tumor site. Their ability to maintain Th2 cell phenotype and effector function is supported by our earlier studies showing that T cells isolated from experimental breast tumors and transferred to naïve tumor bearing humanized mice can promote tumor development even at low numbers and upon single injection (Aspord et al., 2007).

Three key questions arise from our work: 1) what are the mechanisms allowing TSLP release from cancer cells; 2) the impact of IL-13 (and IL-4) on cancer cells, on the stroma and on the immune infiltrate; and 3) can we target the infiltrating DCs to manipulate the immune microenvironment in breast tumors. Our data show that non-malignant breast epithelia can express TSLP. This further demonstrates that cancer cells can exploit pathways that are present in the normal tissue to establish microenvironment facilitating tumor development. The mechanisms regulating TSLP expression and secretion from cancer cells, including a potential link with oncogenic events, remain to be established. It will also be important to determine the impact of TSLP and inflammatory Th2 environment on the stromal fibroblasts. Indeed, recent studies point to the critical role of cross-talk between cancer cells and fibroblasts in determining the type of

microenvironment established by cancer cells originating from different types of breast cancers (Camp et al., 2011).

The innate immune system recognizes antigens through different kinds of pattern recognition receptors (PRRs), including lectins. When the ligands bind to PRRs, the signals induce immune activation to defend against microbial infection. Besides defending infectious diseases, these signals are potent biological modifiers for activating DCs, macrophages and NK cells. Therefore, targeting DCs through those receptors are possible candidates for controlling whether the immune system exhibits immune activation or suppression in the tumor microenvironment.

β-glucan is a natural ligand for dectin-1 expressed on DCs and is known to induce immune activation and phagocytosis. β-glucan is used in a mammary tumor-bearing mice model and shown to convert pro-cancer Th2 immunity to anti-cancer Th1 responses (Jarek Baran, 2007). The tumor infiltrating $CD4^+$ and $CD8^+$ T cells secret IFNγ showing antitumor activity after β-glucan administration (B. Li et al., 2010). However, the mechanisms how β-glucan reverts the immune microenvironment is still unclear. Here we utilized β-glucan (curdlan) in breast tumor system and examine the effects on DCs to see how curdlan modulates the immune microenvironment.

Also, it is reported that dectin1 is expressed on broad range of cell types, including myeloid dendritic cells, plasmacytoid dendritic cells, macrophages and neutrophils. In the breast tumor microenvironment, the infiltrating immune cells include all these cell types. Therefore, we need to characterize the impact of dectin-1 engagement on other cells present in the tumor microenvironment.

In the breast tumor microenvironment, it is reported that there are mature mDCs existing in the peritumoral regions (Diana Bell et al., 1999). It is thought that mDCs that are trapped within breast tumors lose the ability to migrate to draining lymph nodes, resulting in abrogation of their ability to elicit protective immunity. Therefore, we could consider whether the curdlan treatment on DCs would affect the migratory ability.

The molecular mechanism allowing the blockade of iTh2 and enhance Th1 responses by curdlan will need to be confirmed, the gene stand as candidate, *IL1F9 (IL-36γ)*. IL-36 receptor is expressed on DC and T cells. IL-36 promotes T cells proliferation and survival and is also known to polarize Th1 responses. IL-36/IL-36R pathway is involved in the regulation of IFN-γ secretion by $CD4^+$ T cells (Solenne Vigne, 2012) and IL-36γ has been recently shown as downstream of dectin-1/Syk signaling pathway upon exposure to *Aspergillus Fumigatus* (Gresnigt et al., 2013). Thus, curdlan exposure in the presence of soluble tumor factors leads to phenotype switch and enables DC commitment to maturation phenotype associated with enhanced capacity to leave tumor beds and migrate to lymphoid tissues as well as induce IFN-γ secreting $CD4^+$ T cells.

T cells co-cultured with curdlan-treated DCs also produce IL-17A showing the induction of Th17. In tumor microenvironment, the role of Th17 is still controversial which may depend on the cancer type and cause. The studies point out more Th17-polarized cells in prostate cancer correlate to slower tumor progression and in the melanoma study, the number of Th17 is positively associated with $CD8^+$ T cells and their antitumor activity (Martin-Orozco et al., 2009). The in-vitro polarized Th17 cells were tested to treat established melanoma in mice. Upon T cells adoptive transfer, the tumor antigen-specific Th17 cells show effective response against melanoma and promoting the survival in tumor-bearing mice (Pawel Muranski et al., 2008). However, the study done

with hepatoma model shows lower Th17 cells would decrease tumor growth (J. P. Zhang et al., 2009). Thus, the role of Th17 in our breast tumor model could be further investigated. A clinical study showing Th17 infiltration can be seen in breast tumor tissues. The study further analyzed the correlation between the number of Th17 and pathologic parameters such as cancer stages, grades, size and number of metastasis. The results demonstrated that higher number of Th17 is associated with lower pathological stages indicating that Th17 in breast cancer may play an anti-tumor role (Yang et al., 2012). As our preliminary data that shows the breast tumor cell lines (Hs578t and MDA-MB231) and primary breast tumor cells show no IL-17Ra indicating that these breast tumor cells are not able to response to IL-17A secreted in the microenvironment. Therefore, the IL-17A shows low impact on tumor growth in our breast tumor in vivo system.

It is reported that orally administration of β-glucan increases intraepithelial lymphocytes and enhances mucosal immunity (Tsukada et al., 2003). Induction of CD103, the marker of intraepithelial T cells, can enhance anti-tumor CTL function and promote $CD8^+$ T cells retention in tumors (Le Floc'h et al., 2011; Le Floc'h et al., 2007). The effect of curdlan treated-DCs on CD8 T cells give rise higher IFNγ, GzmA and GzmB which perform better tumor rejection effect. Better retention in tumor sites is CD103-mediated which is regulated by integrin β8 induction and TGFβ activation. It is known CD103/E-cadherin interaction is important in enhance lytic granule polarization and exocytosis (Le Floc'h et al., 2011; Le Floc'h et al., 2007) and once the engagement, the cytotoxic mediators, GzmB and perforin, will be quickly upregulated which contribute the tumor lysis effect (Piet et al., 2011). The effect of tumor prevention in our

breast tumor in vivo system is efficient. However, our preliminary result shows that these $CD8^+$ T cells which co-cultured with curdlan-treated-DCs did not give the clear killing effect to established tumors. When analyzing the phenotype of those $CD8^+$ T cells in tumors, we found the $CD8^+$ T cells indeed retain in the tumor better than those co-cultured with BCsup-DC. But large amount of $CD8^+$ T cells expressed PD-1 which represents exhaustion phenotype (Hong, Amancha, Rogers, Ansari, & Villinger, 2013). Therefore, it is important to combine the treatment with anti-PD1 to see if we can rescue the function of $CD8^+$ T cells and help to reduce the tumor size in vivo. And the induction of integrin β8 is specific on curdlan treated-DCs but not CL-075-DCs and polyI:C-DC which also need to be clarified about the mechanisms.

Since seeing the killing function of $CD8^+$ T cells in breast tumors which would be critical through CD103/E-cadherin interaction, we are interested if there are differential expression of E-cadherin between breast tumors and normal epithelial cells. We explored the RNAsequecing database (Craig et al., 2013) which analyzed the comparison between triple negative breast cancers and non-malignant tissues. When pulling out the gene CDH1 which encodes E-cadherin, we found 11/14 breast tumors show upregulated expression of CDH1 gene indicating higher level of E-cadherin expression on breast cancer cells. It suggested the $CD103^+$ $CD8^+$ T cells may have better ability stay in E-cadhein^{high} breast tumor cells performing CTL function.

Here we show that breast cancer is infiltrated with inflammatory Th2 cells and that such T cells are driven by OX40L on DCs. Blocking OX40L in vitro prevents generation of these $CD4^+$ T cells without impact on IL-10 producing $CD4^+$ T cells. Blocking OX40L in vivo partially prevents T cell-dependent acceleration of breast cancer tumor

development. OX40L expression by DCs is driven by TSLP secreted from breast cancer cells. Accordingly, TSLP expression can be found in primary as well as metastatic tumors. Blocking TSLP reduces inflammation and partially inhibits tumor development. Taken together, TSLP-OX40L-IL13 axis might offer a novel therapeutic target. To further reprogram non-protective Th2 responses into protective Th1 responses and enhancing function and retention of $CD8^+$ T cells in breast tumor microenvironment, our approach using β-glucan (curdlan) in DC modulation. In the future, we are expecting the clinical application with curdlan. Intratumoral delivery of curdlan would be possible modulate the existing immune responses in the breast cancers. It can be used in the recurring breast cancer which on the chest walls after surgery. And the monocyte-derived DCs which loaded antigens could be activated with curdlan and used as vaccine to induce the Th1 and CTL responses. From our study, we demonstrated that TSLP/curdlan-activated DCs show the capacity to induce good quality of $CD8^+$ T cells. Therefore, we are expecting to ex-vivo generate the $CD8^+$ T cells and adoptively transfer to patients in the future. It opens a novel avenue for immunotherapy by targeting DCs in situ for reprogramming of tumor promoting immunity.

APPENDICES

APPENDIX A

Thymic stromal lymphopoietin fosters human breast tumor growth by promoting type 2 inflammation (J Exp Med, 208(3), 479-490. 2011)

Thymic stromal lymphopoietin fosters human breast tumor growth by promoting type 2 inflammation

Alexander Pedroza-Gonzalez,[1] Kangling Xu,[1,2] Te-Chia Wu,[1,2] Caroline Aspord,[1] Sasha Tindle,[1] Florentina Marches,[1] Michael Gallegos,[1] Elizabeth C. Burton,[4] Daniel Savino,[4] Toshiyuki Hori,[5] Yuetsu Tanaka,[6] Sandra Zurawski,[1] Gerard Zurawski,[1] Laura Bover,[7] Yong-Jun Liu,[7] Jacques Banchereau,[1,8,9] and A. Karolina Palucka[1,3,8,9]

[1]Baylor Institute for Immunology Research, Baylor Research Institute, Dallas, TX 75204
[2]Department of Biomedical Studies, Baylor University, Waco, TX 76706
[3]Sammons Cancer Center, [4]Baylor University Medical Center, Dallas, TX 75246
[5]Department of Hematology and Oncology, Graduate School of Medicine, Kyoto University, Sakyoku, Kyoto 606-8507, Japan
[6]Department of Immunology, University of the Ryukyus, Okinawa 903-0215, Japan
[7]MD Anderson Cancer Center, Houston, TX 77030
[8]Department of Gene and Cell Medicine and [9]Department of Medicine, Immunology Institute, Mount Sinai School of Medicine, New York, NY 10029

The human breast tumor microenvironment can display features of T helper type 2 (Th2) inflammation, and Th2 inflammation can promote tumor development. However, the molecular and cellular mechanisms contributing to Th2 inflammation in breast tumors remain unclear. Here, we show that human breast cancer cells produce thymic stromal lymphopoietin (TSLP). Breast tumor supernatants, in a TSLP-dependent manner, induce expression of OX40L on dendritic cells (DCs). OX40L$^+$ DCs are found in primary breast tumor infiltrates. OX40L$^+$ DCs drive development of inflammatory Th2 cells producing interleukin-13 and tumor necrosis factor in vitro. Antibodies neutralizing TSLP or OX40L inhibit breast tumor growth and interleukin-13 production in a xenograft model. Thus, breast cancer cell–derived TSLP contributes to the inflammatory Th2 microenvironment conducive to breast tumor development by inducing OX40L expression on DCs.

CORRESPONDENCE
A. Karolina Palucka:
karolinp@baylorhealth.edu

Abbreviations used: HPC, hematopoietic progenitor cell; mDC, myeloid DC; NOD/SCID/$\beta 2m^{-/-}$, nonobese diabetic/LtSz-scid/scid β2 microglobulin–deficient; TSLP, thymic stromal lymphopoietin.

There is accumulating evidence that inflammation plays a key role in the initiation and progression of cancer (Grivennikov et al., 2010). There are two types of inflammation that have opposing effects on tumors: (a) chronic inflammation, which promotes cancer cell survival and metastasis (Coussens and Werb, 2002; Condeelis and Pollard, 2006; Mantovani et al., 2008), and (b) acute inflammation, which can trigger cancer cell destruction as illustrated by regressions of bladder cancer after treatment with microbial preparations (Rakoff-Nahoum and Medzhitov, 2009). Although chronic inflammation is often linked with the presence of type 2–polarized macrophages (M2), acute inflammation associated with cancer destruction is linked with type 1–polarized macrophages (M1). M1 macrophages are induced by the type 1 cytokine IFN-γ, whereas, M2 macrophages are induced by the type 2 cytokines IL-4 and IL-13 (Mantovani and Sica, 2010).

Type 2 cytokines can contribute to tumorigenesis in several ways. For example, IL-13 produced by NKT cells induces myeloid cells to

A. Pedroza-Gonzalez's present address is Dept. of Gastroenterology and Hepatology, Erasmus MC, Rotterdam, Netherlands.
T.-C. Wu's present address is College of Life Sciences, Ritsumeikan University, Kusatsu, Shiga 525-8577, Japan.
C. Aspord's present address is Institut National de la Santé et de la Recherche Médicale U823, Immunobiology and Immunotherapy of Cancers, 38701, La Tronche, France.
J. Banchereau's present address is Hoffman-La Roche, Inc., Nutley, NJ.

The Rockefeller University Press $30.00
J. Exp. Med. Vol. 208 No. 3 479-490
www.jem.org/cgi/doi/10.1084/jem.20102131

The Journal of Experimental Medicine

make TGF-β, which ultimately inhibits CTL functions (Berzofsky and Terabe, 2008). Spontaneous autochthonous breast carcinomas arising in Her-2/neu transgenic mice appear more quickly when the mice are depleted of T cells, which is evidence of T cell–mediated immunosurveillance slowing tumor growth (Park et al., 2008). This immunosurveillance could be further enhanced by blockade of IL-13, which slowed the appearance of these autologous tumors compared with control antibody-treated mice (Park et al., 2008). A spontaneous mouse breast cancer model recently highlighted the role of Th2 cells which facilitate the development of lung metastasis through macrophage activation (DeNardo et al., 2009). We identified $CD4^+$ T cells secreting IFN-γ and IL-13 in breast cancer tumors (Aspord et al., 2007). We also found that breast cancer cells express IL-13 on cell surface. Autocrine IL-13 has been shown to be important in the pathophysiology of Hodgkin's disease (Kapp et al., 1999; Skinnider et al., 2001, 2002). IL-13 and IL-13R are frequently expressed by Hodgkin's and Reed-Sternberg cells (Skinnider et al., 2001), and IL-13 stimulates their growth (Kapp et al., 1999; Trieu et al., 2004). Similar to Hodgkin's cells (Skinnider et al., 2002), breast cancer cells express pSTAT6 (Aspord et al., 2007), suggesting that IL-13 actually delivers signals to cancer cells. However, the mechanisms underlying the development of Th2 inflammation in breast cancer are unknown.

Like many other features of the immune response, Th1/Th2 polarization is regulated by DCs. In the steady state, nonactivated (immature) DCs present self-antigens to T cells, which leads to tolerance (Hawiger et al., 2001; Steinman et al., 2003). Once activated (mature), antigen-loaded DCs are geared toward the launching of antigen-specific immunity (Finkelman et al., 1996; Brimnes et al., 2003) leading to the proliferation of T cells and their differentiation into helper and effector cells. DCs are composed of distinct subsets, including myeloid DCs (mDCs) and plasmacytoid DCs (Caux et al., 1997; Maldonado-López et al., 1999; Pulendran et al., 1999; Luft et al., 2002; Dudziak et al., 2007; Klechevsky et al., 2008). DCs are also endowed with functional plasticity, i.e., they respond differentially to distinct activation signals (Steinman and Banchereau, 2007). For example, IL-10–polarized mDCs generate anergic $CD8^+$ T cells that are unable to lyse tumors (Steinbrink et al., 1999), as well as $CD4^+$ T cells with regulatory/suppressor function (Levings et al., 2005). In contrast, thymic stromal lymphopoietin (TSLP)–polarized mDCs are conditioned to express OX40 ligand (OX40L) and to expand T cells producing type 2 cytokines (Soumelis et al., 2002; Gilliet et al., 2003). Both the distinct DC subsets and their distinct response to microenvironment contribute to the generation of unique adaptive immune responses.

Unraveling the mechanisms by which breast cancer polarizes the immune responses might offer novel therapeutic options. This is important because despite declining mortality rates, breast cancer ranks second among cancer-related deaths in women. Worldwide, it is estimated that more than 1 million women are diagnosed with breast cancer every year, and >410,000 will die from the disease (Coughlin and Ekwueme, 2009). Here, we show that inflammatory Th2 cells that promote tumor development are driven by breast cancer–derived TSLP, which induces and maintains OX40L-expressing DCs in the tumor microenvironment. Thus, TSLP, and down-stream molecules, might represent novel potential therapeutic targets.

RESULTS

Inflammatory Th2 cells in primary breast cancer tumors

Our earlier study using a pilot cohort of 19 samples of primary breast cancer tumors revealed the secretion, upon activation with PMA and ionomycin, of both type 1 (IFN-γ) and type 2 (IL-4 and IL-13) cytokines (Aspord et al., 2007). The current study extends the analysis to a total of 99 consecutive samples (Table S1). Supernatants of activated tumor fragments display high levels of IFN-γ, IL-2, IL-4, IL-13, and TNF (Fig. 1 A and Table S1). Supernatants from tumor sites contained significantly higher levels of IL-2, type 2 (IL-4 and IL-13), and inflammatory (TNF) cytokines than those from macroscopically uninvolved surrounding tissue (Fig. 1 B and Table S1). Whereas a significant correlation can be observed between IL-2 levels in tumor and adjacent tissue ($P = 0.02$), IL-4 and IL-13 levels are not correlated ($P = 0.5$), further suggesting polarization of cytokine environment in breast tumors (Fig. 1 B). IFN-γ did not correlate with other cytokine levels (Table S1). However, levels of TNF were correlated with those of IL-13 ($P < 0.0001$; $r = 0.62$; $n = 98$) and IL-4 ($P = 0.0175$; $r = 0.31$; $n = 59$; Fig. 1 C). Thus, this survey of cytokine expression suggested Th2 polarization in the breast tumor microenvironment.

To identify the cells producing these cytokines, single-cell suspensions were prepared from tumors; activated for 5 h with PMA and ionomycin; stained with antibodies against T cells and cytokines; and analyzed by flow cytometry. Gated viable $CD4^+CD3^+$ T cells expressed IL-13 (3.67%), most of them coexpressing IFN-γ and TNF (Fig. 1 D and Fig. S1 A). A small fraction of $IL\text{-}13^+CD4^+$ T cells coexpressed IL-4, but none expressed IL-10 (Fig. 1 D). Such T cells have been referred to as inflammatory Th2 cells that are involved in allergic inflammatory diseases (Liu et al., 2007). Flow cytometry analysis of consecutive tumor infiltrates ($n = 22$) shows the overall increased percentages of IL-4– and IL-13–secreting $CD4^+CD3^+$ T cells ($P = 0.0313$ and $P = 0.0156$, respectively) when compared with adjacent tissue samples (Fig. 1 D and Fig. S1 B). Thus, the difference between tumor tissue and adjacent tissue appears to be caused by both the increased numbers of infiltrating T cells and enhanced polarization. The analysis of frozen tissue sections further demonstrated that infiltrating T cells in primary breast cancer tumors express IL-13 (Fig. 1 E). Thus, breast cancer tumors are infiltrated with inflammatory Th2 cells.

DCs infiltrating breast cancer tumors express OX40 ligand

Because OX40 ligation drives the differentiation of $CD4^+$ T cells into inflammatory Th2 (Ito et al., 2005), we analyzed the presence of OX40L in primary breast cancer tumors.

Immunofluorescence staining of frozen tissue sections of primary breast cancer tumors showed the expression, in 57 out of 60 analyzed tumors, of OX40L by a majority of HLA-DR^{high} cells (Fig. 2 A). These OX40L$^+$ cells are located in peritumoral areas (Fig. 2 A). Flow cytometry analysis of single-cell suspensions further confirmed the expression of OX40L by a fraction of HLA-DR^{high} CD14^{neg} CD11c^{high} mDCs (Fig. 2 B). Paired analysis demonstrated that the tumor beds express higher percentages of OX40L$^+$ mDCs than the surrounding tissue ($P = 0.0156$; $n = 7$ paired samples; mean ± SE for surrounding tissue = 1.5 ± 0.8% [$n = 7$] and for breast cancer tumors 11 ± 1.67% [$n = 12$], respectively; Fig. 2 B). Thus, breast cancer tumors are infiltrated with OX40L$^+$ mDCs.

Breast cancer tumors produce soluble factors that induce functional OX40L expression on DCs

To identify the breast cancer tumor factors that induce OX40L on mDCs, LIN^{neg}HLA-DR$^+$ CD123$^-$ CD11c$^+$ mDCs were sorted from blood of healthy volunteers and

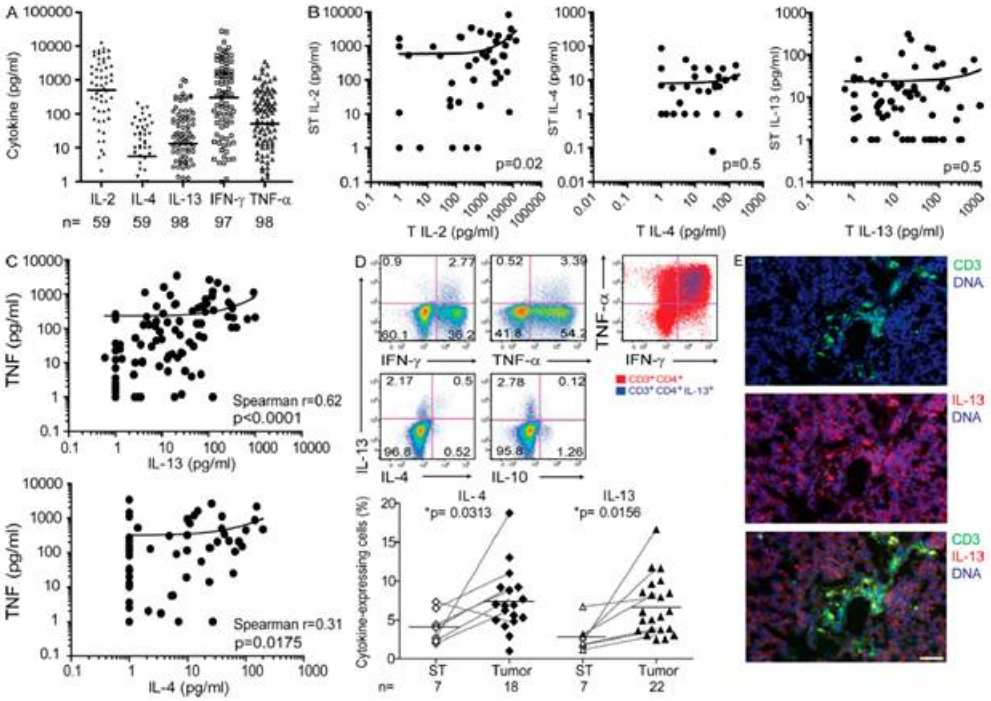

Figure 1. Inflammatory Th2 in breast cancer immune environment. (A) Cytokine profiles as determined by Luminex in supernatants of human breast tumor fragments stimulated for 16 h with PMA and ionomycin. Numbers on the x-axis indicate the number of tissue samples from different patients tested. (B) Cytokine profiles as determined by Luminex in supernatants of tumor fragments (T) and surrounding tissue (ST) from the same patient after PMA and ionomycin stimulation. Cytokine concentration values of IL-2, IL-4, and IL-13 from T and ST samples were plotted and analyzed using linear regression to determine the level of correlation between cytokine concentration in T and ST samples. (C) Cytokine profiles as determined by Luminex in supernatants of tumor fragments after PMA and ionomycin stimulation. Cytokine concentration values of TNF and IL-13 and of TNF and IL-4 were plotted and analyzed using nonparametric Spearman correlation to determine the level of correlation of two cytokines concentration in tumor samples. (D, top) Single-cell suspensions from tumor samples were stimulated for 5 h with PMA and ionomycin. Cytokine production was measured by flow cytometry. Dot plots are gated on CD3$^+$CD4$^+$ T cells. (top right dot plot) Blue indicates gate on CD3$^+$CD4$^+$IL-13$^+$ T cells that coexpress IFN-γ and TNF. Representative of four different patients from whom we have been able to obtain sufficient numbers of cells for 10-color analysis (patient nos. 148, 155, 164, and 169). Bottom, percentages of CD4$^+$ T cells expressing IL-4 and IL-13 in tumor infiltrates and surrounding tissue (ST) were analyzed by flow cytometry. Dotted lines indicate paired samples from the same patient ($n = 7$, Wilcoxon matched-pairs ranked test). Single points indicate the percentage of cytokine expressing cells in tumor samples analyzed by flow cytometry for which we did not obtain sufficient number of cells from surrounding tissue to allow the analysis. (E) Frozen tissue sections from the same patient as in D were analyzed by immunofluorescence. Triple staining with anti-CD3-FITC (green), anti-IL-13–Texas red (red), and DAPI nuclear staining (blue). Bar, 90 µm.

exposed to breast cancer supernatants. These were generated from established breast cancer cell lines expanded in vitro (Hs578T, MDA-MB-231, MDA-MB-468, MCF7, HCC-1806, and T47D; Table S2) and breast cancer tumors established in vivo by implanting breast cancer cell lines in immunodeficient mice (Aspord et al., 2007). As illustrated in Fig. 2 C, mDCs exposed for 48 h to Hs578T and HCC-1806 supernatants expressed OX40L. Four of the five breast cancer cell lines, with the notable exception of T47D, induced OX40L expression on mDCs (Fig. S1 C).

To test whether primary breast cancer tumors could also regulate OX40L expression, fragments of primary tumors were sonicated, centrifuged, filtered, and used in cultures with blood mDCs. As illustrated in Fig. 2 D, mDCs acquired both CD83 (a DC maturation marker) and OX40L. To determine the impact of OX40L on the generation of inflammatory Th2 responses in breast cancer, blood mDCs were first exposed for 48 h to either TSLP or breast tumor–soluble fractions. Exposed mDCs were then used to stimulate naive allogeneic CD4$^+$ T cells with either the anti-OX40L antibody or a relevant

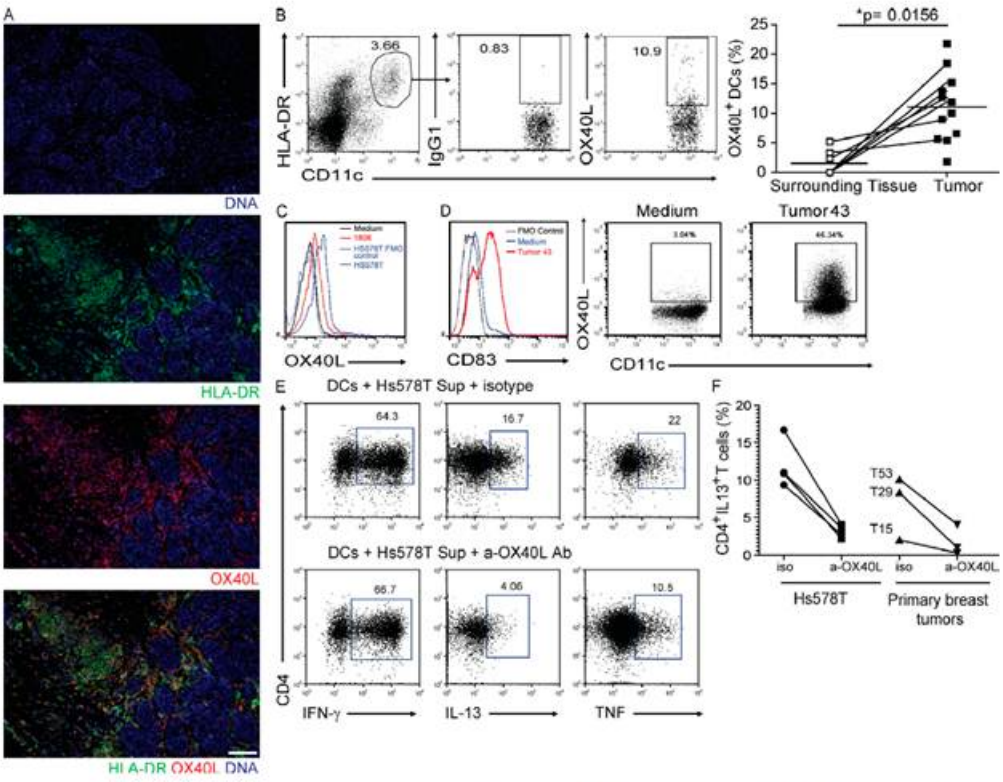

Figure 2. OX40L in breast cancer immune environment. (A) Immunofluorescence of primary breast tumor with indicated antibodies. Bar, 180 µm. Representative of 57/60 tumors analyzed. (B) Flow cytometry analysis of single-cell suspensions of primary breast tumors and surrounding tissue. Dot plots are gated on CD14^{neg} nonlymphocytes. OX40L expression is analyzed on HLA-DR^{high}CD11c^{high} DCs. Graph summarizes percentages of OX40L-expressing DCs in tumor infiltrates and surrounding tissue (ST) analyzed by flow cytometry. Dotted lines indicate paired samples from the same patient (Wilcoxon matched-pairs ranked test). Single points indicate the percentage of OX40L$^+$ DCs in tumor samples for which we did not obtain sufficient number of cells from surrounding tissue to allow the analysis. (C and D) mDCs were exposed to media alone, to supernatant of breast cancer cell lines (1806 or Hs587T), or to sonicate of primary breast cancer tissue from patients (tumor 43). OX40L and CD83 were measured by flow cytometry. FMO, fluorescence minus one indicates controls where one staining fluorescence is omitted to set negative gate. (E and F) mDCs were exposed for 48 h to supernatants of breast cancer cells Hs578T, and then co-cultured with allogeneic naive CD4$^+$ T cells in the presence of 40 µg/ml of anti-OX40L (Ik-5 clone) or isotype control antibody. After 1 wk, cells were collected and restimulated for 5 h with PMA/ionomycin for intracellular cytokine staining. Data in E are representative of four experiments. (F) Summary of the effect of blocking OX40L during T cell stimulation by tumor-activated DCs. Graph shows the proportion of IL-13–secreting cells induced by DCs activated with supernatants from breast cancer cell line Hs578T (left) or primary breast tumors (right, T15, T29, and T53).

isotype control. Blocking OX40L prevented the expansion of $IL13^+CD4^+$ or TNF^+CD4^+ T cells by TSLP-primed mDCs (>50% inhibition; Fig. S2 A), mDCs exposed to Hs578T breast cancer cells ($n = 4$; median inhibition of $IL13^+CD4^+$ cells = 74%; range = 67–80%; Fig. 2, E and F), and mDCs exposed to sonicates of randomly selected primary breast cancer tumors (Fig. 2 F and Fig. S2 B). Thus, breast cancer cells produce factors that activate mDCs and induce them to express OX40L and to elicit inflammatory Th2 cells.

Breast cancer tumors express and secrete TSLP

OX40L can be induced on mDCs by TSLP, an IL-7–like cytokine produced by epithelial cells (Liu et al., 2007; Ziegler and Artis, 2010). All tested breast cancer cell lines expressed and secreted TSLP (Fig. 3 A). Supernatants of some primary breast cancer tumors stimulated with PMA and ionomycin displayed up to 300 pg/ml TSLP (Fig. 3 B). The expression of TSLP by cancer cells was further analyzed using an anti-TSLP antibody and immunofluorescence of frozen breast cancer tumors generated in the xenograft model (Aspord et al., 2007). There, subcutaneous MDA-MB-231 tumors transplanted in mice expressed TSLP (Fig. 3 C). The specificity of the staining is demonstrated by pretreatment of the antibody with recombinant TSLP (Fig. S3).

Importantly, TSLP is expressed in 35 out of 38 analyzed primary breast cancer tumors obtained from patients regardless of grade, histology, or stage of analyzed tumors. Fig. 3 D illustrates the pattern of TSLP staining and coexpression with

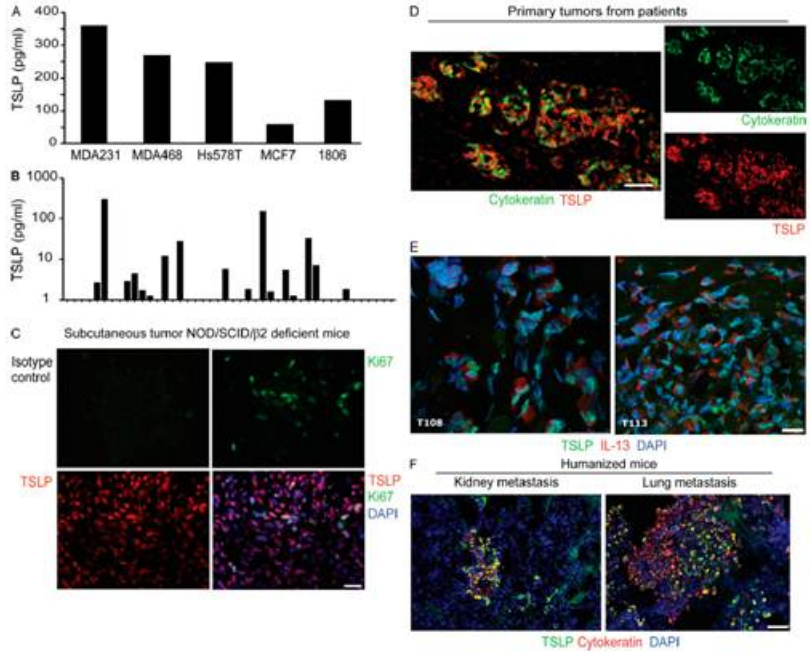

Figure 3. TSLP in breast cancer environment. (A) Luminex analysis of TSLP in supernatants of breast cancer cell lines after 24 h of culture in the presence of PMA and ionomycin. (B) Luminex analysis of TSLP levels in supernatants of primary breast tumors (from 44 patients) activated with PMA and ionomycin. (C) NOD/SCID/$\beta2m^{-/-}$ mice were irradiated the day before tumor implantation and 10×10^6 MDA-MB-231 cells were implanted by subcutaneous injection. Tumors were harvested at 4 wk after implant. Frozen tissue sections were analyzed by immunofluorescence for expression of TSLP (red). Actively dividing cells were identified by expression of Ki67 (green). Bar, 45 µm. (D and E) Frozen tissue sections from primary breast tumors from patients (38 patient samples) were analyzed by immunofluorescence for expression of TSLP. Tissues were also stained for the expression of IL-13 and cytokeratin 19, as indicated, to confirm TSLP expression by cancer cells. Staining pattern is representative of 35 out of 38 analyzed tumor samples from different patients. Bars: (D) 180 µm; (E) 15 µm. (F) NOD/SCID/$\beta2m^{-/-}$ mice were sublethally irradiated and transplanted with human $CD34^+$ HPCs by intravenous injection. 4 wk after HPC transplant, 5×10^6 MDA-MB-231 breast cancer cells were implanted subcutaneously. Tumors at the site of implantation, as well as lungs and kidneys, were harvested at 3 mo after implant. Frozen tissue sections were analyzed by immunofluorescence for expression of TSLP (green) and cytokeratin (red). Staining pattern is representative of tumors from three different mice. Bar, 90 µm.

cytokeratin 19–positive cells. It demonstrates that TSLP is expressed in the cytoplasm and the nucleus of breast cancer cells that display IL-13 on their surface (Fig. 3 E). Importantly, TSLP is also expressed in lung and kidney metastasis of MDA-MB-231 tumors in humanized mice (Fig. 3 F) and in breast cancer tumor metastasis from patients (Fig. S4 A). TSLP expression is specific to epithelial cells as no staining can be found in tumor-infiltrating fibroblasts (Fig. S4 B). Furthermore, non-malignant breast epithelia can also express TSLP (Fig. S4 C).

Thus, similar to normal skin or lung epithelium, breast epithelial cells and breast cancer cells have the capacity to express, produce, and secrete TSLP.

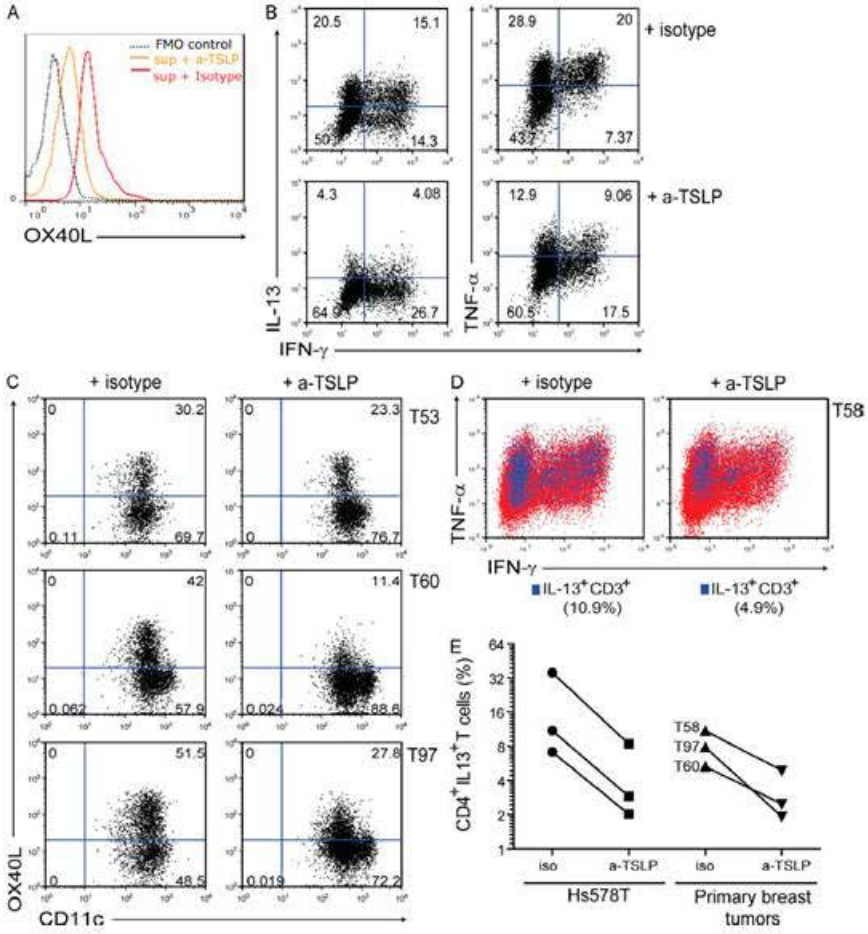

Figure 4. Blocking TSLP in vitro. (A) mDCs were incubated with supernatant of breast cancer cell line Hs578T in the presence or absence of 20 µg/ml of anti-TSLP (AB 19024; rabbit IgG). OX40L expression was measured by flow cytometry after 48 h of incubation. (B) mDCs treated as in A were co-cultured with naive allogeneic CD4+ T cells for 7 d. IL-13 production was measured by intracellular cytokine staining and flow cytometry after cells were restimulated for 5 h with PMA and ionomycin. Data are representative of three experiments. (C) mDCs were incubated with soluble factors from sonicated human breast tumors (T53, T60, and T97) in the presence or absence of 20 µg/ml of anti-TSLP (AB 19024; rabbit IgG). OX40L expression was measured by flow cytometry after 48 h of incubation. (D) mDCs treated as in C were co-cultured with naive allogeneic CD4+ T cells for 7 d. IL-13 production was measured by intracellular cytokine staining and flow cytometry after cells were restimulated for 5 h with PMA and ionomycin. Representative of three patients tested. Blue dots represent IL-13+ T cells gated in the same sample. (E) Graph shows data from three independent experiments as described in A–D.

Anti-TSLP antibodies block the generation of inflammatory Th2 responses in vitro

To determine the impact of blocking TSLP on the generation of inflammatory Th2 responses in breast cancer, blood mDCs were first exposed for 48 h to either TSLP or breast tumor–soluble fractions. Addition of anti-TSLP–neutralizing antibodies to breast cancer tumor supernatants inhibited their ability to induce OX40L on mDCs (Fig. 4 A). Such mDCs displayed a diminished capacity to expand $IL13^+CD4^+$ or TNF^+CD4^+ T cells ($n = 3$; median inhibition = 73%, range = 72–77%; Fig. 4, B and E). Likewise, adding anti-TSLP–neutralizing antibody to sonicate of randomly selected primary breast cancer tumors led to down-regulation of OX40L expression by mDCs (Fig. 4 C) and decreased expansion of $IL13^+TNF^+CD4^+$ T cells (Fig. 4, D and E). Finally, when anti-TSLP receptor β chain (TSLPR) antibody was added to mDCs during their exposure to the supernatant of three different breast cancer cell lines (Hs578T, MDA-MB-231, and MCF7; Fig. 5 A), resulting mDCs showed a much diminished expansion of $IL13^+$ $CD4^+$ T cells (Fig. 5 B). Thus, TSLP is the factor secreted by breast cancer cells that contributes to generation of inflammatory Th2 responses.

Antibodies neutralizing TSLP–OX40L axis block tumor development in vivo

Our results thus far suggest a role for the TSLP–OX40L axis in generation of $IL13^+TNF^+CD4^+$ T cells, but do not establish whether this axis might actually contribute to breast cancer tumor development. To address this question, humanized mice were reconstituted with both Hs578T cells and T cells with or without anti-OX40L–, anti-TSLPR–, and anti-TSLP–neutralizing antibodies. As shown in Fig. 6 A, the administration of neutralizing anti-OX40L antibodies leads to significant inhibition of tumor development.

The administration of a neutralizing anti-TSLP antibody also results in the inhibition of tumor development (Fig. 6 B). TSLP blockade also leads to decreased secretion of IL-4 and IL-13 by tumor infiltrating T cells upon PMA and ionomycin activation (Fig. 6 C). Finally, the administration of antibody blocking TSLPR nearly completely blocks tumor development driven by $CD4^+$ T cells (Fig. 6 D). These results indicate that the TSLP contributes to breast cancer pathogenesis.

DISCUSSION

Here, we show that breast cancer is infiltrated with inflammatory Th2 cells and that such T cells are driven by OX40L on DCs. Blocking OX40L in vitro prevents generation of these $CD4^+$ T cells without impact on IL-10–producing $CD4^+$ T cells. Blocking OX40L in vivo partially prevents T cell–dependent acceleration of breast cancer tumor development. OX40L is not constitutively expressed, but can be induced on DCs, macrophages, and B cells; e.g., upon CD40 engagement or cytokine signals such as TSLP or IL-18, as well as upon TLR stimulation (Ito et al., 2005; Croft et al., 2009). Thus, the

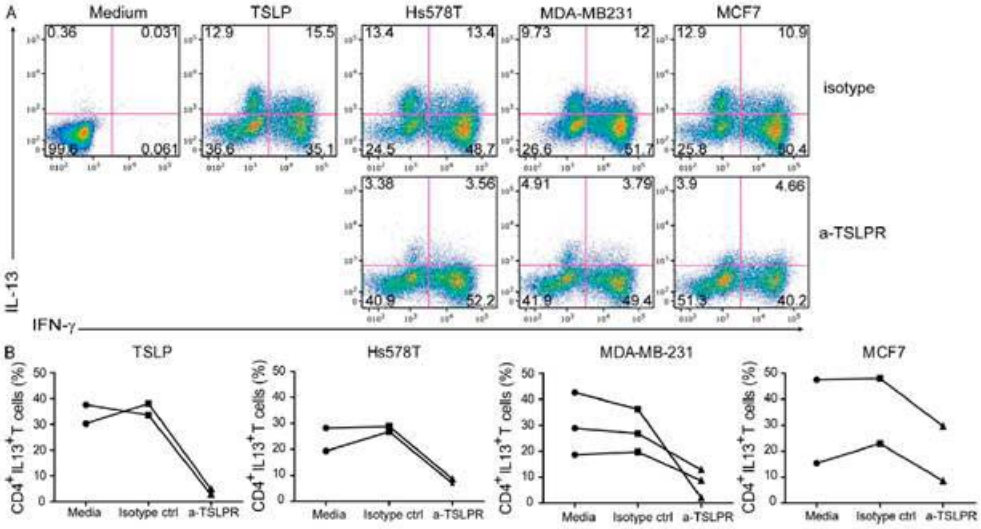

Figure 5. Blocking TSLP-R in vitro. (A) mDCs were treated with anti-TSLP-R (clone AB81_85.1F11, mouse IgG1), media or control antibody during activation with TSLP or with supernatant of one of the three different breast cancer cell lines (Hs578T, MDA-MB-231, and MCF7). mDCs were then co-cultured with allogeneic naive $CD4^+$ T cells. After 1 wk, cells were collected, restimulated for 5 h with PMA and ionomycin, and analyzed by flow cytometry. (B) Analysis of different experiments showing the effect of blocking TSLP-R on the induction of IL-13 secreting cells as described in A.

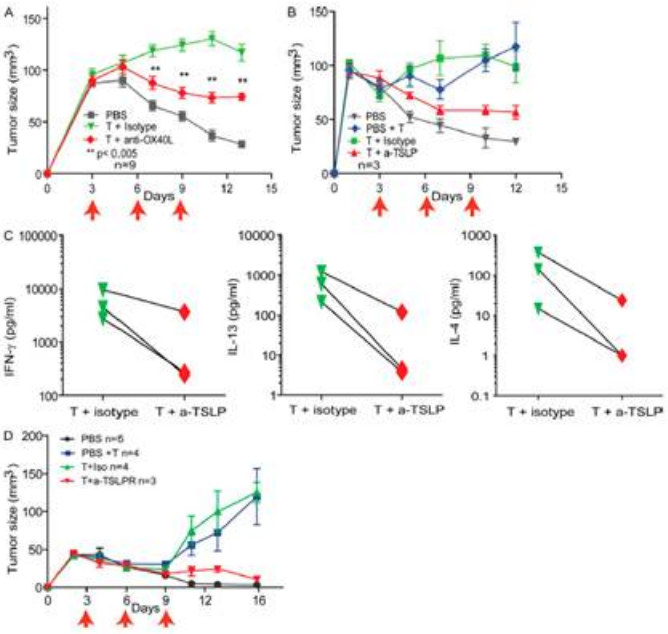

Figure 6. Blocking OX40L-TSLP in vivo. (A) NOD/SCID/$\beta 2m^{-/-}$ mice were sublethally irradiated and transplanted with human $CD34^+$ HPCs by intravenous injection. 4 wk after HPC transplant, 10×10^6 Hs578T breast cancer cells were implanted subcutaneously. 3, 6, and 9 d after, mice were reconstituted with autologous total T cells together with 200 µg per injection of blocking anti-OX40L or isotype control antibody (mouse Ig; red arrows). PBS group was injected with tumor cells but not with T cells (gray line). Tumor size was measured at indicated times. Mean values from three experiments representing nine mice per each condition. Anti-OX40L and isotype-treated cohorts were compared statistically. (B) NOD/SCID/$\beta 2m^{-/-}$ mice were irradiated and implanted with 10×10^6 Hs578T breast cancer cells together with 200 µg per injection of neutralizing anti-TSLP (rabbit), rabbit isotype control antibody, or PBS. 3, 6, and 9 d after, mice were reconstituted with immature DCs and autologous total T cells together with 200 µg per injection of neutralizing anti-TSLP (rabbit), rabbit isotype control antibody or PBS. Representative of three independent experiments with a total of nine mice in TSLP blockade group. (C) Cytokine secretion in single-cell suspensions from tumors after 16-h restimulation with PMA and ionomycin. (D) Same as in B, but mice were injected with anti-TSLPR or isotype control at days 3, 6, and 9. Representative of two independent experiments. *n* indicates number of mice per cohort in this representative experiment.

presence of $OX40L^+$ mDCs in breast tumors indicate sustained activation of DCs in tumor environment. Indeed, OX40L expression by DCs is driven by TSLP secreted from breast cancer cells. Accordingly, TSLP expression can be found in primary and metastatic tumors. Blocking TSLP reduces inflammation and partially inhibits tumor development.

Based on our results presented herein and in our earlier studies, we propose a vicious circle of smoldering type 2 inflammation that perpetuates breast cancer and which is maintained by TSLP. There, breast cancer attracts DCs, possibly through macrophage inflammatory protein 3 α (MIP3-α; Bell et al., 1999). Tumor-infiltrating DCs are then exposed to TSLP secreted by breast cancer cells, which triggers their maturation and OX40L expression. This might explain the aseptic mDC maturation that we found in breast cancer (Bell et al., 1999; Aspord et al., 2007). $OX40L^+$ mDCs induce $CD4^+$ T cells to secrete IL-13, as well as TNF. These inflammatory $CD4^+$ T cells contribute to tumor development in an IL-13–dependent pathway (Aspord et al., 2007). Thus far, TSLP represents the only factor that activates mDCs without inducing them to produce Th1-polarizing cytokines (Liu et al., 2007). Under normal physiological conditions, TSLP appears to play a critical role in $CD4^+$ T cell homeostasis in the peripheral mucosa-associated lymphoid tissues and in the positive selection and/or expansion of regulatory T (T reg) cells in the thymus (Watanabe et al., 2005a,b). In inflammatory conditions such as atopic dermatitis and asthma, epithelial cells markedly increase TSLP expression (Liu et al., 2007). The TSLP-activated DCs migrate to the draining lymph nodes, prime $CD4^+$ T cells via OX40L to differentiate into inflammatory Th2 effector and memory cells, and thus initiate the adaptive phase of allergic immune responses. Interestingly, in breast cancer, $OX40L^+$ mDCs are present in the tumor. It remains to be determined whether this reflects their inability to migrate from the tumor to draining lymph nodes. Indeed, such an evasion mechanism has been documented recently in human and mouse tumors showing an inhibition of DC migration from tumors to tumor-draining lymph nodes (Villablanca et al., 2010). This effect depends on tumor-derived ligands of the liver X receptors (Villablanca et al., 2010). It also remains to be determined whether these DCs are able to prime Th2 immunity in situ in tertiary lymphoid structures or whether their main role is to maintain the activation and survival of Th2 cells at the tumor site. Their ability to maintain Th2 cell phenotype and effector function is supported by our earlier studies showing that T cells isolated from experimental breast tumors and transferred to naive tumor-bearing humanized mice can promote tumor development even at low numbers and upon single injection (Aspord et al., 2007).

Our results add another feature to the role of OX40L in tumors. Indeed, several studies in mouse models of transplantable tumors suggested that engaging OX40 via an agonist antibody, OX40L.Fc, or transfected tumor cells and DCs appears to promote antitumor effects (Weinberg et al., 2000; Morris et al., 2001; Ali et al., 2004; Piconese et al., 2008). However, *Tnfsf4* (gene coding OX40L) is regulated by the mRNA MIRN125B (Smirnov and Cheung, 2008), whose expression is down-regulated in breast cancer (Iorio et al., 2005). *Tnfsf4* is up-regulated in ataxia telangiectasia carriers and patients (Smirnov and Cheung, 2008), who have been shown to have an increased risk of breast cancer (Swift et al., 1987). Furthermore, a recent pilot study described the expression of OX40 and OX40L in >100 tissue samples from invasive ductal carcinomas, and suggested a possible association of OX40 expression and lymph node metastatic status (Xie et al., 2010). OX40L signaling has several important features that might help explain the results observed in our and other studies. Thus, OX40L triggers Th2 polarization independent of IL-4, promotes TNF production, and inhibits IL-10 production by the developing Th2 cells, but only in the absence of IL-12. In the presence of IL-12, OX40L signaling instead promotes the development of Th1 cells that, like inflammatory Th2 cells, produce TNF but not IL-10 (Liu et al., 2007).

Interestingly, inflammatory Th2 cells coexist within the tumor immune environment alongside IL-10–secreting $CD4^+$ T cells. Recent studies demonstrate a colocalization of cells with the phenotype of T reg cells) with mature DCs in lymphoid infiltrates in breast cancer (Gobert et al., 2009). A high number of $FoxP3^+$ T reg cells was associated with disease relapse (Gobert et al., 2009). Thus, the niche finding and metastasis formation might be facilitated by inflammatory Th2 response, whereas in the established tumor a T reg cell response might prevail. Interestingly, CCL22 (a macrophage-derived chemokine) appears involved in the attraction of T reg cells (Gobert et al., 2009), but also, in cooperation with CCL17 (TARC), of inflammatory Th2 cells (Liu et al., 2007). How this fine balance between T reg cells and Th2 responses is regulated will require further study.

Two key questions arise from our work: (1) what are the mechanisms allowing TSLP release from cancer cells; and (2) what is the impact of IL-13 (and IL-4) on cancer cells, on the stroma, and on the immune infiltrate? Our data show that nonmalignant breast epithelia can express TSLP. This further demonstrates that cancer cells can exploit pathways that are present in the normal tissue to establish a microenvironment facilitating tumor development. The mechanisms regulating TSLP expression and secretion from cancer cells, including a potential link with oncogenic events, remain to be established. It will also be important to determine the impact of TSLP and inflammatory Th2 environment on the stromal fibroblasts. Indeed, recent studies point to the critical role of cross talk between cancer cells and fibroblasts in determining the type of microenvironment established by cancer cells originating from different types of breast cancers (Camp et al., 2011).

Interestingly, studies in mice suggest the role of Th2 cytokines in mammary gland development. Indeed, the differentiation of the luminal epithelial lineage appears to require autocrine signaling by Th2 cytokines, as shown by reduced differentiation and alveolar morphogenesis in both Stat6 and IL-4–/IL-13–deficient mice during pregnancy (Khaled et al., 2007). Yet, in the murine model of endogenous breast cancer type 2, polarized $CD4^+$ T cells are essential to the metastatic process via secretion of IL-4, which induces macrophages to secrete epidermal growth factor (DeNardo et al., 2009). Similar to endogenous mouse model, in our model of transplanted metastatic human breast cancer IL-13 is derived from microenvironment. IL-13 can exert pro-cancer activity in several ways, including the triggering of TGF-β secretion (Terabe et al., 2000, 2003; Park et al., 2005; Shimamura et al., 2010). Furthermore, IL-4 exposure of cancer cells leads to the up-regulation of antiapoptotic pathways via mobilization of STAT6 (Zhang et al., 2008). We have shown that STAT6 is phosphorylated in primary breast cancer tumors (Aspord et al., 2007). All these antiapoptotic pathways are likely to synergize to promote the survival of cancer cells and facilitate metastasis. Importantly, such a protective effect on cancer cell susceptibility to apoptosis might increase their resistance to chemotherapy (Todaro et al., 2008) and immune-mediated cytotoxicity driven by Granzyme B (Sarin et al., 1997; Heibein et al., 2000). Thus, the TSLP–OX40L–IL13 axis might offer a novel therapeutic target.

MATERIALS AND METHODS

Isolation and culture of myeloid dendritic cells. DCs were purified from buffy coat of blood from healthy donors. In brief, DCs were enriched from mononuclear cells by negative selection using a mixture of antibodies against linage markers for CD3, CD14, CD16, CD19, CD56, and glycophorin A (Dynabeads Human DC Enrichment kit; Invitrogen). Cells from negative fraction were immunolabeled with anti–human FITC-labeled lienage cocktail (CD3, CD14, CD16, CD19, CD20, and CD56; BD); PE-labeled CD123 (mIgG1; clone 9F5; BD), QR-labeled HLA-DR (mIgG2a; clone HK14; Sigma-Aldrich) and APC-labeled CD11c (mIgG2b; clone S-HCL-3; BD). DCs (lin^-, $CD123^-$, $HLA\text{-}DR^+$, $CD11c^+$) were sorted in a FACSAria cytometer (BD). DCs were seeded at 100×10^3 cells/well in 200 µl of medium (RPMI supplemented with 2 mM glutamine, 50 U/ml penicillin, 50 µg/ml streptomycin, 0.1 mM MEM nonessential amino acids, 10 mM Hepes buffer, 0.1 mM sodium pyruvate, and 10% of human AB serum). DCs were cultured with medium alone or in the presence of 20 ng/ml of TSLP, or different tumor derived products. After 48 h, DCs were harvested and washed. The stimulated cells were stained for phenotype analysis or co-cultured with allogeneic naive $CD4^+$ T cells.

Immunofluorescence. 6-µm-frozen sections from tissues were fixed with cold acetone for 5 min. The sections were labeled with 5 µg/ml of anti-OX40L antibody (mouse IgG1, 8F4), followed by anti–mouse IgG conjugated to Texas red (Jackson ImmunoResearch Laboratories). For IL-13, tissue was labeled with 10 µg/ml of anti–IL-13 (polyclonal goat IgG; AF-123-NA; R&D System) followed with Texas red anti–goat IgG (Jackson ImmunoResearch Laboratories). TSLP was detected with 10 µg/ml of mouse anti-TSLP antibody prepared in-house (mIgG1; clone 14C3.2E11). Cytokeratin 19 was labeled with monoclonal antibody clone A53-BA2 (IgG2a; Abcam), followed by Alexa Fluor 568 goat anti–mouse IgG2a (Invitrogen). The following direct-labeled antibodies used were as follows: FITC anti–HLA-DR (mouse IgG2a; L243; BD), FITC anti-CD11c (clone; KB 90; Dako), FITC anti-Ki67

(clone ki-67; Dako), and Alexa Fluor 488 anti-CD3 (mIgG1; UCHT1; BD). Finally, sections were counterstained for 2 min with 3 µM of the nuclear stain DAPI (in PBS; Invitrogen). To confirm specificity of TSLP staining, primary anti-TSLP antibody was preincubated with 100 µg of recombinant human TSLP (R&D Systems) for 30 min at room temperature before staining of tissue sections that previously showed to be TSLP positive.

Flow cytometry analysis. Cell suspensions from human breast carcinoma tissue and tumor or draining lymph nodes from humanized mice were used for phenotypic characterization of leukocytes. Cell suspensions were obtained by digestion with 2.5 mg/ml of collagenase D (Roche), and 200 U/ml of DNase I (Sigma-Aldrich) for 30–60 min at 37°C. The anti–human antibodies used were as follows: labeled FITC-labeled lineage cocktail (CD3, CD14, CD16, CD19, CD20, and CD56; BD); PE-labeled OX40L (mIgG1; clone Ik-1; BD); QR-labeled HLA-DR (mIgG2a; clone HK14; Sigma-Aldrich); APC-labeled CD11c (mIgG2b; clone S-HCL-3; BD); PerCP-labeled CD3 (mIgG1; clone SK7; BD); PECy7-labeled CD4 (mIgG1; clone SK3; BD); APCCy7-labeled CD8 (mIgG1; clone SK1; BD); CFS-labeled IL-4 (mIgG1; clone 3007; R&D Systems); Pacific blue–labeled IL-10 (rat IgG1; clone JES3-9D7; eBioscience); PE-labeled IL-13 (rat IgG1; clone JES10-5A2 BD); APC-labeled TNF (mIgG1; clone 6401.1111; BD); Alexa Fluor 700–labeled IFN-γ (mIgG1; clone B27; BD). Cells were incubated with the antibodies for 30 min at 4°C in the dark, and then washed three times and fixed with 1% paraformaldehyde to be analyzed in a FACSCalibur or LSR-II cytometer (BD). For intracellular cytokines, cells were stained using BD Cytofix/Cytoperm fixation/permeabilization kit according to the manufacturer's directions.

Tumor factors preparation. Tumor factors were obtained from supernatant of established breast cancer cell lines cultured in vitro (Table S2; Soule et al., 1973; Hackett et al., 1977; Lacroix and Leclercq, 2004; Neve et al., 2006) or by sonication from tumor cell lines, human breast tumor tissue, or tumors from humanized mice. In brief, cell lines were culture in medium (RPMI supplemented with 2 mM glutamine, 50 U/ml penicillin, 50 µg/ml streptomycin, 0.1 mM MEM nonessential amino acids, 10 mM Hepes buffer, 0.1 mM sodium pyruvate, and 10% fetal calf serum), and when the cells reached 90% of confluence fresh medium was added and the cells were left in culture for an additional 48 h. For sonication, cells or tissues were placed in PBS and disrupted for 30 s at 4°C, with the power output adjusted at 4.5 level of the 60 sonic dismembrator (Thermo Fisher Scientific). Cellular debris was removed by centrifugation, and the supernatant was collected and stored at −80°C.

Cytokine analysis. Tumor samples from patients diagnosed with breast carcinoma (in situ, invasive duct, and/or mucinous carcinoma of the breast, as well as lobular carcinoma) were obtained from the Baylor University Medical Center Tissue Bank (Institutional Review Board no. 005–145). Tumors and draining lymph nodes from mice implanted with breast cancer cell lines H578T and MDA-MB-231 were also analyzed. Whole-tissue fragments (4 × 4 × 4 mm, 0.02 g, approximately) were placed in culture medium with 50 ng/ml of PMA (Sigma-Aldrich) and 1 µg/ml of ionomycin (Sigma-Aldrich) for 16 h. Cytokine production was analyzed in the culture supernatant by Luminex. For intracellular staining, cells were resuspended at a concentration of 10^6 cells/ml in medium and activated for 5 h with PMA and ionomycin; brefeldin A (GolgiPlug; BD) and monensin (GolgiStop; BD) were added for the last 2.5 h.

DC–T cell co-cultures. Total $CD4^+$ T cells were enriched from PBMCs of healthy donors using magnetic depletion of other leukocytes (EasySep Human $CD4^+$ T Cell Enrichment kit; STEMCELL Technologies, Inc.). Naive $CD4^+$ T cells were sorted based on the expression of $CD4^+$ $CD27^+$ and $CD45RA^+$. Activated mDCs with medium, TSLP, or tumor-derived factors were co-cultured with naive $CD4^+$ T cells at a ratio of 1:5 for 7 d. After that, the cells were washed and restimulated for 5 h with 50 ng/ml PMA and 1 µl/ml ionomycin. Brefeldin A and monensin were added for the last 2.5 h, followed by surface and intracellular staining. For blocking OX40L, tumor-activated mDCs were co-cultured with naive $CD4^+$ T cells in the presence of 50 µg of anti-OX40L (Ik-5 clone) or control IgG2a isotype antibody. For blocking TSLP, tumor-derived factors were preincubated with 20 µg/ml of anti-TSLP antibody (rabbit; AB 19024) or normal rabbit IgG (R&D Systems) at room temperature for 30 min after DC activation. DCs were activated with the neutralized tumor-derived factors and finally co-cultured with naive $CD4^+$ T cells for 7 d. For TSLPR blocking, DCs were preincubated with anti-TSLP receptor antibody (clone AB81_85.1F11; mouse IgG1) for 3 min at room temperature.

Tumor-bearing mice. Mice were humanized either by $CD34^+$ hematopoietic progenitor cell (HPC) transplant or by co-administration of DCs and T cells as described previously (Aspord et al., 2007; Institutional Animal Care and Use Committee no. A01-005). $CD34^+$HPCs were obtained from apheresis of adult healthy volunteers mobilized with G-CSF and purified as described previously (Aspord et al., 2007). The $CD34^-$ fraction of apheresis was Ficoll purified, and the PBMCs obtained were stored frozen and used as a source of autologous T cells. 3 million $CD34^+$ HPCs were transplanted intravenously into sublethally irradiated (12 cGy/g body weight of 137Cs γ irradiation) nonobese diabetic/LtSz-scid/scid β2 microglobulin–deficient (NOD/SCID/$\beta2m^{-/-}$) mice (Jackson ImmunoResearch Laboratories). After 4 wk of engraftment, 10 million Hs578T breast cancer cells were harvested from cultures and injected subcutaneously into the flanks of the mice. Mice were reconstituted with 10 million $CD4^+$ T cells and 10 million $CD8^+$ T cells autologous to the grafted $CD34^+$ HPCs. $CD4^+$ and $CD8^+$ T cells were positively selected from thawed PBMCs using magnetic selection according to the manufacturer's instructions (Miltenyi Biotec). The purity was routinely >90%. T cells were transferred at days 3, 6, and 9 after tumor implantation. For experiments with NOD/SCID/$\beta2m^{-/-}$ mice, they were sublethally irradiated the day before tumor implantation. Mice were then reconstituted with 1 million monocyte-derived DCs (MDDCs) and autologous T cells as described in the previous paragraph. MDDCs were generated from the adherent fraction of PBMCs by culturing with 100 ng/ml GM-CSF (Immunex) and 10 ng/ml IL-4 (R&D Systems). Tumor size was monitored every 2–3 d. Tumor volume (ellipsoid) was calculated as follows: ([short diameter]^2 × long diameter)/2.

Blocking in vivo experiments. For different experimental purposes, tumor-bearing mice transferred with autologous T cells were injected intratumorally with 200 µg of anti-OX40L (clone IK-5; mIgG2a) blocking antibody, 100 µg of anti-TSLP antibody (clone AB19024; rabbit IgG), 100 µg of anti-IL-13 neutralizing antibody prepared in-house (clone 13G1.B2; mIgG1), 200 µg of anti-TSLPR neutralizing antibody (clone AB81_85.1F11; mouse IgG1), or isotype control, respectively at days 3, 6, and 9 after tumor implantation. For blocking TSLP, anti-TSLP antibody injection was also given at day 0 while the tumor was implanted.

Online supplemental material. Fig. S1 illustrates gating strategy for flow cytometry analysis of tumor-infiltrating lymphocytes and the accumulation of lymphocytes in tumor beds as compared with surrounding tissue. Fig. S2 shows that mDCs exposed to TSLP or to soluble tumor factors in the presence of anti-OX40L are unable to drive the differentiation of inflammatory Th2 cells. Fig. S3 shows the specificity of anti-TSLP antibody staining in frozen tissue sections. Fig. S4 shows the expression of TSLP in breast cancer cells and in nonmalignant breast tissue. Table S1 provides the pathological diagnosis information and Luminex data for cytokine levels of all 99 breast cancer patients used for cytokine analysis. Table S2 describes the characteristics of breast cancer cell lines studied. Online supplemental material is available at http://www.jem.org/cgi/content/full/jem.20102131/DC1.

We are grateful to Albert Barnes, Sebastien Coquery, Elizabeth Kraus, Mark Michnevitz, Gina Stella Garcia-Romo, Jenny Smith, and Lynnette Walters for help; Dr. Joseph Fay for help with healthy volunteers; Cindy Samuelsen for continuous support; and Drs. Sally M. Knox and Michael Grant at the Department of Surgery

and Ms. Dan Su at the Department of Pathology at Baylor University Medical Center. We thank Dr. Michael Ramsay for continuous support.

This work was supported by the Baylor Health Care Systems Foundation, and the National Institutes of Health (grants R0-1 CA89440 and R21 AI056001 to A. Karolina Palucka; grants U19 AI057234, R0-1 CA78846, and CA85540 to J. Banchereau).

J. Banchereau holds the Caruth Chair for Transplantation Immunology Research.

A. Karolina Palucka holds the Ramsay Chair for Cancer Immunology Research.

The authors have no conflicting financial interests.

Submitted: 7 October 2010
Accepted: 27 January 2011

REFERENCES

Ali, S.A., M. Ahmad, J. Lynam, C.S. McLean, C. Entwisle, P. Loudon, E. Choolun, S.E. McArdle, G. Li, S. Mian, and R.C. Rees. 2004. Anti-tumour therapeutic efficacy of OX40L in murine tumour model. *Vaccine*. 22:3585–3594. doi:10.1016/j.vaccine.2004.03.041

Aspord, C., A. Pedroza-Gonzalez, M. Gallegos, S. Tindle, E.C. Burton, D. Su, F. Marches, J. Banchereau, and A.K. Palucka. 2007. Breast cancer instructs dendritic cells to prime interleukin 13–secreting CD4+ T cells that facilitate tumor development. *J. Exp. Med.* 204:1037–1047. doi:10.1084/jem.20061120

Bell, D., P. Chomarat, D. Broyles, G. Netto, G.M. Harb, S. Lebecque, J. Valladeau, J. Davoust, K.A. Palucka, and J. Banchereau. 1999. In breast carcinoma tissue, immature dendritic cells reside within the tumor, whereas mature dendritic cells are located in peritumoral areas. *J. Exp. Med.* 190:1417–1426. doi:10.1084/jem.190.10.1417

Berzofsky, J.A., and M. Terabe. 2008. A novel immunoregulatory axis of NKT cell subsets regulating tumor immunity. *Cancer Immunol. Immunother.* 57:1679–1683. doi:10.1007/s00262-008-0495-4

Brimnes, M.K., L. Bonifaz, R.M. Steinman, and T.M. Moran. 2003. Influenza virus–induced dendritic cell maturation is associated with the induction of strong T cell immunity to a coadministered, normally nonimmunogenic protein. *J. Exp. Med.* 198:133–144. doi:10.1084/jem.20030266

Camp, J.T., F. Elloumi, E. Roman-Perez, J. Rein, D.A. Stewart, J.C. Harrell, C.M. Perou, and M.A. Troester. 2011. Interactions with fibroblasts are distinct in Basal-like and luminal breast cancers. *Mol. Cancer Res.* 9:3–13. doi:10.1158/1541-7786.MCR-10-0372

Caux, C., C. Massacrier, B. Vanbervliet, B. Dubois, I. Durand, M. Cella, A. Lanzavecchia, and J. Banchereau. 1997. CD34+ hematopoietic progenitors from human cord blood differentiate along two independent dendritic cell pathways in response to granulocyte-macrophage colony-stimulating factor plus tumor necrosis factor alpha: II. Functional analysis. *Blood.* 90:1458–1470.

Condeelis, J., and J.W. Pollard. 2006. Macrophages: obligate partners for tumor cell migration, invasion, and metastasis. *Cell.* 124:263–266. doi:10.1016/j.cell.2006.01.007

Coughlin, S.S., and D.U. Ekwueme. 2009. Breast cancer as a global health concern. *Cancer Epidemiol.* 33:315–318. doi:10.1016/j.canep.2009.10.003

Coussens, L.M., and Z. Werb. 2002. Inflammation and cancer. *Nature.* 420:860–867. doi:10.1038/nature01322

Croft, M., T. So, W. Duan, and P. Soroosh. 2009. The significance of OX40 and OX40L to T-cell biology and immune disease. *Immunol. Rev.* 229:173–191. doi:10.1111/j.1600-065X.2009.00766.x

DeNardo, D.G., J.B. Barreto, P. Andreu, L. Vasquez, D. Tawfik, N. Kolhatkar, and L.M. Coussens. 2009. CD4(+) T cells regulate pulmonary metastasis of mammary carcinomas by enhancing protumor properties of macrophages. *Cancer Cell.* 16:91–102. doi:10.1016/j.ccr.2009.06.018

Dudziak, D., A.O. Kamphorst, G.F. Heidkamp, V.R. Buchholz, C. Trumpfheller, S. Yamazaki, C. Cheong, K. Liu, H.W. Lee, C.G. Park, et al. 2007. Differential antigen processing by dendritic cell subsets *in vivo*. *Science.* 315:107–111. doi:10.1126/science.1136080

Finkelman, F.D., A. Lees, R. Birnbaum, W.C. Gause, and S.C. Morris. 1996. Dendritic cells can present antigen in vivo in a tolerogenic or immunogenic fashion. *J. Immunol.* 157:1406–1414.

Gilliet, M., V. Soumelis, N. Watanabe, S. Hanabuchi, S. Antonenko, R. de Waal-Malefyt, and Y.J. Liu. 2003. Human dendritic cells activated by TSLP and CD40L induce proallergic cytotoxic T cells. *J. Exp. Med.* 197:1059–1063. doi:10.1084/jem.20030240

Gobert, M., I. Treilleux, N. Bendriss-Vermare, T. Bachelot, S. Goddard-Leon, V. Arfi, C. Biota, A.C. Doffin, I. Durand, D. Olive, et al. 2009. Regulatory T cells recruited through CCL22/CCR4 are selectively activated in lymphoid infiltrates surrounding primary breast tumors and lead to an adverse clinical outcome. *Cancer Res.* 69:2000–2009. doi:10.1158/0008-5472.CAN-08-2360

Grivennikov, S.I., F.R. Greten, and M. Karin. 2010. Immunity, inflammation, and cancer. *Cell.* 140:883–899. doi:10.1016/j.cell.2010.01.025

Hackett, A.J., H.S. Smith, E.L. Springer, R.B. Owens, W.A. Nelson-Rees, J.L. Riggs, and M.B. Gardner. 1977. Two syngeneic cell lines from human breast tissue: the aneuploid mammary epithelial (Hs578T) and the diploid myoepithelial (Hs578Bst) cell lines. *J. Natl. Cancer Inst.* 58:1795–1806.

Hawiger, D., K. Inaba, Y. Dorsett, M. Guo, K. Mahnke, M. Rivera, J.V. Ravetch, R.M. Steinman, and M.C. Nussenzweig. 2001. Dendritic cells induce peripheral T cell unresponsiveness under steady state conditions in vivo. *J. Exp. Med.* 194:769–779. doi:10.1084/jem.194.6.769

Heibein, J.A., I.S. Goping, M. Barry, M.J. Pinkoski, G.C. Shore, D.R. Green, and R.C. Bleackley. 2000. Granzyme B-mediated cytochrome c release is regulated by the Bcl-2 family members bid and Bax. *J. Exp. Med.* 192:1391–1402. doi:10.1084/jem.192.10.1391

Iorio, M.V., M. Ferracin, C.G. Liu, A. Veronese, R. Spizzo, S. Sabbioni, E. Magri, M. Pedriali, M. Fabbri, M. Campiglio, et al. 2005. MicroRNA gene expression deregulation in human breast cancer. *Cancer Res.* 65:7065–7070. doi:10.1158/0008-5472.CAN-05-1783

Ito, T., Y.H. Wang, O. Duramad, T. Hori, G.J. Delespesse, N. Watanabe, F.X. Qin, Z. Yao, W. Cao, and Y.J. Liu. 2005. TSLP-activated dendritic cells induce an inflammatory T helper type 2 cell response through OX40 ligand. *J. Exp. Med.* 202:1213–1223. doi:10.1084/jem.20051135

Kapp, U., W.C. Yeh, B. Patterson, A.J. Elia, D. Kägi, A. Ho, A. Hessel, M. Tipsword, A. Williams, C. Mirtsos, et al. 1999. Interleukin 13 is secreted by and stimulates the growth of Hodgkin and Reed-Sternberg cells. *J. Exp. Med.* 189:1939–1946. doi:10.1084/jem.189.12.1939

Khaled, W.T., E.K. Read, S.E. Nicholson, F.O. Baxter, A.J. Brennan, P.J. Came, N. Sprigg, A.N. McKenzie, and C.J. Watson. 2007. The IL-4/IL-13/Stat6 signalling pathway promotes luminal mammary epithelial cell development. *Development.* 134:2739–2750. doi:10.1242/dev.003194

Klechevsky, E., R. Morita, M. Liu, Y. Cao, S. Coquery, L. Thompson-Snipes, F. Briere, D. Chaussabel, G. Zurawski, A.K. Palucka, et al. 2008. Functional specializations of human epidermal Langerhans cells and CD14+ dermal dendritic cells. *Immunity.* 29:497–510. doi:10.1016/j.immuni.2008.07.013

Lacroix, M., and G. Leclercq. 2004. Relevance of breast cancer cell lines as models for breast tumours: an update. *Breast Cancer Res. Treat.* 83:249–289. doi:10.1023/B:BREA.0000014042.54925.cc

Levings, M.K., S. Gregori, E. Tresoldi, S. Cazzaniga, C. Bonini, and M.G. Roncarolo. 2005. Differentiation of Tr1 cells by immature dendritic cells requires IL-10 but not CD25+CD4+ Tr cells. *Blood.* 105:1162–1169. doi:10.1182/blood-2004-03-1211

Liu, Y.J., V. Soumelis, N. Watanabe, T. Ito, Y.H. Wang, Rde.W. Malefyt, M. Omori, B. Zhou, and S.F. Ziegler. 2007a. TSLP: an epithelial cell cytokine that regulates T cell differentiation by conditioning dendritic cell maturation. *Annu. Rev. Immunol.* 25:193–219. doi:10.1146/annurev.immunol.25.022106.141718

Luft, T., M. Jefford, P. Luetjens, T. Toy, H. Hochrein, K.A. Masterman, C. Maliszewski, K. Shortman, J. Cebon, and E. Maraskovsky. 2002. Functionally distinct dendritic cell (DC) populations induced by physiologic stimuli: prostaglandin E(2) regulates the migratory capacity of specific DC subsets. *Blood.* 100:1362–1372. doi:10.1182/blood-2001-12-0360

Maldonado-López, R., T. De Smedt, P. Michel, J. Godfroid, B. Pajak, C. Heirman, K. Thielemans, O. Leo, J. Urbain, and M. Moser. 1999. CD8alpha+ and CD8alpha- subclasses of dendritic cells direct the development of distinct T helper cells in vivo. *J. Exp. Med.* 189:587–592. doi:10.1084/jem.189.3.587

Mantovani, A., and A. Sica. 2010. Macrophages, innate immunity and cancer: balance, tolerance, and diversity. *Curr. Opin. Immunol.* 22:231–237. doi:10.1016/j.coi.2010.01.009

Mantovani, A., P. Romero, A.K. Palucka, and F.M. Marincola. 2008. Tumour immunity: effector response to tumour and role of the microenvironment. *Lancet*. 371:771–783. doi:10.1016/S0140-6736(08)60241-X

Morris, A., J.T. Vetto, T. Ramstad, C.J. Funatake, E. Choolun, C. Entwisle, and A.D. Weinberg. 2001. Induction of anti-mammary cancer immunity by engaging the OX-40 receptor in vivo. *Breast Cancer Res. Treat.* 67:71–80. doi:10.1023/A:1010649303056

Neve, R.M., K. Chin, J. Fridlyand, J. Yeh, F.L. Baehner, T. Fevr, L. Clark, N. Bayani, J.P. Coppe, F. Tong, et al. 2006. A collection of breast cancer cell lines for the study of functionally distinct cancer subtypes. *Cancer Cell*. 10:515–527. doi:10.1016/j.ccr.2006.10.008

Park, J.M., M. Terabe, L.T. van den Broeke, D.D. Donaldson, and J.A. Berzofsky. 2005. Unmasking immunosurveillance against a syngeneic colon cancer by elimination of CD4+ NKT regulatory cells and IL-13. *Int. J. Cancer*. 114:80–87. doi:10.1002/ijc.20669

Park, J.M., M. Terabe, D.D. Donaldson, G. Forni, and J.A. Berzofsky. 2008. Natural immunosurveillance against spontaneous, autochthonous breast cancers revealed and enhanced by blockade of IL-13-mediated negative regulation. *Cancer Immunol. Immunother.* 57:907–912. doi:10.1007/s00262-007-0414-0

Piconese, S., B. Valzasina, and M.P. Colombo. 2008. OX40 triggering blocks suppression by regulatory T cells and facilitates tumor rejection. *J. Exp. Med.* 205:825–839. doi:10.1084/jem.20071341

Pulendran, B., J.L. Smith, G. Caspary, K. Brasel, D. Pettit, E. Maraskovsky, and C.R. Maliszewski. 1999. Distinct dendritic cell subsets differentially regulate the class of immune response in vivo. *Proc. Natl. Acad. Sci. USA*. 96:1036–1041. doi:10.1073/pnas.96.3.1036

Rakoff-Nahoum, S., and R. Medzhitov. 2009. Toll-like receptors and cancer. *Nat. Rev. Cancer*. 9:57–63. doi:10.1038/nrc2541

Sarin, A., M.S. Williams, M.A. Alexander-Miller, J.A. Berzofsky, C.M. Zacharchuk, and P.A. Henkart. 1997. Target cell lysis by CTL granule exocytosis is independent of ICE/Ced-3 family proteases. *Immunity*. 6:209–215. doi:10.1016/S1074-7613(00)80427-6

Shimamura, T., T. Fujisawa, S.R. Husain, B. Joshi, and R.K. Puri. 2010. Interleukin 13 mediates signal transduction through interleukin 13 receptor alpha2 in pancreatic ductal adenocarcinoma: role of IL-13 Pseudomonas exotoxin in pancreatic cancer therapy. *Clin. Cancer Res.* 16:577–586. doi:10.1158/1078-0432.CCR-09-2015

Skinnider, B.F., A.J. Elia, R.D. Gascoyne, L.H. Trümper, F. von Bonin, U. Kapp, B. Patterson, B.E. Snow, and T.W. Mak. 2001. Interleukin 13 and interleukin 13 receptor are frequently expressed by Hodgkin and Reed-Sternberg cells of Hodgkin lymphoma. *Blood*. 97:250–255. doi:10.1182/blood.V97.1.250

Skinnider, B.F., A.J. Elia, R.D. Gascoyne, B. Patterson, L. Trumper, U. Kapp, and T.W. Mak. 2002. Signal transducer and activator of transcription 6 is frequently activated in Hodgkin and Reed-Sternberg cells of Hodgkin lymphoma. *Blood*. 99:618–626. doi:10.1182/blood.V99.2.618

Smirnov, D.A., and V.G. Cheung. 2008. ATM gene mutations result in both recessive and dominant expression phenotypes of genes and microRNAs. *Am. J. Hum. Genet.* 83:243–253. doi:10.1016/j.ajhg.2008.07.003

Soule, H.D., J. Vazguez, A. Long, S. Albert, and M. Brennan. 1973. A human cell line from a pleural effusion derived from a breast carcinoma. *J. Natl. Cancer Inst.* 51:1409–1416.

Soumelis, V., P.A. Reche, H. Kanzler, W. Yuan, G. Edward, B. Homey, M. Gilliet, S. Ho, S. Antonenko, A. Lauerma, et al. 2002. Human epithelial cells trigger dendritic cell mediated allergic inflammation by producing TSLP. *Nat. Immunol.* 3:673–680.

Steinbrink, K., H. Jonuleit, G. Müller, G. Schuler, J. Knop, and A.H. Enk. 1999. Interleukin-10-treated human dendritic cells induce a melanoma-antigen-specific anergy in CD8(+) T cells resulting in a failure to lyse tumor cells. *Blood*. 93:1634–1642.

Steinman, R.M., and J. Banchereau. 2007. Taking dendritic cells into medicine. *Nature*. 449:419–426. doi:10.1038/nature06175

Steinman, R.M., D. Hawiger, and M.C. Nussenzweig. 2003. Tolerogenic dendritic cells. *Annu. Rev. Immunol.* 21:685–711. doi:10.1146/annurev.immunol.21.120601.141040

Swift, M., P.J. Reitnauer, D. Morrell, and C.L. Chase. 1987. Breast and other cancers in families with ataxia-telangiectasia. *N. Engl. J. Med.* 316:1289–1294. doi:10.1056/NEJM198705213162101

Terabe, M., S. Matsui, N. Noben-Trauth, H. Chen, C. Watson, D.D. Donaldson, D.P. Carbone, W.E. Paul, and J.A. Berzofsky. 2000. NKT cell-mediated repression of tumor immunosurveillance by IL-13 and the IL-4R-STAT6 pathway. *Nat. Immunol.* 1:515–520. doi:10.1038/82771

Terabe, M., S. Matsui, J.M. Park, M. Mamura, N. Noben-Trauth, D.D. Donaldson, W. Chen, S.M. Wahl, S. Ledbetter, B. Pratt, et al. 2003. Transforming growth factor-beta production and myeloid cells are an effector mechanism through which CD1d-restricted T cells block cytotoxic T lymphocyte-mediated tumor immunosurveillance: abrogation prevents tumor recurrence. *J. Exp. Med.* 198:1741–1752. doi:10.1084/jem.20022227

Todaro, M., Y. Lombardo, M.G. Francipane, M.P. Alea, P. Cammareri, F. Iovino, A.B. Di Stefano, C. Di Bernardo, A. Agrusa, G. Condorelli, et al. 2008. Apoptosis resistance in epithelial tumors is mediated by tumor-cell-derived interleukin-4. *Cell Death Differ.* 15:762–772. doi:10.1038/sj.cdd.4402305

Trieu, Y., X.Y. Wen, B.F. Skinnider, M.R. Bray, Z. Li, J.O. Claudio, E. Masih-Khan, Y.X. Zhu, S. Trudel, J.A. McCart, et al. 2004. Soluble interleukin-13Ralpha2 decoy receptor inhibits Hodgkin's lymphoma growth in vitro and in vivo. *Cancer Res.* 64:3271–3275. doi:10.1158/0008-5472.CAN-03-3764

Villablanca, E.J., L. Raccosta, D. Zhou, R. Fontana, D. Maggioni, A. Negro, F. Sarvito, M. Ponzoni, B. Valentinis, M. Bregni, et al. 2010. Tumor-mediated liver X receptor-alpha activation inhibits CC chemokine receptor-7 expression on dendritic cells and dampens antitumor responses. *Nat. Med.* 16:98–105. doi:10.1038/nm.2074

Watanabe, N., S. Hanabuchi, M.A. Marloie-Provost, S. Antonenko, Y.J. Liu, and V. Soumelis. 2005a. Human TSLP promotes CD40 ligand-induced IL-12 production by myeloid dendritic cells but maintains their Th2 priming potential. *Blood*. 105:4749–4751. doi:10.1182/blood-2004-09-3622

Watanabe, N., Y.H. Wang, H.K. Lee, T. Ito, Y.H. Wang, W. Cao, and Y.J. Liu. 2005b. Hassall's corpuscles instruct dendritic cells to induce CD4+CD25+ regulatory T cells in human thymus. *Nature*. 436:1181–1185. doi:10.1038/nature03886

Weinberg, A.D., M.M. Rivera, R. Prell, A. Morris, T. Ramstad, J.T. Vetto, W.J. Urba, G. Alvord, C. Bunce, and J. Shields. 2000. Engagement of the OX-40 receptor in vivo enhances antitumor immunity. *J. Immunol.* 164:2160–2169.

Xie, F., Q. Wang, Y. Chen, Y. Gu, H. Mao, W. Zeng, and X. Zhang. 2010. Costimulatory molecule OX40/OX40L expression in ductal carcinoma in situ and invasive ductal carcinoma of breast: an immunohistochemistry-based pilot study. *Pathol. Res. Pract.* 206:735–739. doi:10.1016/j.prp.2010.05.016

Zhang, W.J., B.H. Li, X.Z. Yang, P.D. Li, Q. Yuan, X.H. Liu, S.B. Xu, Y. Zhang, J. Yuan, G.S. Gerhard, et al. 2008. IL-4-induced Stat6 activities affect apoptosis and gene expression in breast cancer cells. *Cytokine*. 42:39–47. doi:10.1016/j.cyto.2008.01.016

Ziegler, S.F., and D. Artis. 2010. Sensing the outside world: TSLP regulates barrier immunity. *Nat. Immunol.* 11:289–293. doi:10.1038/ni.1852

APPENDIX B

Ligation of dectin-1 on tumor infiltrating dendritic cells promotes breast cancer rejection
(Submitted)

Ligation of dectin-1 on tumor infiltrating dendritic cells promotes breast cancer rejection.

Te-Chia Wu[1,2], Kangling Xu[1,2], Romain Banchereau[1], Florentina Marches[1], Chun I Yu[1], Jan Martinek[1], Esperanza Anguiano[1], Alexander Pedroza-Gonzalez[1], G. Jackson Snipes[3], Joyce O'Shaughnessy[4], Stephen Nishimura[5], Yong-Jun Liu[1], Virginia Pascual[1], Jacques Banchereau[1], Sangkon Oh[1] and Karolina Palucka[1,6]

From [1]Ralph Steinman Center for Cancer Vaccines, Baylor Institute for Immunology Research, Baylor Research Institute, Dallas, TX; [2]Baylor University, Waco, TX; [3]Baylor University Medical Center, Sammons Cancer Center, Dallas, TX; [4] Baylor Sammons Cancer Center, Texas Oncology, US Oncology, Dallas, TX; [5] Department of Pathology, USCF, San Francisco, CA; and [6]Department of Oncological Sciences, Mount Sinai School of Medicine, New York, NY.

Correspondence to Karolina Palucka, MD, PhD at karolinp@baylorhealth.edu

Breast cancer displays pro-tumor inflammation driven by tumor-infiltrating dendritic cells (DCs) and inflammatory T helper 2 (iTh2) cells. We show that intratumoral delivery of the β-glucan curdlan, a ligand of dectin-1, blocks the generation of iTh2 cells, and prevents breast cancer development in vivo. Curdlan reprograms tumor-infiltrating DCs which become resistant to cancer-derived thymic stromal lymphopoietin (TSLP), produce IL12p70 and help the generation of T helper 1 (Th1) cells. Curdlan-exposed DCs induce $CD8^+$ T cells to express CD103, a ligand for cancer cells E-cadherin. These $CD103^+CD8^+$ T cells accumulate in the tumors thereby increasing their necrosis and preventing their development in vivo. Thus, reprogramming tumor-infiltrating DCs represents a new strategy for enhancing tumor rejection.

Despite declining mortality rates due to improved therapies, breast cancer ranks second among cancer-related deaths in women (*1*). Thus, novel therapies are needed for these patients and immunotherapy, buttressed by its successes with PD-1- (*2*), CD40- (*3*) and CTLA-4-targeted therapy (*4*) represents an attractive option. Recent years witnessed an improved understanding of the tumor microenvironment critical roles for tumor growth, evasion from host immunity, and resistance to therapeutic agents (*5*). Thus, a better definition of the molecular and cellular components of tumor microenvironment will help us improve the clinical efficacy of current immunotherapy approaches and enable tailoring tumor specific-immunotherapies.

Breast and pancreatic cancer are infiltrated with inflammatory Th2 (iTh2) cells, which co-express IL-4/IL-13 and TNF-α but lack IL-10 (*6, 7*). Clinically, the Th2 signature in breast cancer (*8, 9*) and the expression of the Th2 master regulator GATA-3 in pancreatic cancer (*10*) are associated with poor outcomes. Experimentally, iTh2 cells accelerate tumor development in humanized mouse models of breast cancer through IL-13 (*6*). In genetically engineered mouse models of mammary cancer, iTh2 cells accelerate the development of pulmonary metastasis via IL-4 (*11*). IL-4 and IL-13 exert pro-tumor activity through several pathways including: 1. The triggering of TGF-β secretion (*12*); 2. The up-regulation of anti-apoptotic pathways in cancer cells (*13*); and 3. The generation of type-2 polarized macrophages that foster tumor growth directly, via secretion of growth factors, and indirectly via inhibitory effects on $CD8^+$ T cell function (*14*). Indeed, $CD8^+$ T cells are essential for tumor rejection through the generation of cytotoxic effectors. The presence of $CD8^+$ T cells in primary tumors is associated with the long-term survival of patients with colorectal and breast cancer (*14, 15*). Thus, iTh2 cells have a broad and profound impact on tumor microenvironment and tumor development.

The generation of iTh2 cells in breast cancer depends on mature tumor-infiltrating $OX40L^+$ dendritic cells (DCs) (*7*). In experimental models of breast cancer this DC phenotype is driven by cancer-derived thymic stromal lymphopoietin (TSLP) (*7, 16*). Previous studies have demonstrated that Dectin-1, an innate immune receptor with activating motifs (ITAMs), can

reprogram DC from inducing Th2 responses into Th1 responses (*17, 18*). We therefore investigated whether Curdlan, a natural ligand of Dectin-1 (*19*), could reprogram the function of breast tumor infiltrating DCs and promote anti-tumor immunity.

Immunofluorescence analysis of tissue samples from 27 primary breast cancers revealed the presence of Dectin-1 positive cells in all samples (**Supplement Figure 1 and Supplement Table 1**). In all tumors, $CD11c^{+}CD20^{-}HLA\text{-}DR^{+}CD83^{+}$ mature DCs expressing dectin-1 could be found in the peri-tumoral areas (**Figure 1A and Supplement Figure 1**). To establish whether ligation of Dectin-1 by curdlan in the tumor microenvironment might impact breast cancer development in vivo, we relied on a humanized mouse model of human breast cancer we described earlier (*6, 7*). As shown in **Figure 1B,** intratumoral administration of 10 μg of curdlan prevented the development of breast cancer and was as effective as the neutralizing anti-TSLP receptor antibody. The antitumor effect of curdlan has been observed in five independent experiments with a total of 23 mice that had been grafted with DCs and T cells isolated from different donors (**Figure 1C**). As breast tumor development is dependent on IL-13 (*6, 7*), we analyzed the cytokine profile of breast cancers that were harvested from humanized mice and activated with PMA and ionomycin (PMA/Iono). When compared to controls, curdlan-treated tumors produced significantly less IL-13 (DC+T: 1038±115 pg/ml; DC+T+curdlan: 361±62 pg/ml; n=23; $p<0.0001$) but similar levels of IFN-γ (DC+T: 6880±1796 pg/ml; DC+T+curdlan:10669±2081 pg/ml; n=23; p=0.17) and IL-10 (DC+T: 41±7.7 pg/ml; DC+T+curdlan:38±8 pg/ml; n=23; p=0.83) (**Figure 1D and Supplement Figure 2**). We have shown earlier that blood DCs exposed to breast cancer cell supernatants (BCsups) such as MDA-MB231, Hs578T and MCF-7 (**Supplement Table 2**) can induce the differentiation of naïve T cells into iTh2 cells (*6, 7*). To determine whether curdlan prevents the breast cancer induced polarization of DCs, purified blood $Lin^{neg}CD123^{neg}HLA\text{-}DR^{+}CD11c^{+}$ DCs were exposed for 48 hours to BCsups with and without curdlan, and subsequently co-cultured with naïve $CD4^{+}$T cells

for seven days. The cultured T cells were activated for 5 hrs with PMA/Iono and their cytokine profile was analyzed using intracellular cytokine staining (ICS) and flow cytometry. As expected, $CD4^+$ T cells exposed to DCs that had been pretreated with BCsups alone produced both IL-13 and TNF-α (22±3% of $CD4^+$ T cells). In contrast, T cells exposed to DCs treated with both BCsups and curdlan produced less IL-13 (6±0.3% of $CD4^+$ T cells; n=13; p<0.0001) (**Figures 1E and 1F**). In both cases, $CD4^+$ T cells produced IFN-γ (+BCsup-DC: 26 ± 0.5%; and +BCsup/curdlan-DC: 33±1.5% of CD4+ T cells, respectively; n=13; p=0.0002) (**Figures 1E and 1F**, **Supplement Figure 2**). To determine whether curdlan can reprogram the function of tumor-conditioned DCs, we sorted $OX40L^+$ DCs and $OX40L^-$ DCs that arise in response to BCsups. The sorted DCs were then exposed to curdlan for 24 hours, washed and co-cultured with naïve allogeneic T cells. As expected, $OX40L^+$ DCs induced T cells to express IL-13 while $OX40L^-$ DCs did not. Treatment of $OX40L^+$ DCs with curdlan altered their T cell polarization capacity as no IL-13 production was induced (**Figure 1G**). Thus, curdlan inhibits the development of human breast cancer by preventing the generation of pro-tumor iTh2 cells.

Adding curdlan to DCs prevented the induction of OX40L by BCsups (breast tumor-treated DCs=25 ± 2%; n=10; breast tumor-treated DCs+curdlan=6 ± 1.1%, n=10; P<0.0001 **(Figure 2A and Supplement Figure 3**). The inhibition of OX40L expression by curdlan was also observed when DCs were treated with human recombinant TSLP (**Supplement Figure 3)**. Conversely, the addition of anti-dectin-1 antibodies, which are not agonistic but block curdlan binding to DCs ((*17*) and **Supplement Figure 4**) before curdlan treatment allowed OX40L expression by DCs exposed to BCsups (**Figure 2B),** demonstrating that curdlan does indeed engage dectin-1. In vivo, administration of anti-dectin-1 antibodies to developing breast cancer tumors prevented the protective effect of curdlan (**Figure 2C**). These results confirm that curdlan acts through dectin-1 expressed by tumor-infiltrating DCs in breast cancer.

To determine whether curdlan can reprogram DC maturation rather than simply block it, we analyzed the expression of classical maturation markers. DCs treated with BCsups and curdlan showed high levels of CD83, CD80, CD86, CD70 and MHC class I (**Supplement Figure 5**). Thus, curdlan blocks specifically OX40L expression without interfering with other components of DC maturation program. OX40L transcription in DCs depends upon the phosphorylation of STAT5 and STAT6 (*20*). As we showed earlier, STAT6 in both the leukocyte infiltrate and the cancer cells is activated in breast cancer microenvironment (*17*). Exposure to Curdlan of BCsups-DCs led to enhanced phosphorylation of STAT4 and decreased phosphorylation of STAT6 (**Figure 2D**) thereby resulting in an increased pSTAT4/pSTAT6 ratio (**Supplement Figure 5**). This switch in STATs activation pattern likely explains the increased secretion of IL-12p70 by curdlan-treated DCs that leads to Th1 differentiation (**Figure 2E**). Adding anti-IL-12 neutralizing antibodies to co-cultures of naïve T cells with curdlan-treated BCsups-DCs restored generation of iTh2 cells (**Figure 2F**). Thus, curdlan enables STAT4 activation in BCsups-DCs resulting in increased IL-12 production and subsequent Th1 response.

The impact of dectin-1 ligation on tumor-conditioned DCs was further analyzed by transcriptional profiling. Curdlan treated BCsup-DCs over-expressed 314 transcripts and under-expressed 873 transcripts (**Figure 2G and H**). Ingenuity pathway analysis (IPA) of over-expressed transcripts revealed networks centered on NfκB, IL-6 and TNF (**Figure 2G and I**). The under-expressed transcripts formed networks centered on several transcription factors (**Figure 2J**). Curdlan-exposed DCs showed abundant transcription of DC maturation markers such as *CD86* and *TNFSF9* (4-1BBL); cytokines such as *GM-CSF, TNF, IL-6, IL-12, IL-15 and IL-23;* integrins including *ITGB8* which is involved in the activation of TGF-β (*21*); and several molecules possibly facilitating their migration including matrix metalloproteinase 7 (MMP7) (**Figure 2G and Supplement Table 3**). The latter one might facilitate DC migration to the

draining lymph nodes, a feature that appears blocked in breast cancer infiltrating DCs (*22*). Conversely, curdlan-exposed DCs under-expressed *CD14*, *CD68* and *CSF1R*, all of which are associated with an immature DCs phenotype. In addition, *CCR6* which contributes to immature DC retention at the tumor site by binding to MIP3-α (*22*), was also under-expressed consistent with DC maturation. Thus, curdlan prevents the polarization of DCs induced by soluble tumor factors and TSLP.

As $CD8^+$T cells are essential effectors of anti-tumor immunity, naïve allogeneic $CD8^+$T cells were co-cultured with BCsup-DCs, exposed or not to curdlan. ICS at day 7 revealed that $CD8^+$ T cells cultured with BCsup-DCs produce, upon PMA/Iono restimulation, IL-13 (+BCsup-DC: 23±1.3%; n=9), IFN-γ and TNF (**Figure 3A and 3B**), indicating a partial Type 2 polarization. However, $CD8^+$ T cells cultured with curdlan-treated BCsup-DCs displayed a Type 1 phenotype with few IL-13-producing $CD8^+$ T cells (+BCsup-DC: 23±1.3%; +BCsup/curdlan-DC: 2±1%; n=9; $p<0.0001$), and predominantly IFN-γ-producing $CD8^+$ T cells (+BCsup-DC: 53±1%; +BCsup/curdlan-DC: 68±1.6%; n=9; $p<0.001$) (**Figure 3A and 3B**). $CD8^+$ T cells cultured with BCsup-DCs expressed high levels of perforin but low levels of granzymes (Gzm) A and B (**Figure 3C and 3D**). Similarly to monocyte-derived DCs (*17, 23*), curdlan exposed BCsup-DCs allowed the generation of $CD8^+$ T cells expressing high levels of Gzm A and B (**Figures 3C and 3D**). To test their effector function, $CD8^+$ T cells were labeled with CFSE and cultured with BCsup-DCs treated or not with curdlan for 6 days. Then, proliferating CFSE-negative $CD8^+$ T cells were sorted and injected into breast cancer tumors established in immunodeficient mice. At day 3 post-injection, $CD8^+$ T cells generated with curdlan-treated BCsup-DCs persisted in the breast cancer microenvironment better than $CD8^+$ T cells generated by BCsup-DCs (**Figure 3E**). $CD8^+$ T cell persistence within the tumor was associated with tumor necrosis (**Figure 3F**). Curdlan exposure of BCsup-DCs resulted in the enhanced transcription of *IL-15, IL15-RA* and *4-1BBL* (**Figure 2G, Supplement Figure 6 and Supplement Table 3**), molecules that are known

to play important role in generation of high avidity $CD8^+$ effector T cells facilitating cancer rejection (*24-26*).

To control tumor in vivo, the expression of effector molecules such as Gzms by $CD8^+$ T cells is necessary but not sufficient. Indeed, the accumulation and persistence of $CD8^+$ T cells in cancer nests is also critical for cancer rejection. CD103 integrins allow the retention of effector and memory T cells in epithelial compartments (*27*) via binding to their ligand E-cadherin on epithelial cells (*28-31*). As shown in Figure 4, DCs exposed to curdlan showed an increased ability to induce CD103 on $CD8^+$ T cells (**Figure 4A and B**). To assess whether these $CD103^+CD8^+$ T cells adhered to breast cancer cells, we used a modified Stamper-Woodruff tissue binding assay (*22*). Proliferating CFSE-negative allogeneic $CD8^+$ T cells were sorted from co-cultures with DCs, re-labeled with CFSE (green) and overlaid on frozen breast cancer tissue sections to allow adherence. After a 60-minute contact, tissue sections were washed and counter-stained with anti-cytokeratin mAbs (red) to visualize the cancer cells. Numbers of bound T cells per 0.15 mm^2 $cytokeratin^+$ areas were assessed using a series of consecutive tissues sections. $CD8^+$ T cells exposed to curdlan-treated DCs adhered significantly more to frozen breast cancer tissue sections (**Figure 4C**) (+BCsup-DC: 7±1; +BCsup/curdlan-DC: 26±2; n=20; $p<0.0001$) and blocking CD103 with a monoclonal antibody decreased their numbers (**Figure 4D**) (+BCsup/curdlan-DC+isotype Ab: 22±3; +BCsup/curdlan-DC+aCD103: 2±0.5; n=20; $p<0.0001$). The binding of $CD8^+$ T cells to breast cancer tissue sections was also decreased when BCsup-DCs were pre-treated with anti-dectin-1 antibody prior to curdlan (**Figure 4E**) (+BCsup/curdlan-DC:32±4; +BCsup/aDectin/curdlan-DC: 15±3; n=10; p=0.003). Thus, curdlan exposure enables DCs to expand $CD103^+CD8^+$ T cells in a dectin-1-dependent manner. Accordingly, intratumoral injection of curdlan increased the frequency of $CD103^+CD8^+$ T cells in breast cancer tumors *in vivo* (**Figure 4F**) (DC+T: 9±0.3 % of $CD8^+$ T cells; n=3; DC+T+curdlan: 31±1.2 of $CD8^+$ T cells; n=4; $p<0.0001$). When sorted, these $CD8^+$ T cells triggered tumor

necrosis upon transfer into tumors established in immunodeficient mice (**Figure 4G).** A single injection of $CD8^+$ T cells elicited by BCsup-DCs treated with curdlan completely inhibited breast cancer development in a manner dependent upon the expression of CD103 (**Figure 4H**). Indeed, breast cancer tumors grew out in mice which received control $CD8^+$ T cells expanded by BCsup-DCs or in the presence of CD103 blocking Ab **(Figure 4H).** To establish how DCs enabled induction of CD103 expression in $CD8^+$ T cells, we analyzed the role of TGF-β1 as it induces CD103 expression on T cells (*32, 33*). Accordingly, TGF-β1-neutralizing antibodies and pharmacological blockade of TGF-β1 using TGF-β RI kinase inhibitor II (*34*) in DC-T cocultures substantially reduced the ability of curdlan-treated DCs to induce the differentiation of $CD103^+CD8^+$ T cells (**Figure 4I**). Transcriptional profiling revealed that curdlan exposure enables over-expression of *ITGB8* in DCs (**Figure 2H and Supplement Figure 6**). The product of this gene is a cell surface receptor for the latent domain (LAP) of TGF-β (*35*). Through its association with LAP, TGF-β is maintained in a latent form and the binding to the integrin αvβ8 with subsequent metalloproteolytic cleavage of LAP represents a major mechanism of TGF-β activation in vivo (*36*). Consistent with RNA expression, curdlan-treated BCsup-DCs showed substantially increased cell surface expression of αvβ8 (**Figure 4J and Supplement Figure 6**). Furthermore, adding antibodies neutralizing αvβ8 to $CD8^+$ T cell co-cultures with curdlan-treated BCsup-DCs resulted in the complete inhibition of CD103 expression by $CD8^+$ T cells triggered as the result of DC exposure to curdlan (**Figure 4J**). Thus, curdlan-treated DCs activate TGF-β1 through αvβ8 to expand $CD103^+CD8^+$ T cells that reject breast cancer cells.

Our previous studies have established the role of the tumor cells, DCs and iTh2 cells as well as their secreted molecules in the development of breast cancer. Here, we demonstrated a novel immunotherapy strategy for breast cancer based on the reprogramming of tumor-infiltrating DCs *in situ* by targeting pattern recognition receptor dectin-1. Indeed, the direct engagement of dectin-1 via intratumoral delivery of its ligand (β-glucan) initiated reprogramming

of DC maturation resulting in the broad modulation of tumor-infiltrating $CD4^+$ and $CD8^+$ T cell function leading to breast cancer rejection. The key principle is a simultaneous blockade of pro-tumor inflammatory Th2 response, a switch to Th1 immunity and an amplification of a potent anti-tumor $CD8^+$ T cell immunity. Specifically, the direct binding of β-glucan to tumor-infiltrating DCs allows reprogramming of their function including the blockade of iTh2 cells secreting IL-4 and IL-13, in favor of generation of IFN-γ secreting $CD4^+$ T cells. β-glucan-exposed DCs generate $CD8^+$ T cells expressing CD103, a ligand for E-cadherin, with superior capacity to accumulate in and to reject breast cancer in vivo.

Altogether, our studies have identified a number of targets generated by tumor-infiltrating DCs and T cells the ligation of which results in tumor destruction in vivo by the human immune system in humanized mice. These include OX40L, IL-13 and now dectin-1. All these agents act in a unique pathway that we have characterized. It is likely that a combination of antagonists to independent pathway will synergize for tumor eradication which always proves to be more challenging in patients that it is in mouse models. Also, we need to characterize the impact of dectin-1 engagement on other cells present in the tumor microenvironment. Nevertheless, our approach opens a novel avenue for immunotherapy by targeting DCs in situ for reprogramming of tumor promoting inflammation.

ACKNOWLEDGEMENT

We thank all of our patients and healthy volunteers who agreed to participate in this research. We thank Luz S. Muniz, MD and Joseph Fay, MD, the Clinical Core, the Apheresis Core, the Flow Cytometry Core, the Imaging Core and the Animal Facility team at BIIR for help. We thank Dr Jennifer L. Smith for help and discussion. K.P. acknowledges the support from the BIIR, Baylor University Medical Center foundation, Susan B. Komen Foundation, Cancer Prevention Research Institute of Texas, and NIH/NCI.

REFERENCES

1. C. DeSantis, R. Siegel, P. Bandi, A. Jemal, *CA Cancer J Clin* **61**, 409 (Nov-Dec, 2011).
2. S. L. Topalian, G. J. Weiner, D. M. Pardoll, *J Clin Oncol*, (Oct 31, 2011).
3. G. L. Beatty *et al.*, *Science* **331**, 1612 (Mar 25, 2011).
4. F. S. Hodi *et al.*, *N Engl J Med* **363**, 711 (Aug 19, 2010).
5. D. G. DeNardo, P. Andreu, L. M. Coussens, *Cancer Metastasis Rev* **29**, 309 (Jun, 2010).
6. C. Aspord *et al.*, *J Exp Med* **204**, 1037 (May 14, 2007).
7. A. Pedroza-Gonzalez *et al.*, *J Exp Med* **208**, 479 (Mar 14, 2011).
8. A. E. Teschendorff *et al.*, *BMC Cancer* **10**, 604 (2010).
9. V. N. Kristensen *et al.*, *Proc Natl Acad Sci U S A* **109**, 2802 (Feb 21, 2012).
10. L. De Monte *et al.*, *J Exp Med* **208**, 469 (Mar 14, 2011).
11. D. G. DeNardo *et al.*, *Cancer Cell* **16**, 91 (Aug 4, 2009).
12. M. Terabe, J. A. Berzofsky, *Curr Opin Immunol* **16**, 157 (Apr, 2004).
13. W. J. Zhang *et al.*, *Cytokine* **42**, 39 (Apr, 2008).
14. D. G. Denardo *et al.*, *Cancer Discov* **1**, 54 (Jun 1, 2011).
15. J. Galon *et al.*, *Science* **313**, 1960 (Sep 29, 2006).
16. P. B. Olkhanud *et al.*, *J Immunol* **186**, 5656 (May 15, 2011).
17. S. I. Gringhuis *et al.*, *Nat Immunol* **10**, 203 (Feb, 2009).
18. J. Baran, D. J. Allendorf, F. Hong, G. D. Ross, *Folia Histochem Cytobiol* **45**, 107 (2007).
19. H. S. Goodridge *et al.*, *Nature* **472**, 471 (Apr 28, 2011).
20. K. Arima *et al.*, *Science signaling* **3**, ra4 (2010).
21. J. A. Markovics *et al.*, *J Biol Chem* **285**, 24695 (Aug 6, 2010).
22. D. Bell *et al.*, *J Exp Med* **190**, 1417 (1999).
23. S. Leibundgut-Landmann, F. Osorio, G. D. Brown, C. Reis e Sousa, *Blood* **112**, 4971 (Dec 15, 2008).
24. P. Dubsky *et al.*, *Eur J Immunol* **37**, 1678 (Jun, 2007).
25. E. Romano *et al.*, *Blood* **119**, 5182 (May 31, 2012).
26. M. Wolfl *et al.*, *Blood* **110**, 201 (Jul 1, 2007).
27. K. L. Cepek *et al.*, *Nature* **372**, 190 (Nov 10, 1994).
28. W. W. Agace, J. M. Higgins, B. Sadasivan, M. B. Brenner, C. M. Parker, *Curr Opin Cell Biol* **12**, 563 (Oct, 2000).
29. M. P. Schon *et al.*, *J Immunol* **162**, 6641 (Jun 1, 1999).
30. A. Le Floc'h *et al.*, *J Exp Med* **204**, 559 (Mar 19, 2007).
31. A. Le Floc'h *et al.*, *Cancer Res* **71**, 328 (Jan 15, 2011).
32. C. M. Parker *et al.*, *Proc Natl Acad Sci U S A* **89**, 1924 (Mar 1, 1992).
33. S. Rihs *et al.*, *Am J Respir Cell Mol Biol* **15**, 600 (Nov, 1996).
34. T. Ito *et al.*, *Immunity* **28**, 870 (Jun, 2008).
35. H. Kitamura *et al.*, *J Clin Invest* **121**, 2863 (Jul, 2011).
36. M. O. Li, R. A. Flavell, *Cell* **134**, 392 (Aug 8, 2008).

FIGURE LEGENDS

Figure 1: Curdlan blocks iTh2 in human breast cancer.

(A) Immunofluorescence on patient primary breast tumor frozen tissue sections. Columns left to right: Dectin-1 (red)/HLA-DR (green); Dectin-1 (red)/CD11c (green), Cytokeratin (red)/Dectin-1 (green); CD83 (red)/Dectin-1 (green). Top to bottom: single fluorescence for each antibody and overlay. Blue: nuclear staining with DAPI. Representative of 27 tumors analyzed. Bar: 90μm. (B) Hs578T breast tumor-bearing NOD/SCID/β2m−/− mice were reconstituted with monocyte-derived DCs (MDCs) and autologous T cells with/without curdlan (100μg/ml) or anti-TSLPR (200μg/mouse). Empty circles: PBS; red: DC+T; blue: DC+T+curdlan; black: DC+T+anti-TSLPR. (C) Mean value from five independent experiments, 23 mice per group. (D) Cytokines in the activated tumor supernatant measured by Luminex. Single points indicate individual mouse. (E) Blood sorted mDCs were pre-treated with 100μg/ml curdlan, incubated with supernatant of MDA-MB231 breast cancer cell line (BCsup) for 48 hrs and co-cultured with allogenic naive $CD4^+$ T cells. Cells were re-stimulated for ICS at day 7. (F) Summary of different experiments. Single points represent the percentage from individual experiment with mDCs from 13 different healthy donors. (G) Blood sorted mDCs were incubated with BCsup for 48hrs; DCs were sorted based on OX40-L expression; $OX40L^+$ DCs were treated with/without curdlan for 24 hrs and co-cultured with allogenic naïve total T cells. At day 7, cells were re-stimulated for ICS.

Figure 2: Curdlan modulates mDCs maturation in breast cancer via dectin 1.

(A) Blood sorted mDCs were exposed to BCsup for 48 hrs with/without 3min pre-treatment with curdlan (100μg/ml) and analyzed by flow cytometry. Each point indicates the percentage of $OX40L^+$ DCs in 10 individual experiments. (B) DCs were pre-treated with anti-Dectin 1 non-agonistic antibody, followed by curdlan and BCsup. Representative flow cytometry plots of

OX40L expression and summary of four experiments. (C) Hs578T breast tumor-bearing NOD/SCID/β2m−/− mice were reconstituted with MDCs and autologous T cells with/without curdlan (100μg/ml) or anti-Dectin 1 plus. White circles: PBS; black: DC+T; blue: DC+T+curdlan; red: DC+T+anti-Dectin1+curdlan; empty squares: curdlan. (D) Blood sorted mDCs were harvested after 1 hr incubation with curdlan, stained as indicated and analyzed with flow cytometry. Grey: isotype; red: BCsup-DC; blue: BCsup/curdlan-DC; black: BCsup/aDectin/curdlan-DC. Representative histogram of 4 individual experiments. (E)The supernatant from DC culture was collected for IL-12p70 Luminex. Single points indicate individual experiment. (F) anti-IL-12 neutralizing antibody was used to pre-treat the curdlan/BCsup-DCs prior to their co-culture with allogenic naïve T cells. ICS at day 7, 3 experiments. (G) Transcritional profiles of BCsup-DCs from 3 donors cultured for 6 hours in vitro in the presence of Polymyxene B (PMB), PMB+Curdlan or BCsup alone; (Illumina HT12v4). Heatmap representing the clustered (Pearson) 314 transcripts over-expressed 1.5 fold in Curdlan + PMB treatment compared to BCsup alone (Welch T-Test 0.05). Samples were normalized to each donor's untreated reference sample. (H) Heatmap representing the clustered (Pearson) 873 transcripts under-expressed 1.5 fold in Curdlan + PMB treatment compared to BCsup alone (Welch T-Test 0.05). (I) Ingenuity pathway analysis (IPA) of the 314 transcripts identified in the top left panel. The color scale represents the fold-change of the molecules selected in the average of PMB+curdlan-treated DCs as compared to untreated reference samples. The major over-expressed regulators are represented in the center of the network. Edges represent literature-based connections between molecules (full: direct connection, dashed: indirect connection). (J) Ingenuity pathway analysis (IPA) of the 873 transcripts identified in the bottom left panel.

Figure 3: Curdlan enables mDCs in breast cancer to generate $CD8^+$ T cells able to reject tumors.

(A) Curdlan/BCsup-DCs were co-cultured with allogenic naïve T cells. ICS at day 7 on gated $Aqua^-CD3^+CD8^+$ T cells. (B) Summary of 9 individual experiments. (C) Expression of Granzyme A, Granzyme B and perforin. (D) Summary of 3 individual experiments. (E) $CD8^+$ T cells were sorted from in vitro culture and injected into MDA-MB231 breast tumors in NOD-SCID mice. Single cell suspensions from tumors harvested at day 3 were stained with anti human-CD45 mAb and analyzed by flow cytometry. The percentage of $CD45^+$ cells from 4 individual experiments. (F) H&E staining of tumor sections. The necrosis level is rated and calculated in each region. Summary of Points x areas/total area in each section=necrosis index. Necrosis index from 5 sections.

Figure 4: Curdlan enables mDCs in breast cancer to generate $CD103^+CD8^+$ T cells able to prevent tumor development.

(A) Curdlan/BCsup-DCs were co-cultured with allogenic naïve T cells. CD103 expression at day 6. (B) Summary of 7 individual experiments. (C) $CD8^+$ T cells were sorted from DC-T coculture and labeled with CFSE for Stamper-Woodruff assays on breast tumor sections. The sections were fixed and stained with cytokeratin (red). The $CD8^+$ T cells (green) were counted in each 0.15 mm^2 $cytokeratin^+$ area. Twenty fields were counted from two individual breast tumor sections. (D)The T cells were pre-incubated with anti-CD103 or isotype antibodies and then overlaid on breast tumor sections. The sections were fixed and stained with cytokeratin. The $CD8^+$ T cells (green) were counted in each 0.15 mm^2 $cytokeratin^+$ area. Twenty fields were counted from two individual breast tumor sections. (E) $CD8^+$ T cells were co-cultured with DCs which were pre-treated with anti-Dectin1 neutralizing antibody, followed by curdlan and BCsup.

$CD8^+$ T cells were sorted from DC-T coculture and labeled with CFSE for Stamper-Woodruff assays as above. Ten fields were counted from two individual breast tumor sections. (F) Hs578T-bearing NOD/SCID/β2m−/− mice were reconstituted with MDCs) and autologous T cells with or without Curdlan (100μg/ml). Gating of single cell suspension for human $CD45^+$ cells and $CD103^+CD8^+$ T cells. Single dots represent the percentage of $CD103^+CD8^+$ T cells from each mouse. (G) $CD8^+$ T cells were sorted from the tumor cell suspension harvested from mice and injected into MDA-MB231 tumors in NOD-SCID mice. Frozen sections from the tumors at day 3, H&E staining. The necrosis level is rated and calculated with each region as above. (H) The NOD/SCID/β2m−/− mice were subcutaneously injected with $10x10^6$ MDA-MB231 cells. 500K sorted $CD8^+$ T cells were injected into tumors. Black: PBS, n=6; Red: $CD8^+$ T cells from BCsup-DC-T co-culture, n=6; Blue: $CD8^+$ T cells from BCsup/curdlan-DC-T co-culture, n=7; Green: $CD8^+$ T cells from BCsup/curdlan-DC-T co-culture with pre-treatment with anti-CD103 mAb, n=8. (I) DCs were pre-treated with anti-TGF-β1 and TGF-β1 receptor kinase inhibitor for 30 min and then co-cultured with T cells. Single points represent individual experiment. (J) αvβ8 staining. Grey: isotype, red: BCsup-DC, blue: curdlan/BCsup-DC. Blood sorted mDCs were pre-treated with curdlan, activated by BCsup for 48 hrs, pre-treated with anti-β8 mAb and co-cultured with allogenic naïve T cells. The percentage of $CD103^+CD8^+$ T cells at day 6. Single point indicates the percentage of $CD103^+CD8^+$ T cells from 3 individual DC donors.

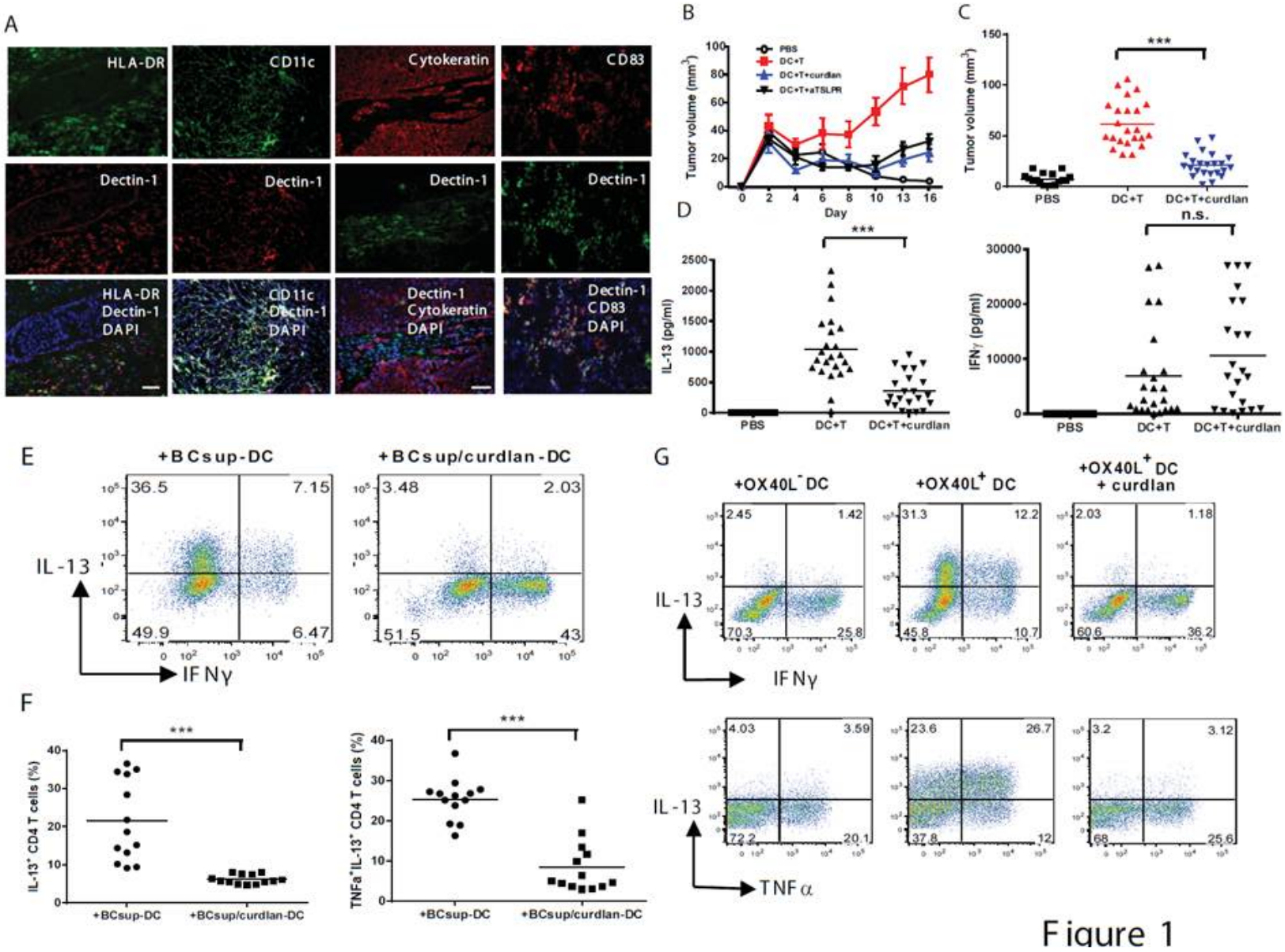
A
HLA-DR
CD11c
Cytokeratin
CD83
Dectin-1
HLA-DR Dectin-1 DAPI
CD11c Dectin-1 DAPI
Dectin-1 Cytokeratin DAPI
Dectin-1 CD83 DAPI
B
PBS
DC+T
DC+T+curdlan
DC+T+αTSLPR
Tumor volume (mm3)
Day
C
***
PBS
DC+T
DC+T+curdlan
D
***
n.s.
IL-13 (pg/ml)
IFNγ (pg/ml)
E
+BCsup-DC
+BCsup/curdlan-DC
IL-13
IFNγ
36.5
7.15
49.9
6.47
3.48
2.03
51.5
43
F
***
IL-13+ CD4 T cells (%)
TNFa+IL-13+ CD4 T cells (%)
+BCsup-DC
+BCsup/curdlan-DC
G
+OX40L- DC
+OX40L+ DC
+OX40L+ DC + curdlan
IL-13
IFNγ
TNFα

Figure 1

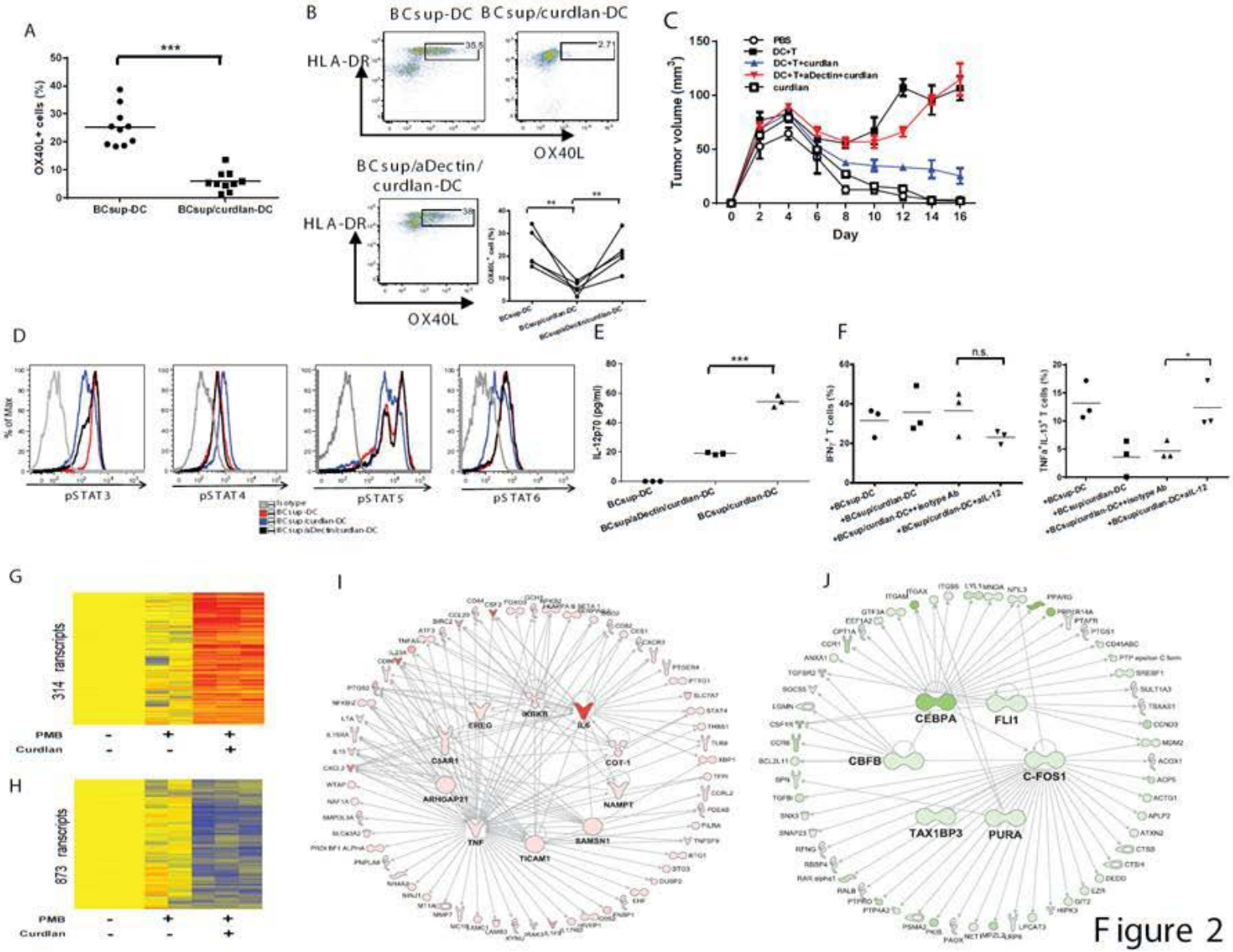
A
OX40L+ cells (%)
BCsup-DC
BCsup/curdlan-DC
B
BCsup-DC
BCsup/curdlan-DC
HLA-DR
OX40L
BCsup/aDectin/
curdlan-DC
C
Tumor volume (mm3)
Day
PBS
DC+T
DC+T+curdlan
DC+T+aDectin+curdlan
curdlan
D
% of Max
pSTAT3
pSTAT4
pSTAT5
pSTAT6
Isotype
BCsup-DC
BCsup/curdlan-DC
BCsup/aDectin/curdlan-DC
E
IL-12p70 (pg/ml)
F
IFN-γ+ T cells (%)
TNFα+IL-13+ T cells (%)
n.s.
G
314 ranscripts
PMB
Curdlan
H
873 ranscripts
I
J
CEBPA
FLI1
CBFB
C-FOS1
TAX1BP3
PURA

Figure 2

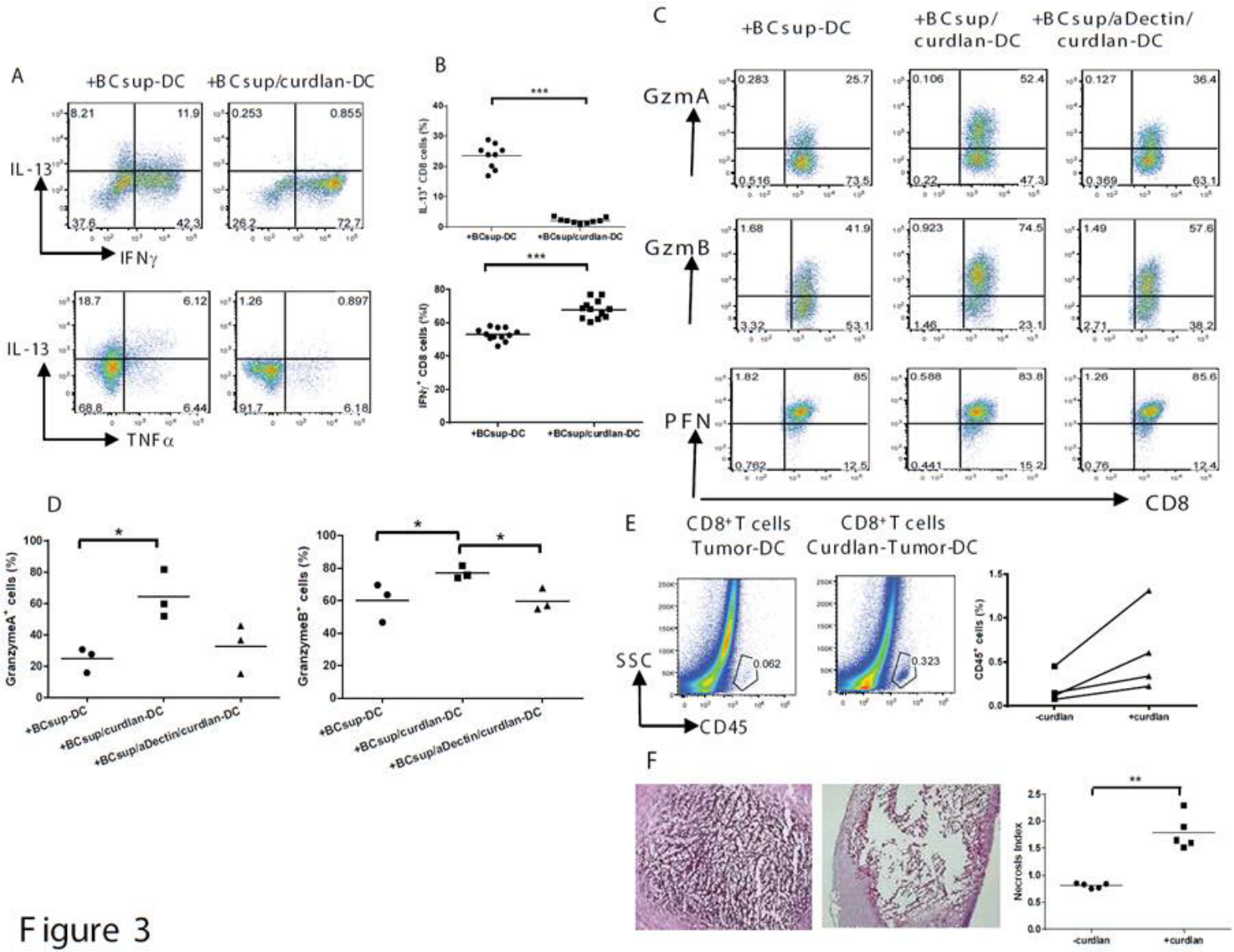
A
+BCsup-DC
+BCsup/curdlan-DC
IL-13
IFNγ
TNFα
B
IL-13+ CD8 cells (%)
IFNγ+ CD8 cells (%)
C
+BCsup-DC
+BCsup/ curdlan-DC
+BCsup/aDectin/ curdlan-DC
GzmA
GzmB
PFN
CD8
D
GranzymeA+ cells (%)
GranzymeB+ cells (%)
+BCsup-DC
+BCsup/curdlan-DC
+BCsup/aDectin/curdlan-DC
E
CD8+T cells Tumor-DC
CD8+T cells Curdlan-Tumor-DC
SSC
CD45
CD45+ cells (%)
-curdlan
+curdlan
F
Necrosis index

Figure 3

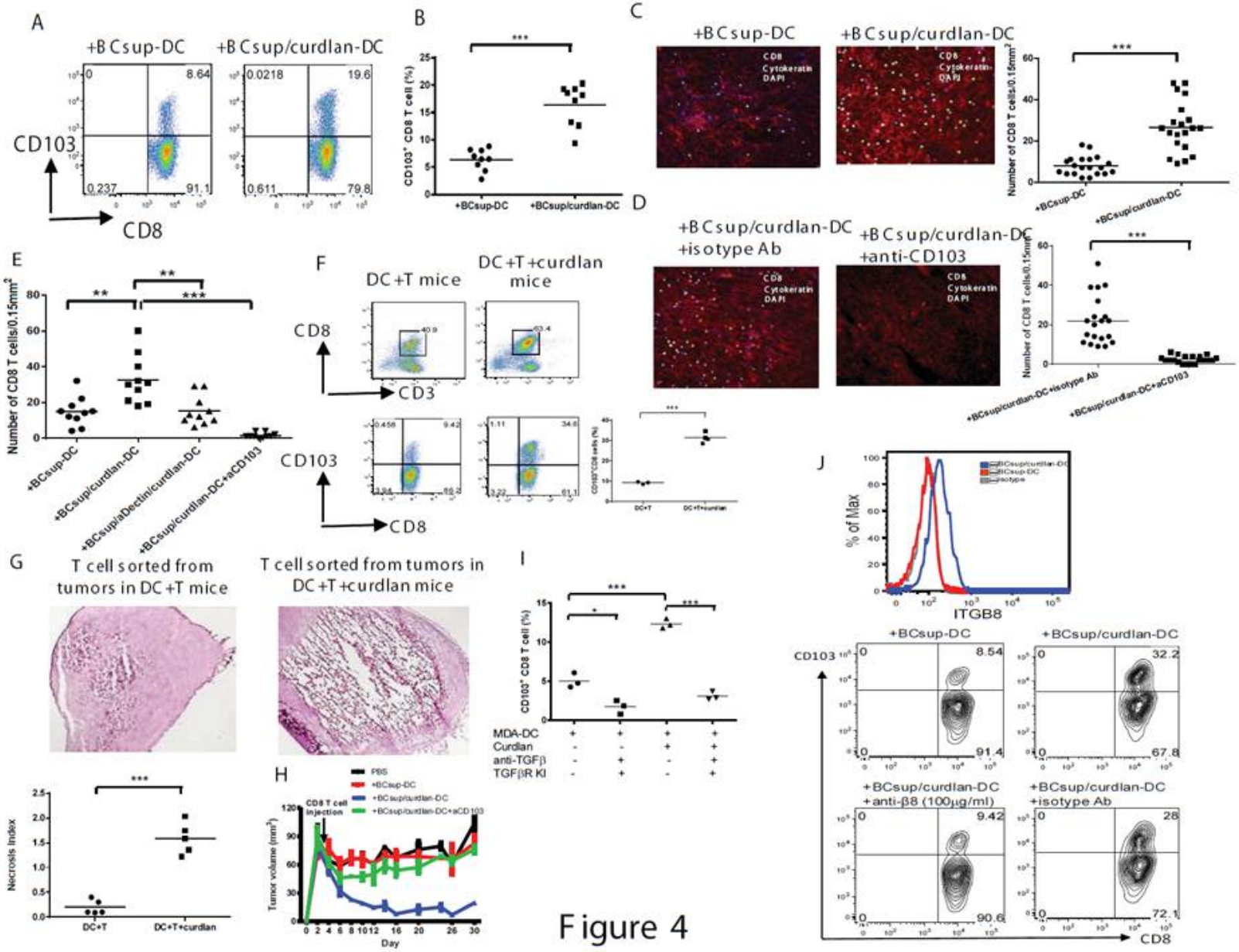
A
+BCsup-DC
+BCsup/curdlan-DC
CD103
CD8
0
8.64
0.237
91.1
0.0218
19.6
0.611
79.8
B
CD103+ CD8 T cell (%)
+BCsup-DC
+BCsup/curdlan-DC
C
+BCsup-DC
+BCsup/curdlan-DC
CD8
Cytokeratin
DAPI
Number of CD8 T cells/0.15mm2
D
+BCsup/curdlan-DC
+isotype Ab
+BCsup/curdlan-DC
+anti-CD103
+BCsup/curdlan-DC+isotype Ab
+BCsup/curdlan-DC+aCD103
E
Number of CD8 T cells/0.15mm2
+BCsup-DC
+BCsup/curdlan-DC
+BCsup/aDectin/curdlan-DC
+BCsup/curdlan-DC+aCD103
F
DC+T mice
DC+T+curdlan mice
CD8
CD3
CD103
40.9
63.4
0.458
9.42
1.11
34.6
3.84
86.2
3.22
61.1
DC+T
DC+T+curdlan
G
T cell sorted from tumors in DC+T mice
T cell sorted from tumors in DC+T+curdlan mice
Necrosis Index
DC+T
DC+T+curdlan
H
PBS
+BCsup-DC
+BCsup/curdlan-DC
+BCsup/curdlan-DC+aCD103
CD8 T cell injection
Tumor volume (mm3)
Day
I
CD103+ CD8 T cell (%)
MDA-DC
Curdlan
anti-TGFβ
TGFβR KI
J
% of Max
ITGB8
+BCsup-DC
+BCsup/curdlan-DC
CD103
8.54
91.4
32.2
67.8
+BCsup/curdlan-DC
+anti-β8 (100μg/ml)
+BCsup/curdlan-DC
+isotype Ab
9.42
90.6
28
72.1
CD8

Figure 4

BIBLIOGRAPHY

Andersen, R. S., C. A. Thrue, N. Junker, R. Lyngaa, M. Donia, E. Ellebaek, I. M. Svane, T. N. Schumacher, P. Thor Straten and S. R. Hadrup. "Dissection of T-Cell Antigen Specificity in Human Melanoma." *Cancer Res* 72, no. 7 (2012): 1642-50.

Arima, K., N. Watanabe, S. Hanabuchi, M. Chang, S. C. Sun and Y. J. Liu. "Distinct Signal Codes Generate Dendritic Cell Functional Plasticity." *Sci Signal* 3, no. 105 (2010): ra4.

Aspord, C., A. Pedroza-Gonzalez, M. Gallegos, S. Tindle, E. C. Burton, D. Su, F. Marches, J. Banchereau and A. K. Palucka. "Breast Cancer Instructs Dendritic Cells to Prime Interleukin 13-Secreting Cd4+ T Cells That Facilitate Tumor Development." *J Exp Med* 204, no. 5 (2007): 1037-47.

Bates, G. J., S. B. Fox, C. Han, R. Launchbury, R. D. Leek, A. L. Harris and A. H. Banham. "Expression of the Forkhead Transcription Factor Foxp1 Is Associated with That of Estrogen Receptor-Beta in Primary Invasive Breast Carcinomas." *Breast Cancer Res Treat* 111, no. 3 (2008): 453-9.

Bing Li, Daniel J. Allendorf, Richard Hansen, Jose Marroquin, Daniel E. Cramer, Claire and and Jun Yan L. Harris. "Combined Yeast B-Glucan and Antitumor Monoclonal Antibody Therapy Requires C5a-Mediated Neutrophil Chemotaxis Via Regulation of Decay-Accelerating Factor Cd55." *Cancer Res*, (2007).

Brian Ruffell, Alfred Aua, Hope S. Rugo, Laura J. Esserman, E. Shelley Hwang, and Lisa M. Coussens. "<Leukocyte Composition of Human Breast Cancer.Pdf>." *PNAS*, (2012).

Camp, J. T., F. Elloumi, E. Roman-Perez, J. Rein, D. A. Stewart, J. C. Harrell, C. M. Perou and M. A. Troester. "Interactions with Fibroblasts Are Distinct in Basal-Like and Luminal Breast Cancers." *Mol Cancer Res* 9, no. 1 (2011): 3-13.

Carl G. Figdor, Yvette van Kooyk and Gosse J. Adema. "C-Type Lectin Receptors on Dendritic Cells and Langerhans Cells." *Nat Rev Immunol*, (2002).

Chacon, J. A., R. C. Wu, P. Sukhumalchandra, J. J. Molldrem, A. Sarnaik, S. Pilon-Thomas, J. Weber, P. Hwu and L. Radvanyi. "Co-Stimulation through 4-1bb/Cd137 Improves the Expansion and Function of Cd8(+) Melanoma Tumor-Infiltrating Lymphocytes for Adoptive T-Cell Therapy." *PLoS One* 8, no. 4 (2013): e60031.

Chan, G. C., W. K. Chan and D. M. Sze. "The Effects of Beta-Glucan on Human Immune and Cancer Cells." *J Hematol Oncol* 2, (2009): 25.

Condeelis, J. and J. W. Pollard. "Macrophages: Obligate Partners for Tumor Cell Migration, Invasion, and Metastasis." *Cell* 124, no. 2 (2006): 263-6.

Coussens, L. M. and Z. Werb. "Inflammation and Cancer." *Nature* 420, no. 6917 (2002): 860-7.

Coussens, L. M., L. Zitvogel and A. K. Palucka. "Neutralizing Tumor-Promoting Chronic Inflammation: A Magic Bullet?" *Science* 339, no. 6117 (2013): 286-91.

Craig, D. W., J. A. O'Shaughnessy, J. A. Kiefer, J. Aldrich, S. Sinari, T. M. Moses, S. Wong, J. Dinh, A. Christoforides, J. L. Blum, C. L. Aitelli, C. R. Osborne, T. Izatt, A. Kurdoglu, A. Baker, J. Koeman, C. Barbacioru, O. Sakarya, F. M. De La Vega, A. Siddiqui, L. Hoang, P. R. Billings, B. Salhia, A. W. Tolcher, J. M. Trent, S. Mousses, D. Von Hoff and J. D. Carpten. "Genome and Transcriptome Sequencing in Prospective Metastatic Triple-Negative Breast Cancer Uncovers Therapeutic Vulnerabilities." *Mol Cancer Ther* 12, no. 1 (2013): 104-16.

De Monte, L., M. Reni, E. Tassi, D. Clavenna, I. Papa, H. Recalde, M. Braga, V. Di Carlo, C. Doglioni and M. P. Protti. "Intratumor T Helper Type 2 Cell Infiltrate Correlates with Cancer-Associated Fibroblast Thymic Stromal Lymphopoietin Production and Reduced Survival in Pancreatic Cancer." *J Exp Med* 208, no. 3 (2011): 469-78.

DeNardo, D. G., P. Andreu and L. M. Coussens. "Interactions between Lymphocytes and Myeloid Cells Regulate Pro- Versus Anti-Tumor Immunity." *Cancer Metastasis Rev* 29, no. 2 (2010): 309-16.

Diana Bell, Pascale Chomarat, Denise Broyles,George Netto,, Serge Lebecque Ghada Moumneh Harb, Jenny Valladeau and Karolina A. Palucka Jean Davoust, and Jacques Banchereau. "In Breast Carcinoma Tissue, Immature Dendritic Cells Reside within the Tumor, Whereas Mature Dendritic Cells Are Located in Peritumoral Areas." *Journal of Experimental Medicine*, (1999).

Doedens, A. L., C. Stockmann, M. P. Rubinstein, D. Liao, N. Zhang, D. G. DeNardo, L. M. Coussens, M. Karin, A. W. Goldrath and R. S. Johnson. "Macrophage Expression of Hypoxia-Inducible Factor-1 Alpha Suppresses T-Cell Function and Promotes Tumor Progression." *Cancer Res* 70, no. 19 (2010): 7465-75.

Du, J., Z. Wu, S. Ren, Y. Wei, M. Gao, G. J. Randolph and C. Qu. "Tlr8 Agonists Stimulate Newly Recruited Monocyte-Derived Cells into Potent Apcs That Enhance Hbsag Immunogenicity." *Vaccine* 28, no. 38 (2010): 6273-81.

Dubsky, P., H. Saito, M. Leogier, C. Dantin, J. E. Connolly, J. Banchereau and A. K. Palucka. "Il-15-Induced Human Dc Efficiently Prime Melanoma-Specific Naive Cd8+ T Cells to Differentiate into Ctl." *Eur J Immunol* 37, no. 6 (2007): 1678-90.

Fridman, W. H., J. Galon, F. Pages, E. Tartour, C. Sautes-Fridman and G. Kroemer. "Prognostic and Predictive Impact of Intra- and Peritumoral Immune Infiltrates." *Cancer Res* 71, no. 17 (2011): 5601-5.

Georgiannos, Stavros N., Andrew Renaut, Anthony W. Goode and Michael Sheaff. "The Immunophenotype and Activation Status of the Lymphocytic Infiltrate in Human Breast Cancers, the Role of the Major Histocompatibility Complex in Cell-Mediated Immune Mechanisms, and Their Association with Prognostic Indicators." *Surgery* 134, no. 5 (2003): 827-834.

Gordon D. Brown, Siamon Gordon. "Immune Recognition. A New Receptor for Beta-Glucans." *Nature* (2001).

Gresnigt, M. S., B. Rosler, C. W. Jacobs, K. L. Becker, L. A. Joosten, J. W. van der Meer, M. G. Netea, C. A. Dinarello and F. L. van de Veerdonk. "The Il-36 Receptor Pathway Regulates Aspergillus Fumigatus-Induced Th1 and Th17 Responses." *Eur J Immunol* 43, no. 2 (2013): 416-26.

Gringhuis, S. I., J. den Dunnen, M. Litjens, M. van der Vlist, B. Wevers, S. C. Bruijns and T. B. Geijtenbeek. "Dectin-1 Directs T Helper Cell Differentiation by Controlling Noncanonical Nf-Kappab Activation through Raf-1 and Syk." *Nat Immunol* 10, no. 2 (2009): 203-13.

Grivennikov, S. I., F. R. Greten and M. Karin. "Immunity, Inflammation, and Cancer." *Cell* 140, no. 6 (2010): 883-99.

Hong, J. J., P. K. Amancha, K. Rogers, A. A. Ansari and F. Villinger. "Re-Evaluation of Pd-1 Expression by T Cells as a Marker for Immune Exhaustion During Siv Infection." *PLoS One* 8, no. 3 (2013): e60186.

Humrich, J. Y., J. H. Humrich, M. Averbeck, P. Thumann, C. Termeer, E. Kampgen, G. Schuler and L. Jenne. "Mature Monocyte-Derived Dendritic Cells Respond More Strongly to Ccl19 Than to Cxcl12: Consequences for Directional Migration." *Immunology* 117, no. 2 (2006): 238-47.

Ito, T. "Interferon-Alpha and Interleukin-12 Are Induced Differentially by Toll-Like Receptor 7 Ligands in Human Blood Dendritic Cell Subsets." *Journal of Experimental Medicine* 195, no. 11 (2002): 1507-1512.

Ito, T., S. Hanabuchi, Y. H. Wang, W. R. Park, K. Arima, L. Bover, F. X. Qin, M. Gilliet and Y. J. Liu. "Two Functional Subsets of Foxp3+ Regulatory T Cells in Human Thymus and Periphery." *Immunity* 28, no. 6 (2008): 870-80.

Ito, T., Y. H. Wang, O. Duramad, T. Hori, G. J. Delespesse, N. Watanabe, F. X. Qin, Z. Yao, W. Cao and Y. J. Liu. "Tslp-Activated Dendritic Cells Induce an Inflammatory T Helper Type 2 Cell Response through Ox40 Ligand." *J Exp Med* 202, no. 9 (2005): 1213-23.

Jarek Baran, Daniel J. Allendorf, Feng Hong and Gordon D. Ross. "Oral B-Glucan Adjuvant Therapy Converts Nonprotective Th2 Response to Protective Th1 Cell-Mediated Immune Response in Mammary Tumor-Bearing Mice." *Folia Histochemica Et Cytobiologica*, (2007).

Kanazawa, N. "Dendritic Cell Immunoreceptors: C-Type Lectin Receptors for Pattern-Recognition and Signaling on Antigen-Presenting Cells." *J Dermatol Sci* 45, no. 2 (2007): 77-86.

Kaoru Morikawa, Reiko Takeda, Masatoshi Yamazaki, and Den'ichi Mizuno. "Induction of Tumoricidal Activity of Polymorphonuclear Leukocytes by a Linear Beta-1,3-D-Glucan and Other Immunomodulators in Murine Cells." *Cancer Res*, (1985).

Ken Shirabe, Mitsuo Shimada, Kiyoshi Kajiyama, Tomonobu Gion, Yasuharu Ikeda, Hirofumi Hasegawa, Kenichi Taguchi, Kenji Takenaka, Keizo Sugimachi. "Clinicopathologic Features of Patients with Hepatocellular Carcinoma Surviving 10 Years after Hepatic Resection." *Cancer*, (1998).

Klechevsky, E., M. Liu, R. Morita, R. Banchereau, L. Thompson-Snipes, A. K. Palucka, H. Ueno and J. Banchereau. "Understanding Human Myeloid Dendritic Cell Subsets for the Rational Design of Novel Vaccines." *Hum Immunol* 70, no. 5 (2009): 281-8.

Koido, S., S. Homma, M. Okamoto, Y. Namiki, K. Takakura, A. Takahara, S. Odahara, S. Tsukinaga, T. Yukawa, J. Mitobe, H. Matsudaira, K. Nagatsuma, K. Uchiyama, M. Kajihara, S. Arihiro, H. Imazu, H. Arakawa, S. Kan, H. Komita, M. Ito, T. Ohkusa, J. Gong and H. Tajiri. "Combined Tlr2/4-Activated Dendritic/Tumor Cell Fusions Induce Augmented Cytotoxic T Lymphocytes." *PLoS One* 8, no. 3 (2013): e59280.

Koontongkaew, S. "The Tumor Microenvironment Contribution to Development, Growth, Invasion and Metastasis of Head and Neck Squamous Cell Carcinomas." *J Cancer* 4, no. 1 (2013): 66-83.

Le Floc'h, A., A. Jalil, K. Franciszkiewicz, P. Validire, I. Vergnon and F. Mami-Chouaib. "Minimal Engagement of Cd103 on Cytotoxic T Lymphocytes with an E-Cadherin-Fc Molecule Triggers Lytic Granule Polarization Via a Phospholipase Cgamma-Dependent Pathway." *Cancer Res* 71, no. 2 (2011): 328-38.

Le Floc'h, A., A. Jalil, I. Vergnon, B. Le Maux Chansac, V. Lazar, G. Bismuth, S. Chouaib and F. Mami-Chouaib. "Alpha E Beta 7 Integrin Interaction with E-Cadherin Promotes Antitumor Ctl Activity by Triggering Lytic Granule Polarization and Exocytosis." *J Exp Med* 204, no. 3 (2007): 559-70.

Lewis, K. L., M. L. Caton, M. Bogunovic, M. Greter, L. T. Grajkowska, D. Ng, A. Klinakis, I. F. Charo, S. Jung, J. L. Gommerman, Ivanov, II, K. Liu, M. Merad and B. Reizis. "Notch2 Receptor Signaling Controls Functional Differentiation of Dendritic Cells in the Spleen and Intestine." *Immunity* 35, no. 5 (2011): 780-91.

Li, B., Y. Cai, C. Qi, R. Hansen, C. Ding, T. C. Mitchell and J. Yan. "Orally Administered Particulate Beta-Glucan Modulates Tumor-Capturing Dendritic Cells and Improves Antitumor T-Cell Responses in Cancer." *Clin Cancer Res* 16, no. 21 (2010): 5153-64.

Li, B. H., X. Z. Yang, P. D. Li, Q. Yuan, X. H. Liu, J. Yuan and W. J. Zhang. "Il-4/Stat6 Activities Correlate with Apoptosis and Metastasis in Colon Cancer Cells." *Biochem Biophys Res Commun* 369, no. 2 (2008): 554-60.

Li, M. O. and R. A. Flavell. "Tgf-Beta: A Master of All T Cell Trades." *Cell* 134, no. 3 (2008): 392-404.

Liu, Y. J., V. Soumelis, N. Watanabe, T. Ito, Y. H. Wang, W. Malefyt Rde, M. Omori, B. Zhou and S. F. Ziegler. "Tslp: An Epithelial Cell Cytokine That Regulates T Cell Differentiation by Conditioning Dendritic Cell Maturation." *Annu Rev Immunol* 25, (2007): 193-219.

Mantovani, A. and A. Sica. "Macrophages, Innate Immunity and Cancer: Balance, Tolerance, and Diversity." *Curr Opin Immunol* 22, no. 2 (2010): 231-7.

Martin-Orozco, N., P. Muranski, Y. Chung, X. O. Yang, T. Yamazaki, S. Lu, P. Hwu, N. P. Restifo, W. W. Overwijk and C. Dong. "T Helper 17 Cells Promote Cytotoxic T Cell Activation in Tumor Immunity." *Immunity* 31, no. 5 (2009): 787-98.

Mazzoni, A. and D. M. Segal. "Controlling the Toll Road to Dendritic Cell Polarization." *J Leukoc Biol* 75, no. 5 (2004): 721-30.

Medzhitov, Seth Rakoff-Nahoum and Ruslan. "Toll-Like Receptors and Cancer." *NATURE REVIEWS CANCER*, (2009).

Murphy, K. M. and S. L. Reiner. "The Lineage Decisions of Helper T Cells." *Nat Rev Immunol* 2, no. 12 (2002): 933-44.

Naoko Inoshima, Yoichi Nakanishi, Miiru Izumi Takahiro Minami, Ichiro Yoshino Koichi Takayama, and and Nobuyuki Hara. "The Influence of Dendritic Cell Infiltration and Vascular Endothelial Growth Factor Expression on the Prognosis of Non-Small Cell Lung Cancer." *Clinical Cancer Research*, (2002).

Ni, L., I. Gayet, S. Zurawski, D. Duluc, A. L. Flamar, X. H. Li, A. O'Bar, S. Clayton, A. K. Palucka, G. Zurawski, J. Banchereau and S. Oh. "Concomitant Activation and Antigen Uptake Via Human Dectin-1 Results in Potent Antigen-Specific Cd8+ T Cell Responses." *J Immunol* 185, no. 6 (2010): 3504-13.

Palucka, K. and J. Banchereau. "Cancer Immunotherapy Via Dendritic Cells." *Nat Rev Cancer* 12, no. 4 (2012): 265-77.

Parker CM, Cepek KL, Russell GJ, Shaw SK, Posnett DN, Schwarting R, Brenner MB. "A Family of Beta 7 Integrins on Human Mucosal Lymphocytes." *Proc Natl Acad Sci U S A.*, (1992).

Partha P. Manna, Andr´es Jaramillo, Kanchana Majumder, Lacey G. Campbell, and Jill R. Dietz Timothy P. Fleming, John F. Dipersio, and T. Mohanakumar. "Generation of Cd8 Cytotoxic T Lymphocytes against Breast Cancer Cells by Stimulation with Mammaglobin a Pulsed Dendritic Cells." *Breast Cancer Research and Treatment*, (2003).

Pawel Muranski, Andrea Boni, Paul A. Antony, Lydie Cassard, Kari R. Irvine, Andrew Kaiser, Chrystal M. Paulos, Douglas C. Palmer, Christopher E. Touloukian, Krzysztof Ptak, Luca Gattinoni, Claudia Wrzesinski, Christian S. Hinrichs, Keith W. Kerstann, Lionel Feigenbaum, Chi-Chao Chan and and Nicholas P. Restifo. "<Tumor-Specific Th17-Polarized Cells Eradicate Large Established Melanoma.Pdf>." *Blood*, (2008).

Pedroza-Gonzalez, A., K. Xu, T. C. Wu, C. Aspord, S. Tindle, F. Marches, M. Gallegos, E. C. Burton, D. Savino, T. Hori, Y. Tanaka, S. Zurawski, G. Zurawski, L. Bover, Y. J. Liu, J. Banchereau and A. K. Palucka. "Thymic Stromal Lymphopoietin Fosters Human Breast Tumor Growth by Promoting Type 2 Inflammation." *J Exp Med* 208, no. 3 (2011): 479-90.

Piet, B., G. J. de Bree, B. S. Smids-Dierdorp, C. M. van der Loos, E. B. Remmerswaal, J. H. von der Thusen, J. M. van Haarst, J. P. Eerenberg, A. ten Brinke, W. van der Bij, W. Timens, R. A. van Lier and R. E. Jonkers. "Cd8(+) T Cells with an Intraepithelial Phenotype Upregulate Cytotoxic Function Upon Influenza Infection in Human Lung." *J Clin Invest* 121, no. 6 (2011): 2254-63.

Pulendran, Bali. "Variegation of the Immune Response with Dendritic Cells and Pathogen Recognition Receptors." *Journal of Immunology*, (2005).

Qi, C., Y. Cai, L. Gunn, C. Ding, B. Li, G. Kloecker, K. Qian, J. Vasilakos, S. Saijo, Y. Iwakura, J. R. Yannelli and J. Yan. "Differential Pathways Regulating Innate and Adaptive Antitumor Immune Responses by Particulate and Soluble Yeast-Derived Beta-Glucans." *Blood* 117, no. 25 (2011): 6825-36.

Qian, B. Z., J. Li, H. Zhang, T. Kitamura, J. Zhang, L. R. Campion, E. A. Kaiser, L. A. Snyder and J. W. Pollard. "Ccl2 Recruits Inflammatory Monocytes to Facilitate Breast-Tumour Metastasis." *Nature* 475, no. 7355 (2011): 222-5.

Radtke, F. and K. Raj. "The Role of Notch in Tumorigenesis: Oncogene or Tumour Suppressor?" *Nat Rev Cancer* 3, no. 10 (2003): 756-67.

Raz, Y. and N. Erez. "An Inflammatory Vicious Cycle: Fibroblasts and Immune Cell Recruitment in Cancer." *Exp Cell Res*, (2013).

Saito, H., P. Dubsky, C. Dantin, O. J. Finn, J. Banchereau and A. K. Palucka. "Cross-Priming of Cyclin B1, Muc-1 and Survivin-Specific Cd8+ T Cells by Dendritic Cells Loaded with Killed Allogeneic Breast Cancer Cells." *Breast Cancer Res* 8, no. 6 (2006): R65.

Salomé LeibundGut-Landmann, Fabiola Osorio, Gordon D. Brown and Caetano Reis e Sousa. "Stimulation of Dendritic Cells Via the Dectin-1syk Pathway Allows Priming of Cytotoxic T-Cell Responses." *Blood*, (2008).

Schön MP, Arya A, Murphy EA, Adams CM, Strauch UG, Agace WW, Marsal J, Donohue JP, Her H, Beier DR, Olson S, Lefrancois L, Brenner MB, Grusby MJ, Parker CM. "Mucosal T Lymphocyte Numbers Are Selectively Reduced in Integrin Alpha E (Cd103)-Deficient Mice." *J Immunol.*, (1999).

Solenne Vigne, Gaby Palmer, Praxedis Martin, Céline Lamacchia, Deborah Strebel, Emiliana Rodriguez, Maria L. Olleros, Dominique Vesin, Irene Garcia, Francesca Ronchi, Federica Sallusto, John E. Sims and Cem Gabay. "Il-36 Signaling Amplifies Th1 Responses by Enhancing Proliferation and Th1 Polarization of Naive Cd4+ T Cells." *Blood*, (2012).

Solinas, G., G. Germano, A. Mantovani and P. Allavena. "Tumor-Associated Macrophages (Tam) as Major Players of the Cancer-Related Inflammation." *J Leukoc Biol* 86, no. 5 (2009): 1065-73.

Stenger, E. O., H. R. Turnquist, M. Y. Mapara and A. W. Thomson. "Dendritic Cells and Regulation of Graft-Versus-Host Disease and Graft-Versus-Leukemia Activity." *Blood* 119, no. 22 (2012): 5088-103.

Sudhanshu Agrawal, Sudhir Gupta, Anshu Agrawal. "Human Dendritic Cells Activated Via Dectin-1 Are Efficient at Priming Th17, Cytotoxic Cd8 T and B Cell Responses." *PLoS ONE*, (2010).

Tsukada, Chika, Hisashi Yokoyama, Chikako Miyaji, Yuiko Ishimoto, Hiroki Kawamura and Toru Abo. "Immunopotentiation of Intraepithelial Lymphocytes in the Intestine by Oral Administrations of B-Glucan." *Cellular Immunology* 221, no. 1 (2003): 1-5.

Ueno, H., N. Schmitt, E. Klechevsky, A. Pedroza-Gonzalez, T. Matsui, G. Zurawski, S. Oh, J. Fay, V. Pascual, J. Banchereau and K. Palucka. "Harnessing Human Dendritic Cell Subsets for Medicine." *Immunol Rev* 234, no. 1 (2010): 199-212.

Unger, W. W. and Y. van Kooyk. "'Dressed for Success' C-Type Lectin Receptors for the Delivery of Glyco-Vaccines to Dendritic Cells." *Curr Opin Immunol* 23, no. 1 (2011): 131-7.

Vahedi, G., H. Takahashi, S. Nakayamada, H. W. Sun, V. Sartorelli, Y. Kanno and J. J. O'Shea. "Stats Shape the Active Enhancer Landscape of T Cell Populations." *Cell* 151, no. 5 (2012): 981-93.

Vessela N. Kristensen, Charles J. Vaske, Josie Ursini-Siegele, Peter Van Loof, Silje H. Nordgard,, Therese Sørlie Ravi Sachidanandam, Fredrik Wärnberg, Vilde D. Haakensen, Åslaug Helland, Bjørn Naume, and David Haussler Charles M. Perou, Olga G. Troyanskaya, and Anne-Lise Børresen-Dale. "Integrated Molecular Profiles of Invasive Breast Tumors and Ductal Carcinoma in Situ (Dcis) Reveal Differential Vascular and Interleukin Signaling." *Proc Natl Acad Sci U S A.*, (2012).

Villablanca, E. J., L. Raccosta, D. Zhou, R. Fontana, D. Maggioni, A. Negro, F. Sanvito, M. Ponzoni, B. Valentinis, M. Bregni, A. Prinetti, K. R. Steffensen, S. Sonnino, J. A. Gustafsson, C. Doglioni, C. Bordignon, C. Traversari and V. Russo. "Tumor-Mediated Liver X Receptor-Alpha Activation Inhibits Cc Chemokine Receptor-7 Expression on Dendritic Cells and Dampens Antitumor Responses." *Nat Med* 16, no. 1 (2010): 98-105.

William W Agace, Jonathan MG Higgins, Bhanu Sadasivan, and Michael B Brenner and Christina M Parker. "T-Lymphocyte-Epithelial-Cell Interactions Integrin Alphaecd103beta7 Leep-Cam and Chemokines." *Curr Opin Cell Biol.*, (2000).

Yang, L., Y. Qi, J. Hu, L. Tang, S. Zhao and B. Shan. "Expression of Th17 Cells in Breast Cancer Tissue and Its Association with Clinical Parameters." *Cell Biochem Biophys* 62, no. 1 (2012): 153-9.

Zhang, J. P., J. Yan, J. Xu, X. H. Pang, M. S. Chen, L. Li, C. Wu, S. P. Li and L. Zheng. "Increased Intratumoral Il-17-Producing Cells Correlate with Poor Survival in Hepatocellular Carcinoma Patients." *J Hepatol* 50, no. 5 (2009): 980-9.

Zhang, W. J., B. H. Li, X. Z. Yang, P. D. Li, Q. Yuan, X. H. Liu, S. B. Xu, Y. Zhang, J. Yuan, G. S. Gerhard, K. K. Masker, C. Dong, W. A. Koltun and M. J. Chorney. "Il-4-Induced Stat6 Activities Affect Apoptosis and Gene Expression in Breast Cancer Cells." *Cytokine* 42, no. 1 (2008): 39-47.

Zhou, L., M. M. Chong and D. R. Littman. "Plasticity of Cd4+ T Cell Lineage Differentiation." *Immunity* 30, no. 5 (2009): 646-55.

Ziegler, S. F. and Y. J. Liu. "Thymic Stromal Lymphopoietin in Normal and Pathogenic T Cell Development and Function." *Nat Immunol* 7, no. 7 (2006): 709-14.